N° d'ordre : 4498 **ANNÉE 2012**

UNIWERSYTET IM. ADAMA MICKIEWICZA W POZNANIU

UNIVERSITÉ DE RENNES 1

**THÈSE**
**en cotutelle**

pour le grade de

**DOCTEUR DE L'UNIVERSITÉ DE RENNES 1**

*Mention : Physique*

**Ecole doctorale « Science de la Matiere »**

présentée par


# Wawrzyniec KASZUB

Préparée à l'unité de recherche :
Institut de Physique de Rennes, Université de Rennes 1, France
et Faculté de Physique, Université Adam Mickiewicz de Poznań, Pologne


---

# Photo-induced phase transitions in molecular materials

**Thèse soutenue à Faculté de Physique, Université Adam Mickiewicz de Poznań, Le 26 Avril 2012**

devant le jury composé de :

**Ryszard PARZYŃSKI**
Professeur, Université Adam Mickiewicz de Poznań, Pologne / *President*

**Azzedine BOUSSEKSOU**
Directeur de Recherche, Laboratoire de Chimie de Coordination du CNRS, Toulouse, France / *rapporteur*

**Czesław RADZEWICZ**
Professeur, Université de Varsovie, Pologne / *rapporteur*

**Marylise BURON**
Professeur, Université de Rennes 1, France / *examinateur*

**Herve CAILLEAU**
Professeur, Université de Rennes 1, France / *directeur de thèse*

**Ryszard NASKRĘCKI**
Professeur, Université Adam Mickiewicz de Poznań, Pologne / *directeur de thèse*

Faculty of Physics, Adam Mickiewicz University in Poznań
Institute of Physics, University of Rennes 1

Doctoral Thesis

# Photo-induced phase transitions in molecular materials

by
**Wawrzyniec KASZUB**

This Ph.D. dissertation was completed under joint supervision and with guidance of two supervisors:

Professor Hervé CAILLEAU
*Institute of Physics, University of Rennes 1, France*

Professor Ryszard NASKRĘCKI
*Faculty of Physics, Adam Mickiewicz University in Poznań, Poland*


RENNES – POZNAŃ
2012

Doctoral Thesis
**Photo-induced phase transitions in molecular materials**
author: Wawrzyniec Kaszub

**2012** Institut de Physique de Rennes UMR UR1 – CNRS 6251,
Universite de Rennes 1, Campus de Beaulieu, 263 av. du General Leclerc,
35042 Rennes Cedex, FRANCE

**2012** Wydział Fizyki,
Uniwersytet im. Adama Mickiewicza w Poznaniu, ul. Umultowska 85,
61-614 Poznań, POLSKA

Printed by:
Service Imprimerie
Campus Scientifique de Beaulieu, 263 av. du General Leclerc, CS 74205
35042 Rennes Cedex, FRANCE

Typesetting: Wawrzyniec Kaszub
Original size : B5 - 17 x 24 cm (6,69 x 9,44 in.)
Number of pages: 162
Number of colour pages: 38
Main fonts: Palatino Linotype, Arial Narrow

This work is available as PDF file at: www.repozytorium.amu.edu.pl
and www.cnrs.fr

*I would like to dedicate this Thesis*
*to my Wife and our whole Family*

## Acknowledgements

Ph.D. thesis wouldn't appear if there would be no helpful hand from many people. I would like to express my appreciation and thanks to my supervisors, prof. Herve Cailleau and prof. Ryszard Naskręcki for their help, knowledge and confidence for young scientist. Without their wisdom, this work would not have been started and completed. They showed me beauty of the physics and how to solve the problems which are very often accompanying to scientific work.

I would like to express my appreciation and thanks to Dr. Maciej Lorenc. He showed me not only a secrets of the lasers experimental work but more: he taught me how to focus on the complex targets without seeing difficulties. He introduced me to people, who I knew only from the scientific papers. He encourages me in many areas (not only scientific one!) and he is a man who is a lucky-given all the time. I would like to thank to him for things which I participate, for the priceless help especially at the final part of writing this thesis.

I would like to thank also to Dr. Marina Servol, for the valuable discussions and help with not only a "EDO-TTF" project. She showed me that computing part of scientific work can be also interesting. Without her, the "EDO-TTF" project would be undiscovered by me. I believe that our collaboration will be fruitful in the future!

I will never forget helpful hand and unfading enthusiasm from the prof. Marylise Buron, prof. Eric Collet and Dr. Gotard Burdziński. I would like to thank them for the help and encourage during my Ph. D. study!

I would like to express my appreciation and thanks to Dr. Jacek Kubicki for valuable discussions and useful remarks. I wish I met him earlier. I hope that after the end of my Ph.D. study our collaboration will be continued.

Anything comes out of nothing. That's why I would like to thank to Dr. Krzysztof Dobek and prof. Antoni Wójcik, because their knowledge is still in my heart and it was very useful during these studies. Thank you very much for this!

To my colleagues from the Faculty and especially: Dr. Elżbieta Trzop, Dr. Michał Berent, Roman Bertoni, Mikołaj Czechlewski, Dr. Wojciech Giera, Dr. Paweł Kurzyński, Dr. Tomasz Kopyciuk, Tomasz Kozioł and Jan Olszanowski I would like to express my thanks for the priceless and everlasting help in every aspect of my life.

I have been extremely fortunate to have worked with the following group of talented individuals from the IPR (UR1) group, especially: Loic Toupet, Jean-Claude Ameline, Dr. Alan Moreac, and from the ZEK (AMU), especially: prof. Ryszard Parzyński, Dr. Marcin Ziółek, Dr. Jerzy Karolczak, Dr. Elżbieta Pawłowska and Dr. Adam Łukaszewicz – who was a great colleague and he supported me before final exams and I believe that he roots me now from Heaven.

I would like to thanks also to: Dr. Azzedine Bousseksou and prof. Czesław Radzewicz, my referees, for their constructive remarks included in this version of thesis. I'm sure that this work became more clear and useful for the next generations.

I would like to thanks also to Katarzyna Panek, who was my first boss. She helped me many times especially after my wedding and removal. Thank you!

To continued support of my family has been paramount to my ability to complete this work. To my wife, sister, brother in law, and our parents, grandparents and whole family for the encourage, help, support and helpful hand in every moment of my life. I expressed my deepest love and appreciation. Thank You very much! It was very important to me!

*Wawrzyniec Kaszub*

*Poznań, June 26th 2012*

# Table of contents

# Abstracts

## Abstract

My thesis concerns phase transitions induced by a light pulse in the solid state. This new field is attracting considerable interests as it promises development of new applications based on photo-switchable molecular materials.[1,2,3,4] During my Ph.D. I have investigated such materials and the mechanisms underlying their transitions upon the action of a laser pulse.

The group in Rennes University is engaged in investigations of Photo-Induced Phase Transitions (PIPT), for which subtle couplings between electronic excitations and relaxation of structural degrees of freedom exist and often lead to spectacular macroscopic effects. In particular, the Rennes group focus on molecular materials which exhibit switching between multi-functional properties. The mechanisms driving photo-induced phase transitions are strongly nonlinear and bring into play different time and space scales. These require thorough analysis of the cooperative effects as well as the physical mechanisms away from thermal equilibrium. From the standpoint of classical thermodynamics we can speak of "hidden phases" of matter, which are now attainable thanks to ultra-short laser pulses. Designing suitable excitation patterns should eventually lead to the photo-control of phase transitions. In brief, the relevant mechanisms can be described as originating from either of two extreme cases:

1) Photon absorption can generate an excited state localized on a molecule following structural relaxation (conformational change, etc…). Initial dynamics of these transformations is related to the elementary atomic motions, and consequently it occurs on timescales spanning few hundreds of femtoseconds (1 fs = $10^{-15}$s) to few picoseconds (1 ps = $10^{-12}$s). Contrary to photochemical processes, in which the phenomena are essentially independent, in cooperative systems there exist strong interactions between excited molecules. When an ultrashort laser pulse simultaneously transforms sufficient number of molecules, these can couple and drive the system towards a new macroscopic phase. Spin-crossover phenomenon illustrates well this case, and the group in Rennes have very recently obtained compelling data on a spin transition compound which underpin the ultrafast nature of the process.[5] Using time resolved optical spectroscopy with one wavelength or broadband chirped probe pulses one can see the dynamics of the transition between High and Low Spin (HS, LS respectively).

2) In the systems with predominant collective phenomena, delocalized electronic excitations initiated by an ultrashort laser pulse perturb the entire atomic network. It generates coherent collective atomic motions, such as optical phonon,[4] which can extremely rapidly lead to a new phase (100 fs – few ps). Beautiful results obtained on a charge transfer molecular crystal $(EDO\text{-}TTF)_2PF_6$, which undergoes metal-insulator transition, illustrate the novel possibilities.[7] New experiments with $(EDO\text{-}TTF)_2SbF_6$ compound were made and new features of this crystal were found. A femtosecond laser pulse induces a new state from the insulating phase through an ultrafast process, within around 1 ps. Generally speaking, all compounds related to charge transfer ordering are very promising candidates for ultrafast phase transitions. Their potential is currently explored via collaboration between Rennes University and Japan.

In addition to generating and evidencing such effects, understanding these non-linear and out of equilibrium phenomena is of fundamental importance and requires coupling several complementary techniques. Time-resolved studies, using femtosecond flashes of light to excite a material and trigger a phase transition, have provided insights into the microscopic description of phase transitions. In my research I have used the well established capabilities of the time-resolved pump-probe experiments, to address the key parameters governing the switching in molecular materials. Both Poznań and Rennes groups have proven record of expertise in applying these techniques, and they are complementary in terms of wavelength range, time resolution, sample environment.[8,9]

During my Ph.D. study, I've made experiments on spin-crossover compounds using two lasers working in synchrony and covers wide range of time delay between pump and probe. Due to collected data, dynamics of relaxation process in femtosecond, nanosecond and microsecond time scale was proposed. What was completely new, during one measurement experimental setup we were able to detect photo response after excitation through femtosecond step, elastic interactions occurs in nanosecond timescale and microseconds thermal relaxation. Additionally I developed new experimental setup with white light and used it to measurements covering wide spectral range of photo-response.

Second compound ((EDO-TTF)$_2$SbF$_6$) crystal, is isostructural compound to (EDO-TTF)$_2$PF$_6$ (all belongs to family of ((EDO-TTF)$_2$XF$_6$ ¼ filled organic crystals) in which first giant photoresponse was observed and published in Science in 2005.[7] Analysis of obtained data widen knowledge about this kind of excitation and dynamics of the metastable photo-induced state.

Besides rather conventional ultrafast optical techniques, as part of my "co-tutelle" thesis I developed and used a single shot set-up to investigate irreversible processes, i.e. inside thermal hysteresis. Because multiple laser shots are typically required to monitor ultrafast dynamics, sample depletion and product accumulation restrict the range of substrates, structural environments, excitation conditions amenable to study. Recent study on irreversible chemical reaction in an organic crystal proved the feasibility of performing single shot experiments, whereby a two-dimensional temporal delay grid is imprinted on the spatial profile of a single femtosecond pulse, which then monitors a reaction until 10 ps following triggering flash.[10] Single shot optical experiments will allow monitoring the transformation dynamics inside the hysteresis, where critical phenomena take place and systems may be irreversibly trapped. The femtosecond pulses have extremely high intensities, which often causes ablation or non-thermal melting of studied materials, both of which evidently preclude common repetitive pump-probe measurements. In my preliminary studies, I chose thin gold layer as a tester for benchmarking this new experimental setup.

**References:**

[1] O. Sato et al., *Angew. Chem. Int. Ed.* **46,** 2152 (2007)
[2] A. Bousseksou et al., *Chem. Soc. Rev.* **40,** 3313 (2011)
[3] E. Collet et al., *Science* **300**, 612 (2003)
[4] E. Trzop et al., *Appl. Crys.* **40**, 158 (2007)
[5] M. Lorenc et al., *Phys. Rev. B* **85**, 054302 (2012)
[6] S. Iwai et al., *Phys. Rev. Lett.* **96**, 057403 (2006)
[7] M. Chollet et al., *Science* **307**, 86 (2005)
[8] J. Przesławski et al., *Ferroelectrics* **269**, 45 (2002)
[9] A.Pajzderska et al., *Mol. Phys.* **104**, 1819 (2006)
[10] P. Poulin et al., *Science* **313**, 1756 (2006)

## Résumé

Ce travail de recherche concerne des transformations à l'état solide induites par la lumière. Ce nouveau champ scientifique présente un intérêt certain du fait d'opportunités nouvelles d'applications basées sur la photo-commutation de matériaux.[1,2,3,4] Durant les travaux de thèse, les mécanismes de transformations photo-induites par un pulse laser dans des matériaux moléculaires ont été étudiés.

Les Transitions de Phase Photo-Induites (Photo-Induced Phase Transitions – PIPT) se produisent à l'état cristallin du fait du couplage des états électroniques photo-excités avec le réseau qui entraîne une relaxation structurale impliquant plusieurs atomes ou molécules. En particulier, c'est le cas des matériaux moléculaires multi-fonctionnels qui présentent une commutation entre états macroscopiques, amenant un changement spectaculaire de leurs propriétés physiques. Les mécanismes de base des transitions de phase photo-induites sont fortement non linéaires et mettent en jeu différentes échelles de temps et d'espace. Ceci nécessite aussi une analyse des effets coopératifs de même que des comportements du matériau loin de l'équilibre thermique. Cet objectif sur le photo-contrôle de transitions de phase dans les matériaux nécessite une compréhension approfondie des différents aspects. Pour simplifier, on peut distinguer entre deux cas limites:

1) L'absorption du photon peut générer un état localisé sur une molécule suite au processus de relaxation structurale (réarrangements intramoléculaires et dans l'environnement local). La dynamique initiale de cette réorganisation locale est gouvernée par des mouvements atomiques élémentaires, et par conséquent elle se produit sur des échelles de temps allant de la centaine de femtosecondes ($1fs = 10^{-15}s$) à quelques picosecondes ($1ps = 10^{-12}s$). Contrairement aux processus photochimiques en solution, qui sont essentiellement des processus indépendants, à l'état solide ils peuvent devenir coopératifs puisque des interactions importantes peuvent se manifester entre molécules excitées. Quand un pulse laser ultra-court transforme simultanément un nombre suffisant de molécules, les interactions entre celles-ci peuvent conduire à un nouvel état macroscopique de nature différente. Les phénomènes de transitions de spin illustre bien cette situation localisée. L'équipe de Rennes s'est récemment intéressé aux processus rapides et ultra-rapides induits par un pulse laser ultra-court dans les composés à transition de spin.[5]

Utilisant la spectroscopie optique résolue en temps dans le cadre de cette thèse, avec un pulse sonde monochromatique ou à large bande, on peut observer les différentes étapes de la transition entre états Bas et Haut Spin (BS, HS).

2) Dans les systèmes où l'excitation électroniques est délocalisée (electrons itinerants) les effets collectifs peuvent dominer avec une relaxation sructurale mettant en jeu l'ensemble du réseau, c'est à dire l'ensemble des atomes du cristal. Ainsi un pulse laser ultra-court peut générer des mouvements atomiques collectifs cohérents, tels que des phonons optiques, qui peuvent conduire rapidement à la formation d'une nouvelle phase (100 fs – quelques ps).[6] Le bismuth qui présente une transition isolant-métal illustre bien cette situation physique. Les cristaux moléculaires à transfert de charge, en particulier ceux de la famille de $(EDO\text{-}TTF)_2PF_6$ qui présentent aussi une transition isolant-métal, pourraient constituer d'autres exemples.[7] On savait qu'un pulse laser femtoseconde induisait un nouvel état à partir de l'état isolant de façon ultra-rapide, de l'ordre de la picoseconde. Ceci se traduit par une réponse optique particulièrement spectaculaire. De façon générale, tous les composés moléculaires à transfert de charge sont très prometteurs dans le champ des transitions de phase photo-induites. Une partie des travaux de thèse se rapporte à cette problématique.

En plus de la génération et de la mise en évidence de ces phénomènes, la compréhension des mécanismes, par essence non linéaires et hors équilibre, nécessite l'utilisation de plusieurs techniques expérimentales complémentaires. Les études résolues en temps, utilisant un flash de lumière femtoseconde pour exciter un matériau et induire une transformation de phase, apportent des informations cruciales sur la description microscopique de ces processus, de l'échelle de la molécule à celle du matériau. Dans ce travail de thèse les possibilités offertes par les expériences optiques pompe-sonde ont été utilisées pour déterminer les paramètres clés gouvernant la photo-commutation de matériaux moléculaires. Pour cela, les expertises et les possibilités expérimentales complémentaires de Rennes et Poznan, en termes de gamme de longueur d'onde, de résolution temporelle et d'environnement échantillon, ont été exploitées.[5,8,9]

Les expériences sur les composés à transition de spin ont utilisées de façon spécifiques deux sources lasers pulsées qui étaient synchronisées électroniquement et qui pouvait ainsi couvrir une très large gamme de délai en temps entre la pompe et la sonde. C'est ainsi que la dynamique de la transformation a pu être observée sur plusieurs échelles de temps, de la femposeconde à la microseconde.

Ce qui a ainsi pu être démontré c'est que la transformation du matériau à partir d'un état BS se réalise en plusieurs étapes successives: à l'échelle des femtosecondes une étape « photo-induite » à proprement parlé vers l'état HS au niveau de la molécule, à l'échelle des nanosecondes une étape « élastique » avec l'augmentation de volume du matériau, à l'échelle des microsecondes une étape « thermique » avec l'activation thermique de BS vers HS et l'homogénéisation de température du matériau. De façon complémentaire un nouveau montage expérimental de « lumière blanche » a été développé pour couvrir une large gamme spectrale pour l'étude de la photo-réponse transitoire.

Le cristal de $(EDO\text{-}TTF)_2SbF_6$ est isostructural au composé prototype $(EDO\text{-}TTF)_2PF_6$ (tous appartiennent à la famille des cristaux organiques conducteurs $(EDO\text{-}TTF)_2XF_6$ à bande ¼ remplie) dans lequel une photo-réponse géante a été observée et publiée dans Science en 2005.[7] Une dynamique mettant en jeu plusieurs phonons optiques cohérents a été clairement observée. Leur comportement en température est cependant similaire à celui à l'équilibre thermique et aucun phénomène d'auto-amplification n'a été observé. Cela semble indiquer que le comportement de ce composé est différent de celui du composé prototype avec transformation photo-induite plus localisé.

En plus des techniques optiques utilisées pendant les travaux se rapportant aux deux parties précédentes, un nouveau montage expérimental « single shot » a aussi été mis en place. Le but est d'étudier des processus irréversibles, comme par exemple la dynamique de la transformation d'un cristal avant son explosion ou dans un régime bistable, c'est-à-dire à l'intérieur d'un cycle d'hystérésis thermique. Récemment des études au MIT ont montré la faisabilité de telles expériences avec l'observation de la dynamique d'une réaction chimiques à l'état cristallin jusqu'à 10 ps après le flash de lumière.[10] De multiple faisceaux laser sont nécessaire pour observer une telle dynamique ultra-rapide. Le comportement du cristal limite cependant les conditions de photo-excitation. Le pulse laser pompe est très intense et peut causer ainsi la fusion non thermique et l'ablation d'un matériau. Un couche mince d'or a ainsi été choisie pour tester notre nouveau montage espérimental.

**Bibliographie:**

[1] O. Sato et al., *Angew. Chem. Int. Ed.* **46,** 2152 (2007)
[2] A. Bousseksou et al., *Chem. Soc. Rev.* **40,** 3313 (2011)
[3] E. Collet et al., *Science* **300**, 612 (2003)
[4] E. Trzop et al., *Appl. Crys.* **40**, 158 (2007)
[5] M. Lorenc et al., *Phys. Rev. B* **85**, 054302 (2012)
[6] S. Iwai et al., *Phys. Rev. Lett.* **96**, 057403 (2006)
[7] M. Chollet et al., *Science* **307**, 86 (2005)
[8] J. Przesławski et al., *Ferroelectrics* **269**, 45 (2002)
[9] A.Pajzderska et al., *Mol. Phys.* **104**, 1819 (2006)
[10] P. Poulin et al., *Science* **313**, 1756 (2006)

## Streszczenie

W październiku 2007 roku został zapoczątkowany międzynarodowy projekt badawczy pomiędzy Institut de Physique de Rennes Uniwersytetu Rennes 1 (Francja), a Wydziałem Fizyki Uniwersytetu im. Adama Mickiewicza w Poznaniu. Celem tego projektu było podjęcie wspólnych badań przejść fazowych indukowanych światłem w kryształach molekularnych, a jednym z elementów składowych tego projektu było powołanie wspólnego polsko-francuskiego doktoratu „en co-tutelle" w tym obszarze badań.

### Wprowadzenie

Wybór potencjalnych ośrodków do badań obejmował zarówno grupy kryształów molekularnych intensywnie badanych na Wydziale Fizyki UAM jak i zupełnie nowe grupy kryształów molekularnych syntetyzowanych i badanych przez grupy badawcze z Japonii[1] [(EDO-TTF)$_2$SbF$_6$] oraz Francji[2] [[(TPA)Fe$^{III}$(TCC)]PF$_6$ i [(TPA)Fe$^{III}$(TCC)]SbF$_6$] na bazie współpracy istniejącej między Uniwersytetami w Rennes (UR1), Kyoto (Kyoto University) i Paryżu (Universite Paris-Sud 11).[3]

Tematyka niniejszej rozprawy doktorskiej koncentruje się wokół badań przejść fazowych indukowanych światłem w ciałach stałych (kryształy organiczne i takie, w których następuje przejście spinowe). Obecnie jest to nowa, dynamicznie rozwijająca się dziedzina badań, która z powodu potencjalnie możliwych zastosowań w szeroko rozumianej informatyce,[4] obejmuje coraz liczniejszą grupę materiałów. Jednak mechanizm powstawania przejść fazowych indukowanych światłem nadal pozostaje do końca nie wyjaśniony. Wiadomo jednak, że różni się on od procesów indukowanych takimi parametrami jak ciśnienie czy temperatura i określany jest on jako stan poza równowagą termodynamiczną, gdzie pod wpływem ultrakrótkiego impulsu laserowego w krysztale dochodzi do silnie nielinowych efektów, zmian dalekich od tych zachodzących w stanie równowagowym.

### Metoda badawcza

Aby badać efekty indukowane światłem należy użyć femtosekundowych układów laserowych typu pompa – sonda w dużą czasową zdolnością rozdzielczą. Impuls „pompujący" indukuje efekt, natomiast impuls sondujący służy do monitorowania zachodzących zmian (np. fazy układu). Otrzymane taką metodą widma czasowo-

rozdzielcze są porównywalne z widmami stacjonarnymi układu w równowadze termodynamicznej. Zaletą tej metody badawczej jest możliwość badania zachowania się układu w czasach rzędu pikosekund od wzbudzenia oraz możliwość obserwacji stanów koherentnych w indukowanej fazie, ktore ulegają stochastycznemu "rozmrażaniu" w stanach tradycyjnie generowanych termicznie. W latach dziewięćdziesiątych na Wydziale Fizyki UAM zbudowano układ typu pompa – sonda z femtosekundową zdolnością rozdzielczą[5,6] służący do badania absorpcji przejściowej w fazie ciekłej. Podjęte wspólne, polsko-francuskie badania pozwoliły efektywniej wykorzystać zaplecze sprzętowe obu laboratoriów, oraz bardzo dobrze rozwiniętą współpracę naukową grupy francuskiej w szczególnosci z laboratoriami japońskimi.

**Obecny stan wiedzy na temat foto-indukowanych przejść fazowych**

Na podstawie obecnie dostępnej literatury mechanizmy rządzące przejściami fazowymi indukowanym światłem można rozpatrywać na dwa sposoby: pierwszy polega na absorpcji fotonu przez cząsteczkę, która relaksując oddziałuje na swoje otoczenie, co w konsekwencji może prowadzić do lokalnych zmian konformacyjnych w krysztale. Pierwotne procesy takiego przejścia zachodzą w czasach od femtosekund do mikrosekund i są związane z elementarnymi ruchami atomów w ciele stałym.[2] W przeciwieństwie do reakcji fotochemicznych, gdzie procesy relaksacyjne atomów są od siebie w większości niezależne - w przypadku układów kooperatywnych (takich jak np. kryształy) istnieją bardzo silne interakcje pomiędzy wzbudzonymi molekułami. Po wzbudzeniu całej grupy atomów, cząsteczki mogą – oddziałując na siebie – wprowadzić układ w nowy stan. Przykładem może być zjawisko typu „spin-crossover”[7] polegające na przejściu pomiędzy różnymi stanami spinowymi w niektórych pierwiastkach (np. metalach przejściowych) pod wpływem zewnętrznego czynnika, jakim jest światło lub temperatura.

W drugim przypadku - w układach, w których wzbudzenie elektronów przez impuls laserowy prowadzi do delokalizacji elektronu, może dojść do „wzbudzenia” całej sieci atomowej. W efekcie powstaje w sieci fonon optyczny, który w czasie rzędu femtosekund zmienia fazę makroskopową układu. Przykładem materiału, gdzie zachodzi takie zjawisko są kryształy, w których występuje przeniesienie ładunku pomiędzy cząsteczkami.[8] W kryształach takich obserwuje się przejście z fazy nieprzewodzącej do fazy przewodzącej. Obecnie wraz z grupą badawczą z Rennes prowadzę badania nad takimi układami. Jednakże na świecie toczy się dyskusja czy faza wysokotemperaturowa jest taka sama (posiada takie same właściwości) jak faza indukowana światłem.

Niektóre źródła literaturowe tę nową fazę nazywają „fazą pseudo-przewodzącą" lub „fazą pseudo-metaliczną".[9] Poznanie i zrozumienie natury tego zjawiska ma więc kluczowe znaczenie do potwierdzenia lub zaprzeczenia istniejącej teorii fotoindukowanych przejść fazowych.

**Cel badań**

Celem badań zrealizowanych w ramach niniejszej pracy doktorskiej było:

1. Zbadanie dynamiki przejść pomiędzy dwoma stanami spinowymi cząsteczki w kryształach typu „spin-crossover" i jej oddziaływanie z całym otoczeniem, poprzez monitorowanie zmian absorbancji (transmitancji) i struktury w czasach od femtosekund do mikrosekund.[2] Wyniki tych badań opisano w rozdziale 3 (chapter 3: „Spincrossover transformation…").

2. Zbadanie właściwości fazy powstałej wskutek działania impulsu femtosekundowego i związanej z tym silnej delokalizacji ładunku w krysztale organicznym w fazie nieprzewodzącej.[10] Uzyskane wyniki oraz wnioski dotyczące tych badań zostały zaprezentowane w rozdziale 4 (chapter 4: „Photo-induced phenomena…").

Znaczny nakład pracy w czasie realizacji niniejszej pracy doktorskiej został poświęcony budowie i rozwojowi nowych laserowych układów pomiarowych typu pompa-sonda. Na rysunku (ryc. 1 na następnej stronie) przedstawiono schemat układów laserowych używanych w czasie badań.

Badania nad kryształami spinowymi przeprowadzono miedzy innymi z wykorzystaniem dwóch zsynchronizowanych laserów femtosekundowych. Czas trwania impulsów pompującego i sondującego wynosiły odpowiednio 40 fs i 100 fs. Układ ten pozwalał na śledzenie dynamiki procesów w szerokiej skali czasu, od femtosekund do mikrosekund, tą samą parą impulsów laserowych na tym samym krysztale i w tych samych warunkach termodynamicznych. Biorąc pod uwagę złożoność zachodzacych procesów fizycznych w badanych układach, zmiana jednego z parametrów eksperymentalnych może zasadniczo wpływać na interpretację wyników. Stąd zastosowane rozwiązanie, unikalne w Europie, pozwalające na jednoznaczną interpretację procesów rozciągających się na dziesięć rzędów wielkości skali czasu, gdzie każda kolejna dekada "odmraża" nowy stopień swobody (elektron, atom, fonon, drgania termiczne).

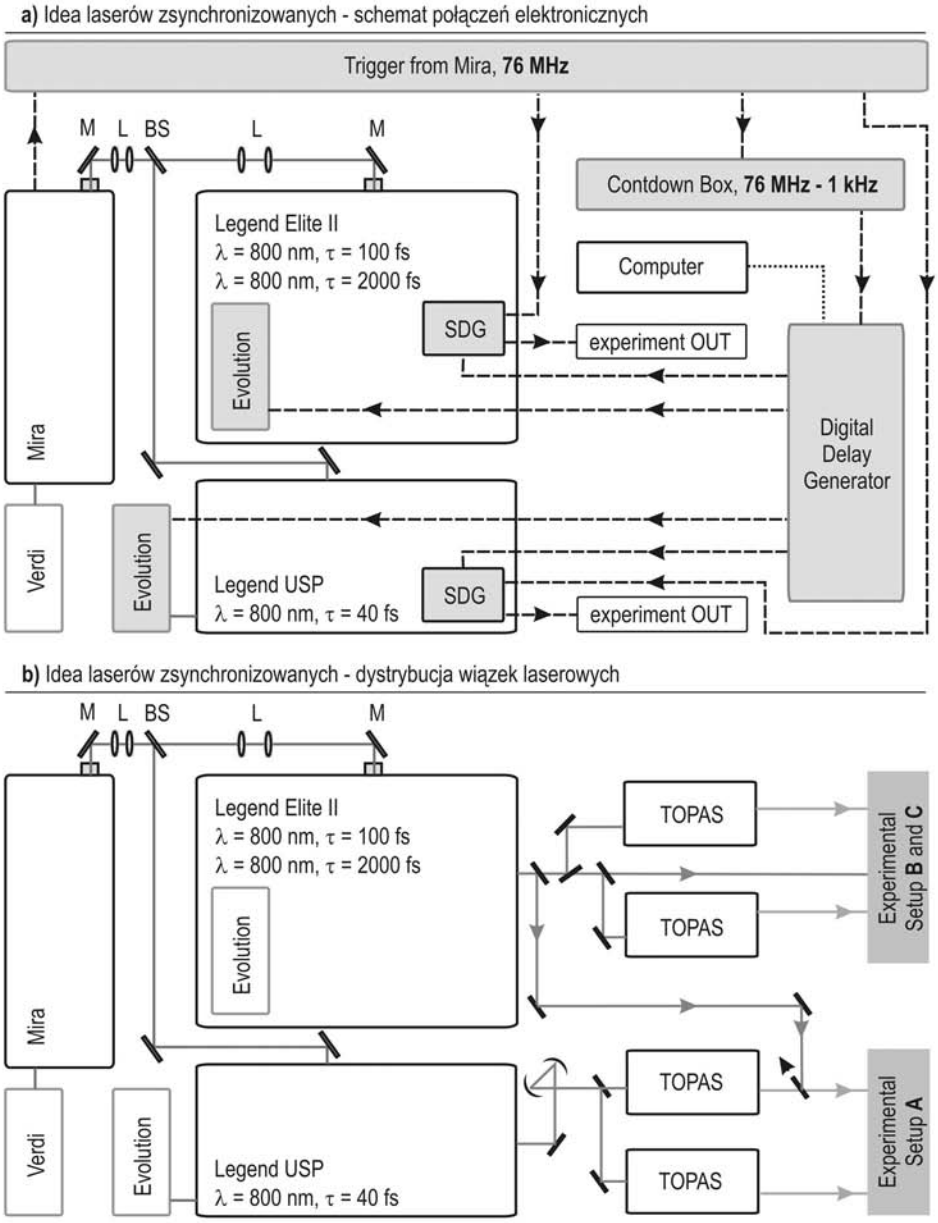


**Ryc. 1:** Schemat układu laserowego wykorzystywanego w eksperymentach. **a)** Idea laserów zsynchronizowanych – schemat połączeń elektronicznych. Sygnał synchronizujący dwa femto sekundowe wzmacniacze regeneratywne (Legend Elite II, Legend USP) pochodzi z generatora opóźnień wyzwalanego sygnałem z oscylatora femtosekundowego, którego częstość została zmniejszona z 76 MHz do 1 kHz („countdown box"). **b)** Schemtat pokazujący dystrybucję wiązek laserowych do każdego z układów eksperymentalnych. Do zmiany długości fali używano czterech optycznych wzmacniaczy parametrycznych (OPA) z Positive Light, (TOPAS).

Przedstawiony powyżej układ pomiarowy nie pozwalał na badania zmian szerokiego rozkładu spektralnego odpowiedzi kryształu (pomiar polichromatyczny). W tym celu zbudowano układ typu pompa – sonda (superkontinuum), w którym detektorem jest szybka i czuła kamera CCD, rejestrująca widma rozdzielone za pomocą spektrometru. Dzięki temu rozwiązaniu stało się możliwe badanie układów molekularnych w szerokim zakresie spektralnym (obecnie 450 - 750 nm, a w niedalekiej przyszłości nawet 350 - 750 nm). Tak zmierzone widma zawierają informacje na temat właściwości kryształu po fotowzbudzeniu.

Ważnym etapem pracy było zbudowanie układu pomiarowego, zdolnego rejestrować całe widmo w czasie jednego cyklu impulsów (ryc. 2), co miało pozwolić na badania procesów nieodwracalnych oraz z praktycznego punktu widzenia pozwalało wyeliminować fluktuacje związane ze zmianami intensywności białego impulsu sondującego. W czasie testów wykonano pomiary na cienkiej (ok. 300 nm) warstwie złota. Szczegóły zagadnienia te omówiono w rozdziale 5 (chapter 5: „Single shot…"), natomiast szczegóły związane z układami eksperymentalnymi zostały zestawione i opisane w rozdziale 6 (chapter 6: „Experimental").

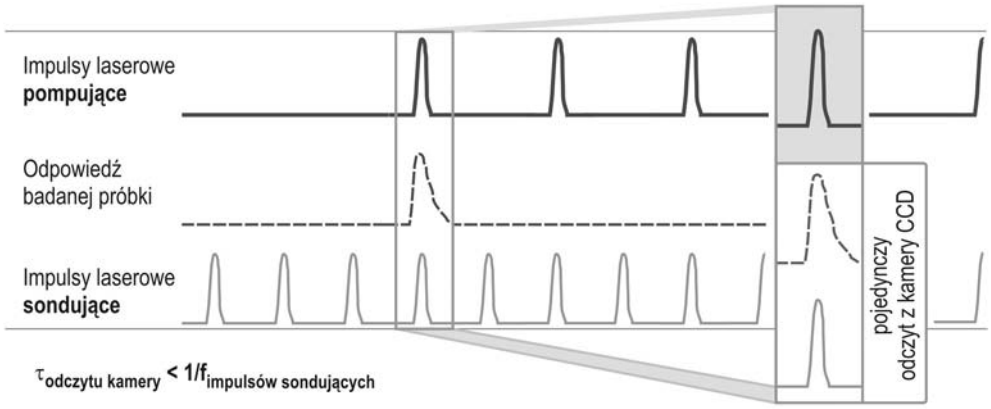


**Ryc. 2:** Idea układu do badań przejść nieodwracalnych. Impuls monitorujący zmiany układu (sonda – jasno-szara linia ciągła) pojawia się z określoną częstotliwością podczas całego eksperymentu. Impulsy indukujące efekt (pompa – ciemno-szara pogrubiona linia ciągła) są zatrzymywane przez szybką migawkę, aż do momentu jej otwarcia. Odpowiedź układu została zaznaczona krzywą przerywaną. Kamera CCD jest zdolna rejestrować odpowiedź układu po każdej ekspozycji (pojedynczy odczyt z kamery). Opóźnienie pomiędzy impulsem „pompującym" i monitorującym dobierane jest za pomocą linii opóźniającej.

**Badania nad kryształami typu spin-crossover**

W badaniach nad kryształami spinowymi użyto dwóch ośrodków: $[(TPA)Fe^{III}(TCC)]PF_6$ i $[(TPA)Fe^{III}(TCC)]SbF_6$, w których przejście pomiędzy stanem wysoko-spinowym (w wysokich temperaturach) i nisko-spinowym (w niskich temperaturach), widoczne jest jako zmiana absorbancji oraz jako zmiana rozkładu spektralnego światła transmitowanego przez ten ośrodek. W przypadku pierwszego z badanych układów ($[[(TPA)Fe^{III}(TCC)]PF_6$) znane były zmiany struktury krystalograficznej, powstające w układzie po wzbudzeniu impulsem pikosekundowym.[11] Badania te pokazały zmiany parametrów komórki elementarnej pojawiające się już w czasie kilku nanosekund od wzbudzenia.

W niniejszej pracy doktorskiej pokazano i omówiono wyniki eksperymentalne uzyskane z wykorzystaniem dwóch synchronizowanych impulsów laserowych. Układ pomiarowy pozwolił na obserwacje zmian absorbancji, a następnie na ich korelacje ze zmianami obserwowanymi w strukturze kryształu w szerokim zakresie czasów opóźnień pomiędzy impulsem wzbudzającym i sondującym badany układ. Dzięki tym obserwacjom przedstawiono procesy, które zachodzą w krysztale po wzbudzeniu. Zmiany absorbancji oraz zmiany struktury w zależności od opóźnienia zostały przedstawione na wykresie (ryc. 3).

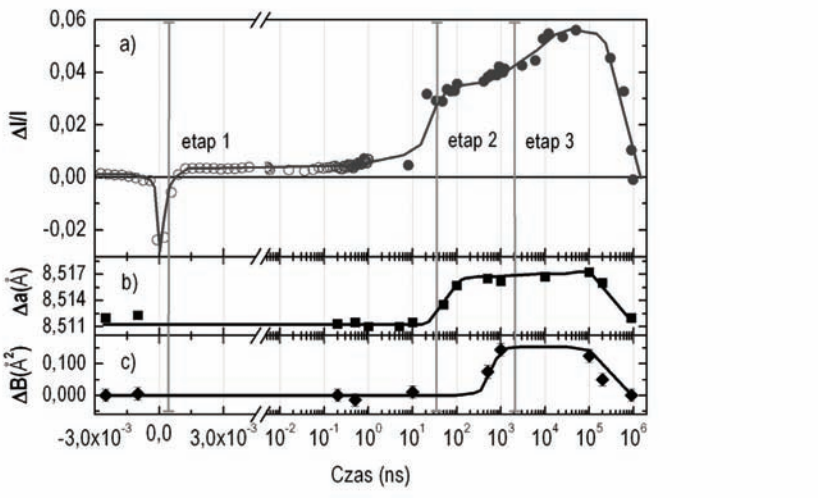


**Ryc. 3: a)** Zmiany intensywności światła transmitowanego przez kryształ w zależności od opóźnienia między impulsem pompy i sondy. **b)** Zmiany stałej sieciowej w zależności od opóźnienia. **(c)** Zmiana współczynnika Debye'a-Wallera. Na rysunku zaznaczono kolejne etapy opisane w tekście (etapy 1-3) Wykres opublikowany w [2].

W czasach rzędu femtosekund zmiany absorbancji utrzymują się na stałym poziomie (etap 1 na ryc. 3). Wiedząc, że jeden foton może być pochłonięty tylko przez jedną cząsteczkę (proces jednofotonowy), tuż po relaksacji ze stanu LMCT (przejście bezpośrednie między stanem nisko-spinowym, a wysoko-spinowym jest zabronione), przez pewien czas liczba wzbudzonych cząsteczek jest stała. Kolejny etap został nazwano etapem „elastycznym", ponieważ różnica w przypadku dwóch różnych stanów spinowych polega na zmianie odległości między atomem metalu, a jego otoczeniem w samej cząsteczce. Zatem cząsteczki w stanie wysoko-spinowym oddziałują elastycznie na sąsiadów, ponieważ zwiększają swoją objętość w sieci zawierającej cząsteczki w stanie nisko-spinowym. Etap ten schematycznie został przedstawiony na ryc. 4, a w badaniach spektroskopowych widoczny jest jako nagła zmiana absorbancji (etap 2 na ryc. 3).

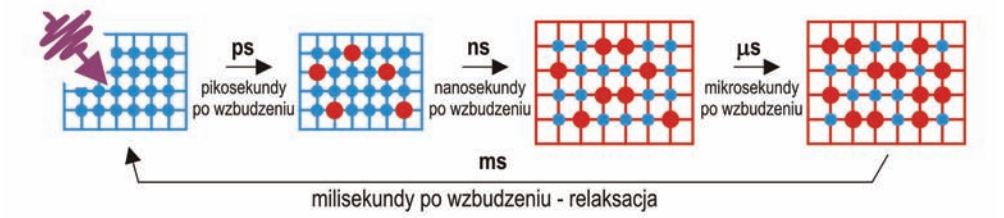


**Ryc. 4:** Rysunek przedstawiający idee relaksacji ze stanu wysoko-spinowego do stanu nisko-spinowego cząsteczek w sieci kryształu typu „spin-crossover" po wzbudzeniu ultrakrótkim impulsem laserowym. Kolejne etapy opisane zostały w tekście. Rysunek publikowany w [11].

Nadmiar zgromadzonej energii po wzbudzeniu zostaje przekazany sieci krystalicznej, co prowadzi do zmian parametrów sieci i rejestrowane jest jako kolejna zmiana absorbancji – tym razem w czasach rzędu mikrosekund (etap 3 na ryc. 3). W tym czasie w krysztale dochodzi także do zamiany stanów spinowych cząsteczek. Te, które znajdowały się w stanie wysoko-spinowym relaksują do stanu niższego, natomiast te, które były w stanie nisko-spinowym, poprzez sieć krystaliczną przechodzą do stanu wysoko-spinowego. Gdy cała zgromadzona energia ulegnie dyssypacji, kryształ powraca do stanu sprzed wzbudzeniem – absorbancja powraca do wartości odpowiadającej danej temperaturze, w jakiej znajduje się kryształ (znanej z pomiarów stacjonarnych). Przejście spinowe jest przejściem nieciągłym, drugiego rodzaju, co znajduje także odzwierciedlenie w badaniach temperaturowych absorbancji w stanie nierównowagowym.

Dodatkowo wykonane zostały pomiary przy użyciu impulsu światła białego (superkontinuum) w czasach krótkich (poniżej 1 nanosekundy).[12] Wyniki te stanowią znaczny postęp w stosunku do publikowanych wcześniej wyników uzyskanych przy pomocy układów z detekcją monochromatyczną.[2,11] Otrzymane wyniki pokazują wyraźnie, że właściwości stanu wysoko-spinowego wzbudzonego termicznie, różnią się od stanu fotoindukowanego (widma obu stanów różnią się).

Wyniki badań układów typu „spin-crossover" w krysztale $[(TPA)Fe^{III}(TCC)]PF_6$, otrzymane przy pomocy układu pompa – sonda (superkontinuum), zostały zaprezentowane podczas konferencji ISSMMM w Argonne, USA. O istotnej wadze tych wyników świadczy fakt, że poster prezentujący te wyniki badań uzyskał II nagrodę w dziedzinie chemii.

**Badania nad kryształem organicznym z rodziny $(EDO\text{-}TTF)_2XF_6$**

Rodzina kryształów organicznych $(EDO\text{-}TTF)_2XF_6$ jest pierwszym tego typu układem, w którym zaobserwowano wydajny proces „metalizacji" w stanie nieprzewodzącym, pod wpływem ultraszybkiego impulsu laserowego. Kryształy te charakteryzują się przejściem fazowym metal – izolator pierwszego rodzaju. Informację na temat stanu kryształu otrzymuje się na podstawie zmian intensywności światła odbitego od powierzchni badanego ośrodka. Celem badań nad kryształami organicznymi $(EDO\text{-}TTF)_2SbF_6$ było znalezienie odpowiedzi na pytanie, czy w tym krysztale dochodzi do zmiany fazy pod wpływem impulsu laserowego oraz czy badane zjawisko ma charakter ciągły czy progowy. Autorzy jednej z pierwszych publikacji[13] na temat $(EDO\text{-}TTF)_2PF_6$ (kryształu należącego do tej samej rodziny związków co badany przeze mnie ośrodek) na podstawie badań optycznych przy użyciu układu pompa – sonda doszli do wniosku, że w krysztale znajdującym się w fazie izolującej doszło do zmiany fazy na metaliczną. W swojej pracy wskazali także, że istnieje pewna wartość progowa gęstości energii światła pompującego, przy której to zjawisko zachodzi. Odpowiedź układu stała się później przedmiotem prac teoretycznych i doświadczalnych przeprowadzonych przez grupę z Japonii.[9] Wyniki tych badań pozwalają zapostulować istnienie stanu, który nie ma właściwości fazy metalicznej, choć – ponieważ dochodzi do delokalizacji ładunku – nie może być nazywany fazą nieprzewodzącą.

Na podstawie danych otrzymanych w eksperymentach czasowo rozdzielczych, stwierdzono, że po wzbudzeniu dochodzi do powstania koherentnych fononów o częstościach występujących w fazie izolującej (otrzymanych na podstawie widm

Ramana). Brak zmiany częstości tychże fononów (ang. *„mode softening"*) w zależności od gęstości energii pompy, sugeruje, że zmiana ładunku w krysztale ma charakter lokalny, a nie zdelokalizowany. Z kolei podobne zmiany w częstościach wzbudzonych fononów w zależności od temperatury uzyskane na podstawie badań czasowo-rozdzielczych i Ramana wskazują, że nie dochodzi do zmiany fazy z nieprzewodzącej na metaliczną – nawet jeśli prowadzone są one w zakresie temperatur, gdzie obserwowana jest histereza. Indukowany stan został nazwany w niniejszej pracy fotoindukowanym stanem metastabilnym.

Wpływ na właściwości tego stanu ma temperatura, ponieważ podczas badań w temperaturach ciekłego helu (10 K), zaobserwowano fakt dłuższego zachowania spójnych drgań. W wyższych temperaturach, ruchy termiczne odgrywają większą rolę powodując szybszą dyssypację energii i dekoherencję wzbudzonych fononów.

Innym zagadnieniem, mającym zasadnicze znaczenie dla kontroli przejść fazowych przez impuls laserowy, jest pytanie o próg gęstości energii światła wzbudzającego, przy jakim dochodzi do powstania nowej fazy. W przypadku badanego kryształu wielkość progu, przy którym dochodzi do fotoindukowanych zmian jest bardzo mała lub nie ma jej wcale – co może mieć daleko idące skutki w opisie i wyjaśnieniu fenomenu indukowanych światłem przejść fazowych. Cytowana już wcześniej praca grupy z Japonii[9] także zawierała stwierdzenie, że w badania nad izostrukturalnym układem $(EDO\text{-}TTF)_2PF_6$ pokazują, że próg przy którym pojawia się nowa faza jest „zaniedbywalnie" mały. Ciekawostką jest fakt, że w bardzo niskich temperaturach (10 K), nie zaobserwowano sygnału świadczącego o występowaniu fazy fotoindukowanej. Jedynie widoczne były oscylacje pochodzące od wzbudzonych fononów.

**Układ pomiarowy do badań procesów nieodwracalnych**

W czasie prac nad układem pompa – sonda (supercontinuum) rozpoczęto także badania nad procesami nieodwracalnymi, zachodzącymi w metalach, wykorzystując tylko jeden impuls laserowy i zdolność kamery CCD do szybkiej rejestracji widm po każdej ekspozycji. Cienka warstwa złota była „wypalana" silną wiązką laserową (pompa). Monitorując zmianę współczynnika odbicia (reflektancji) od powierzchni złota, obserwowano procesy zachodzące podczas samego przejścia fazowego. Dodatkowo nie kompensowano efektu dyspersji grupowej światła (GVD), towarzyszącego generacji światła białego, pozwalając tym samym na dużą dyspersję czasową prędkości grupowej generowanego superkontinuum. Dzięki temu dynamika przejścia była dodatkowo analizowana także samym impulsem sondującym.

Mechanizm przejścia w złocie („*non-termal melting*"?) jest obecnie przedmiotem licznych naukowych dyskusji. Rozważane są różne hipotezy, w tym zjawisko ablacji, stopienia lub odparowania metalu.[14,15]

Zespół badawczy z Uniwersytetu Rennes 1 dzięki temu układowi pomiarowemu rozpoczął także badania procesów nieodwracalnych w kryształach. Do tej pory w tym celu używano układów monochromatycznych, co przy tak prężnie rozwijającej dziedzinie już było cennym źródłem informacji o układach poddanych ekstremalnym bodźcom zewnętrznym indukującym badany efekt. Zastosowanie światła białego pozwala na jeszcze szerszy wgląd w badane procesy. Na tym etapie badane są kryształy metali (m.in. złoto), w których odpowiedz w pomiarach odwracalnych (układ relaksuje do stanu podstawowego) jest znana, natomiast w przypadku pomiarów efektów nieodwracalnych (np. zniszczenie badanej warstwy) można uzyskać informację o dynamice przejścia fazowego.

Badania procesów nieodwracalnych pozwoliły także na istotne polepszenie stosowanej techniki pomiarowej („*single-shot*"). Z uwagi na pewne ograniczenia techniczne w pierwszej kolejności pokazano, że sygnał przychodzący po tzw. „Pierwszym" impulsie pompy rzeczywiście spowodował nieodwracalne zmiany na powierzchni metalu. Badania pod mikroskopem pozwoliły zaobserwować wygląd powierzchni po oddziaływaniu całej serii impulsów pompy. Przeprowadzone badania stacjonarne jednoznacznie pokazały, że kolejny, drugi impuls pompy wzbudza już substrat, na którym znajdowała się warstwa złota.

Wykorzystując dużą wartość współczynnika dyspersji prędkości grupowej odtworzona została zależność opóźnienia impulsu monitorującego względem pompy nieodwracalnie wypalającej złoto. Dalsze prace prowadzone będą w celu uzyskania odpowiedzi, jakie procesy są obecne w trakcie samego oddziaływania pompy z powierzchnią badanej próbki.

**Wnioski**

Wyniki badań przeprowadzonych w ramach niniejszej pracy zostały opublikowane w dwóch artykułach naukowych[2,12] oraz zostały zaprezentowane podczas licznych międzynarodowych konferencji i sympozjów. W fazie końcowej są artykuły, w których zawarte będą wyniki badań przejść fazowych w kryształach $(EDO\text{-}TTF)_2SbF_6$ oraz pomiarów procesów nieodwracalnych (prowadzone także w kryształach spinowych, nie zamieszczone w tej rozprawie). Rozwój technik badawczych związanych

ze skracaniem impulsu laserowego (do 10 fs), prowadzące do uzyskanie jeszcze lepszej zdolności rozdzielczej w układach pompa-sonda stanowią, kolejny ważny etap w badaniach właściwości „początkowej" fazy prowadzącej do powstania stanu fotoindukowanego. Wstępne pomiary zostały już wykonane, jednak ze względu na ich początkowy charakter nie zostały omówione w tej pracy.

**Bibliografia:**

[1] M. Maesato et al., *J. Phys. Conf. Series* **148,** 012004 (2009)
[2] M. Lorenc et al., *Phys. Rev. B* **85**, 054302 (2012)
[3] H. Cailleau et al., *Acta Phys. Pol.* **121**, 45 (2012)
[4] M. Lorenc et al., *J. Phys. Conf. Series* **148,** 012001 (2009)
[5] Naskręcki R. - *Femtosecond transient absorption spectroscopy. Photophysical study of the excited states of molecules and short - living individua*, Wydawnictwo Naukowe UAM, Poznan (2000)
[6] M. Lorenc, *PhD Thesis*, Poznan 2001, Poland
[7] P. Gütlich et al., *Top. Curr. Chem*. **233**, **234**, **235** (2004)
[8] N. Moisan, *PhD Thesis*, Rennes 2008, France
[9] K. Onda et al., *Phys. Rev*. Lett. **101,** 067403 (2008)
[10] M. Servol et al., in preparation
[11] H. Cailleau et al., *Acta Cryst. A* **66**, 189 (2010).
[12] W. Kaszub et al., *Acta Phys. Cryst. A* **121**, 325 (2012)
[13] M. Chollet et al. *Science* **307**, 86 (2005)
[14] P. Poulin et al., *Science* **313**, 1756 (2006)
[15] I. Lindberg, *Science* **310**, 5750 (2005)

Chapters 1&2:

# Introduction

# 1 Introduction

Photo-induced phase transitions constitute a new field of research focusing on today's challenges in science such as the control of emergent, nonlinear, coherent and far away from equilibrium phenomena[1]. Scientists voice their belief in the evolution of human's increasing mastery over the matter, which sooner or later should lead to the age of control over electronic movements during all sorts of reactions and transformation processes, in particular of materials. So, the new stakes in science reach beyond observation and pose another challenge, namely the control over the functionality of materials on the relevant lengths, time and energy scales.[2] This also requires the use of new experimental tools to explore matter on these relevant scales on which processes of interest take place. Thus, ultrafast femtosecond lasers and state-of-the-art detection systems, diversify the observation onto so far un-explored regions, probing matter at a level much deeper than the macroscopic averages studied up to now. Time-resolved experiments determine which elementary phenomena and mechanisms govern the transformations of matter triggered by an intense and ultra-short laser pulse. In general such photo-induced transformations in materialls are multiscale processes from the atomic or molecular scale to crystal scale. The time evolution exhibit successive steps, from coherent dynamics inducing deterministic atomic or molecular motions to stochastic kinetics towards quasi--equilibrium statistical state, giving new light to Feynman's definition of equilibrium "when all the fast things have happened but the slow things have not".[3,4,5,6]

Thanks to a tremendous progress in chemical engineering it is practically possible to design materials with properties "on demand". In parallel, ultrafast techniques are a formidable playground for controlling and exploring such complex systems, pushing further the frontiers of physics. My Ph.D. has been primarily dedicated to developing various ultrafast optical experiments in response to the above challenges.[1]

This work is focused on spin-crossover crystals[4] and organic conductors[10], in chapters 3 and 4, respectively. Ultrafast laser spectroscopy and complementary X-ray structural methods were utilized to observe spin state switching following laser pulse excitation, both on short and long time scales.[7] Laser pulses of time duration from 100 fs down to 40 fs were applied to follow the ultrafast dynamics of organic conductors. Such photo-induced spin-state switching[4,5] or coherent phonons processes[8] touch upon several fields of physics, such as statistical physics, condensed matter, magnetism etc.

In some materials, under certain conditions, photo-processes are irreversible, therefore single shot experiments are required.[9] Chapter 5 is devoted to irreversible phenomena occurring on a metallic surface after the impact of an ultrafast and intense laser pulse. In this chapter I touch upon a problem of non-thermal melting, which I used for benchmarking future investigations of irreversible transformations in crystals.

Chapter 6, entitled "Experimental", contains detailed description of the experimental setups including detection systems, laser synchronization electronics and the camera for single shot white light spectroscopy. Finally, a review on photo-induced phase transitions is given at the beginning of the manuscript. General conclusions at the end.

**References:**

[1] H. Cailleau et al., *Acta Phys. Pol. A* **121**, 297 (2012)
[2] G. Fleming et al., *Physics Today* **61**, 7, 28 (2008)
[3] R.P. Feynman, *"Statistical Mechanics"*, Benjamin (1972)
[4] M. Lorenc et al., *Phys. Rev. Lett.* **103**, 028301 (2009)
[5] E. Collet et al., *Acta Crystallogr. B* **65**, 474 (2009)
[6] H. Cailleau et al., *Acta Crystalogr. A* **66**, 189 (2010)
[7] M. Lorenc et al, *Phys. Rev. B* **85**, 054302 (2012)
[8] M. Chollet et al., *Science* **307**, 86 (2005)
[9] P.Poulin et al., *Science* **313,** 175 (2006)
[10] K. Sokolowski-Tinten et al., *Nature* **422**, 287 (2003)

# 2 Review

Photo-induced phase transitions (PIPT) is an emerging field in science which began almost twenty years ago with pioneering works on neutral-to-ionic instability in crystal carried out in Japan and spin-crossover solids in Europe. These works influenced researchers to explore these new areas, opening a new chapter in condensed matter physics and chemistry. PIPT concerns a number of different kinds of materials which cooperatively respond to light excitation by revealing interesting physical effects in matter.[1,2] Especially the phenomena in condensed matter, triggered by the ultrashort laser pulses, are promising for future applications and new theoretical concepts have to be established for describing them.[3,4,5]

Response from the matter to external stimuli plays a key role in understanding the mechanisms which drive materials to particular macroscopic state or phase. Progress in experimental techniques allows to observe spectacular and subtle, fast and ultrafast phenomena on different time scales.[6] However, not only the observation but also the control of materials on relevant time scale is a challenge set by contemporary science.[7,8,9]

The study of mechanisms occurring during photo-induced phase transitions has essentially two main goals, firstly exploring new way of controlling the functionality of materials, and secondly revealing fundamental physics underlying ultrafast cooperative driven phenomena.[3,4,5,10]

## 2.1 Ultrafast time resolved experimental technique and femto-chemistry

What is essential for experimental studies of ultrafast phenomena in PIPT, is the application of suitable techniques able to detect changes on physically pertinent time scales. Time resolved techniques based on two ultra short pulses, the first one to trigger the sample and the second one to monitor its response, are by far the most common. Although this idea is simple and quite old,[11] measuring ultrafast time scale proves far more difficult in reality, mostly because of complex and expensive technology. However, less technologically demanding steady state experiments and time resolved techniques with pulses longer than hundreds of picoseconds, thus detecting slower processes, are also important and often complement the ultrafast measurements.[12,13,14,15]

Two pulse experiments are commonly called pump-probe experiments. The pump induces a physical effect while the probe interrogates the studied system. Different time delays between those two pulses reproduce, after several shots for reversible photo-induced phenomena, a time course of the triggered phenomena (Fig. 2.1). Time resolution in such experiment depends on the time duration of the pulses. In stroboscopic measurements we should also pay attention for the repetition rate which is crucial for the sensitivity of the experimental setup.[16]

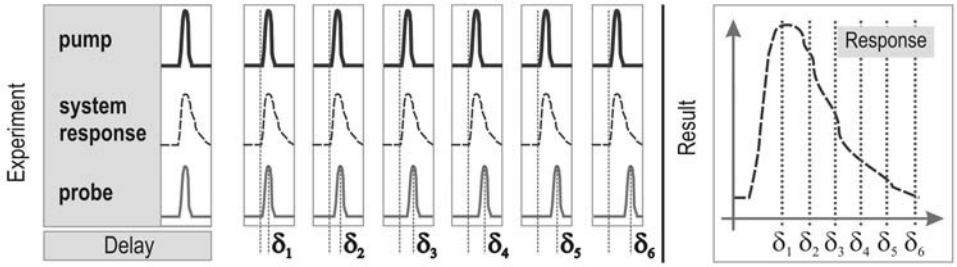


**Fig. 2.1:** Schematic illustration of time resolved pump-probe experiment. Pump and probe pulses are shown as dark and light grey peaks, respectively. Response from the sample was indicated as a grey peak – dashed line. Left side corresponds to idea of pump - probe experiment. Right side corresponds to result's diagram from experiment.

At present, this method is exploited in time-resolved laser spectroscopes where both pulses are optical,[17] or time-resolved X-ray diffraction which combine optical pump pulse from a laser with an X-ray probe pulse from a synchrotron,[18] FEL (Free Electron Laser) or other sources.[17,18,19] The latter gives the possibility to directly observe structural changes, dynamics of molecular switching, collective motions, etc.[20]

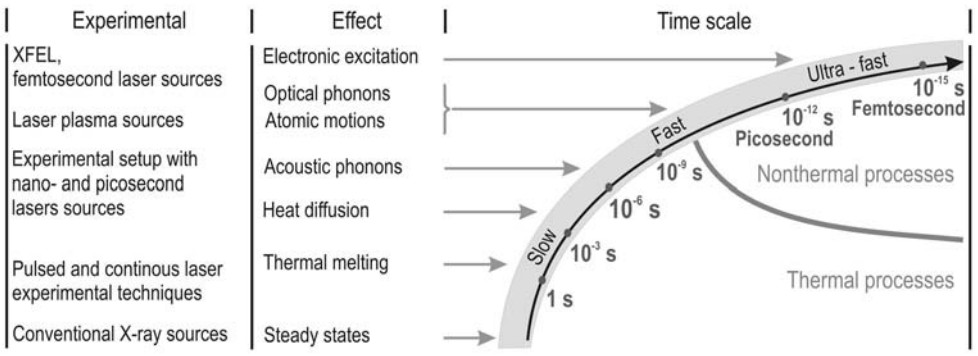


**Fig. 2.2:** Time scales and suitable experimental facilities for selected phenomena occurring in the solid state. Picture shown in [32,45].

Fig. 2.2 shows different processes occurring in matter, starting on femtoseconds and spa-nning a dozen of time decades, together with technology allowing reaching those time scales experimentally. Detailed discussion of experimental solutions exploited during the thesis work are included in chapter 6 (“Experimental”).

### 2.1.1 Femto-chemistry of gases and liquids as an example of “controlling” the matter

First step in research, focused on “light-controlling” the matter, was made in chemistry in the gas or liquid state. By using a train of femtosecond laser pulses and clocking a chemical reaction with two such pulses, the changes of interatomic potentials and the motion of atomic wavepackets could be followed in real-time.[21] Photo-excitation causes drastic effects in matter, such as breaking and making of covalent bonds. Driving a chemical reaction from transient states with appropriately timed femtosecond pulse[11] has been a dream starting to materialize. This field of research was awarded Nobel Prize in 1999 and since then, progress in ultrafast time-resolved experimental techniques has accelerated. This has allowed to explore not only “independent” molecules in liquid- or gas- phase, but also in the solid state, thus unveiling collective and cooperative phenomena triggered and observed in the ultra-short time scale.[11] The emergence of PIPT and its scientific appeal even spreads on the nanomaterials.[22,23,24]

### 2.1.2 Single shot episode

In an ideal situation there would be no need for time-averaging over repeated cycles of supposedly the same measurement. The issues of experimental stability, sample damage, or product accumulation, would no longer cause doubts and problems. The so-called “single shot” methods hold big promise in that matter as they give a possibility to observe irreversible transformations in the material for instance inside the hysteresis loop for a first-order phase transition.[21] Detailed discussion of this method is included in chapter 5 and 6.

## 2.2 The realization of femto-science for photo-induced phase transitions

In the solid state molecules are not independent and the interactions between them may lead to photo-induced collective and/or cooperative phenomena, unlike in the liquid or gase state. Applying ultrafast light pulse, response can be triggered from the whole system, manifested through macroscopic changes of optical, magnetic or structural properties.

Pioneering works on photo-induced phase transitions on ultrafast time scale date to the beginning of 90's, after observation of photo-induced neutral-to-ionic instability in a molecular crystal by Koshihara et al.[25] Inspired by this experiment, Y. Toyozawa, in the paper entitled "Condensation of relaxed excitons in static and dynamic phase transitions",[26] introduced a new conceptual view in condensed matter. PIPT has quickly spread over different directions, such as correlated electron systems, charge density waves, ultrafast magnetism,[27,28] chemical bonding or even molecular switching in materials.[29] PIPT now encompasses diversity of materials and experimental methods, from steady-state to time-resolved studies, extending the field of phenomena due to the interaction of light with matter.

PIPT in ultrafast time scale, where the triggering pulse is shorter than the time scale of atomic motions and also very intense with a macroscopic number of photons, relates to different dynamical processes far away from equilibrium – non thermal and extremely fast. Therefore the appropriate description of such cooperative phenomena resulting from the interaction between photons, electrons and lattice requires new theoretical approaches[30] involving quantum mechanics and condensed matter physics. In contrary to processes at thermal equilibrium, during ultrafast photo-induced processes the system is out of equilibrium with environment – energy transfer from photons occurs so quickly that molecular system cannot exchange with the environment. Nowadays this field is sill in evolution and new models are introduced.[31] One of the first and still the most common picture illustrating changes in energy levels was presented by Nasu[1,3,26,32] after Toyozawa's paper. Fig. 2.3 illustrates that PIPT leads to a completely new world for physics.

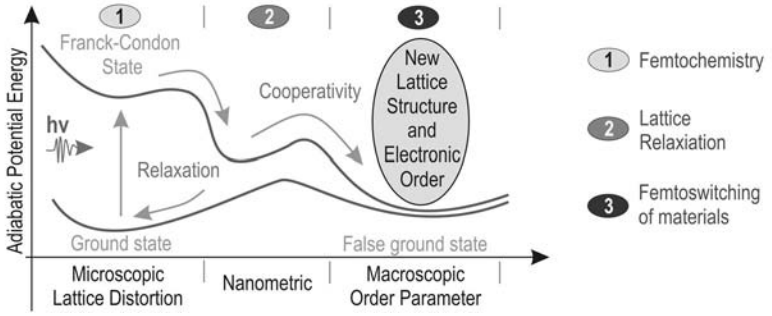


**FIG 2.3:** One of the first – and still actual – simple conceptual view of the behavior after ultrafast excitation – presented by Nasu in [1,3,26]. Nowadays small modification was made: nanometric scale became better known and spotted.

Within PIPT field, we can distinguish between two different types of materials where the photo-excited electronic state is either localized (for instance on a molecule) or delocalized (in case of itinerant electrons).

### 2.2.1 Localized electron excitation (on a molecule)

In the first case, photon absorption promotes a molecule to a localized excited state following structural molecular relaxation (conformational change, etc…). Initial dynamics of these transformations is related to the elementary intra-molecular atomic motions, and consequently it occurs on timescales of the relaxation of molecular vibrations, typically 10s of femtoseconds ($10^{-15}$s) to 1 picosecond ($10^{-12}$s). Contrary to photochemical processes, in which the phenomena are essentially independent, in cooperative systems there may exist strong interactions between excited molecules. When an ultrashort laser pulse simultaneously transforms sufficient number of molecules, these can interact and drive the system towards a new macroscopic phase on longer time scales. Spin-crossover phenomena illustrates well this case. Chapter 3 ("Spin crossover transformation…") in this work presents new results obtained on such kind of compounds.[33]

### 2.2.2 Delocalized electron excitation

In the second case, molecular systems are governed by collective phenomena, in which delocalized electronic excitations initiated by an ultrashort laser pulse perturb the entire atomic network. It can generate coherent collective atomic motions, such as optical phonons,[34] which can extremely rapidly lead to a new phase (100 fs – few ps). Delocalized excitation in Bi, inducing the softening of a coherent dimerization mode, illustrates well this situation.[35] However after the photo-excitation of itinerant electrons the structural relaxation may induce the formation of localized states which extend over a few molecules, as in TTF-CA. Spectacular gigantic response observed in a charge transfer molecular crystal $(EDO\text{-}TTF)_2PF_6$, which undergoes a metal-insulator phase transition at thermal equilibrium, provides a novel possibility.[36] A femtosecond laser pulse induces a "quasi-metallic" state from the insulating phase through an ultrafast process, within around 1ps. Generally speaking, all compounds related to charge transfer ordering are very promising candidates for ultrafast phase transitions. The chapter 4 devoted to $(EDO\text{-}TTF)_2SbF_6$, which is another member of the family, discusses the dynamics observed in such a molecular crystal after an ultrashort photo-excitation.

### 2.2.3 Coherence and cooperativity

Coherence is strongly connected with interaction between light and matter – playing key role especially in PIPT.[37,38] Molecular system in a solid state can provide coherent response via optical phonons. After excitation the collective wave fields vibrate in unison, in phase, and so they interfere. On macroscopic scale they drive drastic changes of physical properties. Recent studies on quasi-metallic photo-induced materials[31,36] show interesting behavior of photo-response and completely new electronic order.

At thermal equilibrium, the system is driven through a phase transition due to cooperative interactions between constituents of the molecular system. Cooperativity in such systems is also important in an out of equilibrium photo-induced phase transition.[12] Molecules, or other entities, interacting after excitation lead to nonlinearities due to positive feedback and showing through self amplified phenomena, thus introducing complexity away from equilibrium. In other words, the simultaneous absorption of a huge number of photons induces more than the sum over individual events.

### 2.2.4 Far away from equilibrium

New sources for ultrafast diffraction experiments, either with electrons or X-rays, ultrafast laser spectroscopies, or their combination, allow to perform experiments on materials far away from equilibrium, when intense laser pulse with a macroscopic number of photons can force the material into new electronic order.[3] PIPT are a perfect illustration of far away from equilibrium phenomena.[39,40,41,42] When materials are forced towards a new macroscopic state by a laser, the possibility to direct its functionality became real. This phenomena is of great interest in today's science.[7,43,44]

References:

[1] K. Nasu (Ed.), *"Photoinduced Phase Transitions"*, World Scientific (2004)
[2] M. Kuwata-Gonokami et al., *J. Phys. Soc. Jpn.* **75**, 011001 (2006)
[3] K. Nasu (Ed.), *"Relaxation of Excited State and Photo-Induced phase Transitions"*, Spr. (1997)
[4] E. Hanamura et al., *J. Phys. Soc. Jpn.* **56**, 2080 (1987)
[5] N. Nagaosa et al., *Phys. Rev. B* **39**, 4472 (1989)
[6] G. Galle et al., *Chem. Phys. Lett*. **500**, 18 (2010)
[7] G. Fleming et al., *Physics Today* **61**, 7, 28 (2008)
[8] M. Buron, E. Collet (Eds), *J. Phys.: Conf. Series* **21**, (2005)

[9] K. Tanaka, T. Ogawa, H. Hashimoto, S. Koshihara (Eds.), *J. Phys.: Conf. Series* **148** (2009)
[10] A.L. Semenov, *JETP* **87**, 764 (1998)
[11] A. Zewail, *"Femtochmistry: Ultafast Dynamics of the Chemical Bond"*, World Scientific (1994)
[12] A. Bousseksou et al., *Chem. Soc. Rev.*, **40**, 3310 (2011)
[13] J-A. Real et al., *J. Am. Chem. Soc.* **114**, 4650 (1992)
[14] D. Boinnard et al., *Inorg. Chem.* **33**, 271 (1994)
[15] S. Bedoui et al., *Chem. Phys. Lett.* **499**, 94 (2010)
[16] R. Naskręcki - *Femtosecond transient absorption spectroscopy. Photophysical study of the excited states of molecules and short - living individua*, Wydawnictwo Naukowe UAM, Poznan 2000
[17] M. Lorenc et al., *Phys. Rev. B* **85**, 054302 (2012)
[18] E. Collet (Ed.), *Special Issue Acta. Cryst. A* **66**, 133 (2010)
[19] Newsletter, *Swiss Physical Soc.* **23**, 4, 16, (2008)
[20] P. Stampfli et al., *Phys. Rev. B* **42**, 7163 (1990)
[21] P.Poulin et al., *Science* **313**, 175 (2006)
[22] K. Koshino et al., *J. Phys. Soc. Jpn*. **67**, 2174 (1998)
[23] S. Iwai et al., *Phys. Rev. Lett*. **96**, 057403 (2006)
[24] S. Koshihara et al., *J. Phys. Chem*. *B* **103**, 2592 (1999)
[25] S. Koshihara et al., *Phys. Rev*. *B* **42**, 6853 (1990)
[26] Y. Toyozawa, *Solid State Commun*. **84**, 255 (1992)
[27] N. Brefuel et al., *Angew. Chem. Int. Ed*. **48**, 9304 (2009)
[28] K. Kamide et al., *Phys. Rev. Lett*. **105**, 056401 (2010)
[29] M. Lorenc et al., *Phys. Rev. Lett*. **103**, 028301 (2009)
[30] K. Yonemitsu et al., *Phys. Rep*. **465**, 1 (2008)
[31] K. Onda et al., *Phys. Rev. Lett*. **101**, 067403 (2008)
[32] N. Moisan, *PhD Thesis,* Rennes 2008, France
[33] H. Cailleau, *Acta Crystalogr*. A66, 189 (2010)
[34] S. Iwai, et al., *Phys. Rev. Lett*., 96, 057403 (2006)
[35] T. K. Cheng, et al., *Appl. Phys. Lett*. **10**, 1004 (1990)
[36] M. Chollet et al., *Science* **307**, 86 (2005)
[37] K. Sokolowski-Titen et al., *Nature* **422**, 287 (2003)
[38] K. Ishida et al., *Phys. Rev. Lett*. **100**, 116403 (2008)
[39] O. Sato et al., *Science* **272**, 704 (1996)
[40] S. Ohkoshi et al., *Nature Chem*. **2**, 539 (2010)
[41] M. Sollogoub et al., *Chem. Biol. Chem.* **9**, 1201 (2008)
[42] S.H. Stroglatz, *"Nonlinear Dynamics and Chaos"*, Westview (2000)
[43] R.D. Averitt, *Nature Phys*. **6**, 639 (2010)
[44] R. Yusupov et al., *Nature Phys*. **6**, 681 (2010)
[45] E. Trzop, *PhD Thesis*, Wrocław - Rennes 2009

Chapter 3:

# Spin-crossover transformation induce by the laser pulse

# 3 Spin crossover transformation induce by laser pulse

Spin crossover (SCO) compounds have been known for 80 years.[1] They exhibit two distinguished spin states, called high and low spin state (HS, LS respectively). The change of molecular spin state is accompanied with a colour change and structural reorganization. In the solid state, they have been intensively studied since the 60's because of their unusual and interesting cooperative switching under external stimuli such as temperature, pressure and even light. Therefore, spin crossover crystals very quickly became a prototype of bistable materials, since the system may exhibit two stable macroscopic states for the same set of control parameters.[2,3,4] New possibilities and progress in chemistry in creating compounds with desired features (in example new switchable nanomaterials) stimulate further experiments in such materials.

Besides conventional techniques, including stationary photo-irradiation, new time resolved pump-probe experiments are carried out to investigate the elementary mechanisms of the photo induced transformation in spin crossover compounds. These sophisticated techniques are essentially based on the use of two ultra-short pulses (pump and probe). They allow to excite macroscopic number of molecules in a ultrafast time scale (comparable to the time scale of electronic transitions and shorter than this one of atomic motions), and trigger coherently a sequence of processes starting from the molecule and ending on the macroscopic entity – the crystal.[5,6] While a laser pulse probes the optical properties of a material related to transitions of valence electrons, an X-ray pulse probes all electrons and so the atomic positions in real-time, thereby providing snapshots of the structure of a material. The combination of the two kinds of probes unveils an otherwise fragmented picture of transformation and relaxation, starting from the molecule and ending on the crystal scale.

Photo-induced spin changes hold big promise for application purposes, what was proved by numerous studies. In optical measurements beside continuous wave (cw) and nanosecond lasers, the femtosecond laser pulses are a formidable gateway to the control over materials. Excitation of a single SCO compounds by femtosecond laser pulse can switch the molecular state from LS to HS, involving different processes and timescales in the out-of-equilibrium dynamics. Molecular system after such light excitation is an interesting object of study for scientist, because it connects differrent domains of physics and chemistry beyond equilibrium properties.

Dynamics appear after femtosecond pulse excitation span vast timescale, starting from sub-picosecond non-thermal molecular transformation to slower thermal switching and diffusive heating through the lattice on the microsecond timescale. Study relied on combined time-resolved X-ray diffraction with ultrafast laser spectroscopy[5-8] permitted to lay ground for the interpretation of the out-of-equilibrium spin-crossover structural dynamics, including the equilibrium recovery.

During my Ph.D. the bottom line of the study in SCO compounds was to cover several decades of time in one experiment also in wide spectroscopic region. In general idea of pump – probe experiments, the femtosecond laser pulse initiates an electronic transition and the second delayed laser pulse monitors the transient absorbance of the crystal. Using two different experimental setups, one with monochromatic beams and second one with supercontinuum pulses, relying on two different gating schemes for probing the time evolution of the material response to light excitation, while utilizing the same laser source, we were able to cover ten time decades beginning with femtosecond Franck-Condon (FC) excitation and ending with microsecond relaxation.

### 3.1 Theory describing SCO complexes

First thermal spin transition, described as "unusual magnetic properties of iron (III)" complex, was discovered by Cambi et al., in 1931.[8,9] Since then, new compounds with different metal atoms i.e. Fe(II, III), Co(II, III), Mn(II) were synthesized in the form of single crystals or microcrystalline powders of different grain size, even down to few nanometers.[4] Structural analysis with X-rays showed that in most cases spin crossover (SCO) materials, made from transition metal ions of $3d^4$ – $3d^7$ electronic configuration, are arranged into pseudo-octahedral complexes with a surrounding ligand ($3d^8$ electrons are present too, but in lower symmetry). SCO crystals exhibit a change in spin state accompanied by an electronic redistribution (colour changes) and a change of molecular geometry (especially of metal to ligand bond length and of unit cell volume).[10] At equilibrium this change can be controlled by temperature and pressure, and obviously by the magnetic field. Fig. 3.1 shows a schematic picture of the change of spin state, in particular the potential energy surface as a function of the metal-ligand bond length. Therefore the structural change from LS to HS state is manifested by the increasing of volume of the unit cell, causing pressure effects inside the crystal and also change of vibrational frequencies, causing entropy driven effects (in addition to that due to the change of spin multiplicity).[1,3,4]

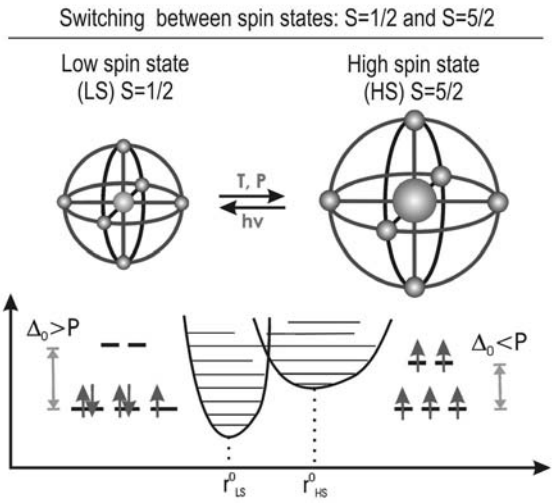


**Fig. 3.1:** Schematic picture of the change of spin state, corresponds to changes in potential energy surface as a function of the metal-ligand bond-length.
Spin change is manifested as a increasing of the volume of the unit cell.[5]

A few years after Cambi's observation of SCO phenomena, a theoretical explanation was proposed and because of the origin of the interaction between metal and ligand, it was referred to as the crystal field theory (CFT), or later the ligand field theory (LFT). Electronic configuration of a free ion and the same molecule in a lattice may be different (Fig. 3.2) and depends on the crystalline structure. In SCO complexes consisting of metal ions and arranged into octahedral (or pseudo-octahedral) ligand geometry, spin transition occurs on 3d orbital. Depending on whether the crystal field energy is lower or higher than the pairing energy (Hund) between electrons, electrons can fill higher ($e_g$, HS state) or lower ($t_{2g}$, LS state) energy levels – and in consequence, respectively S = 2 or S = 0 for Fe II.[11, 12]

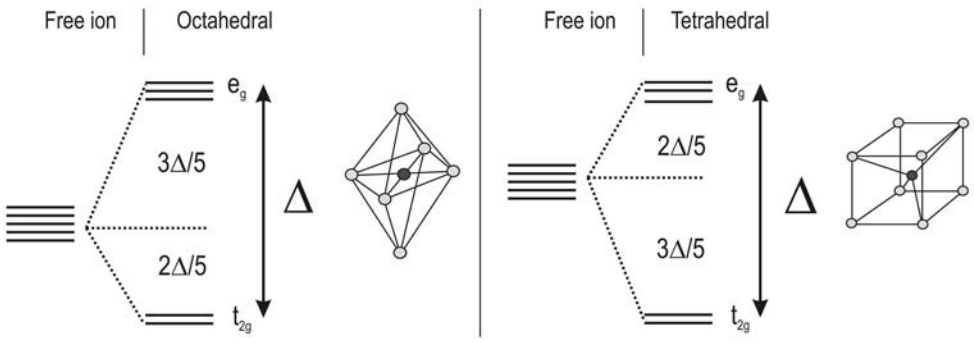


**Fig 3.2**: Electronic configuration of free ion and molecule in the lattice (in two octahedral and tetrahedral structure). Picture taken from [11].

### 3.1.1 Thermal spin state switching

In a phenomenological model describing relative stability of HS and LS state at thermal equilibrium one can use as thermodynamic potential the Gibbs free energy in crystal which is the relevant one when temperature T and pressure P are the thermodynamic control parameters. At atmospheric pressure, this free energy G becomes very similar to the Helmholtz free energy F because the quantity PΔV is small.

Generally spin state switching in spin-crossover materials occurs with no symmetry change (isostuctural transformation). In the solid state, the concentration of HS molecules (noted as $n_{HS}$) plays then the same role in spin transition as the particle density does in liquid to gas phase transition. In this case, we can plot a (P,T) phase diagram and define a critical point C (Fig. 3.3). Above C the spin state switching is gradual (crossover phenomenon) and below C strong cooperative effects take over and a first order transition occurs. Dotted line represents metastability limits below the critical temperature $T_c$, and above $T_c$, the temperature $T_{1/2}$, where $n_{LS} = n_{HS} = 0{,}5$. The black line in Fig. 3.3 corresponds to a situation when two phases of the same symmetry coexist in the crystal and the first order phase transition taking place along this line is manifested by an abrupt change of $n_{HS}$ at temperature $T_0$.

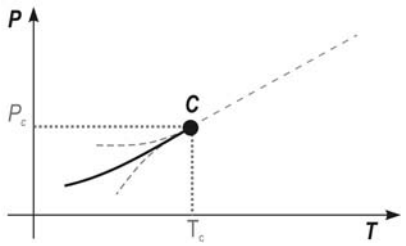


**Fig. 3.3:** Plot (P, T) with defined point C. Above C the spin state switching is gradual. Below C we can observe stronger cooperative effects corresponding to first order phase transition. Black line corresponds to coexistence of two phases with the same symmetry.[13]

As mentioned above – switching between two states with temperature can be understood in terms of phenomenological models used to describe a non-ideal solution within mean field approach (Bragg-Williams). The free energy potential, which is expressed as a function of the internal variable $n_{HS}$, takes into accounts the cooperative interactions between molecules. Using this phenomelogical approach the shape of the thermodynamic potential can change determining at every temperature the crystal's stable, unstable and metastable states. Moreover, the strength of cooperative interactions governs the type of transformation in spin-crossover compounds: abrupt, i.e. a first order phase transition, or gradual, i.e. a crossover change which is no longer a phase transition. In other words, the critical temperature $T_c$ is more or less higher with respect to $T_{1/2}$.[1,4,14]

A similar phenomenological approach can be given by a mapping in terms of an Ising model, where the two molecular states on lattice site are characterized by an Ising variable $s_i = +1$ for HS, and $s_i = -1$ for LS state. Since 1970 an Ising-like model has been presented by Wajnflasz and Pick[13,15] and further developed to express the Hamiltonian:

(3.1) $$H = -\sum_{<i,j>} J s_i s_j - h \sum_i s_i,$$

where J is a coupling parameter, expressing cooperative interactions between sites, $< i , j >$ denoting that the sum is only over the first neighboring pairs in order to simplify. Parameter $h$ is a temperature dependent "field".[13] Indeed it includes not only the site energy difference $\Delta$ between HS and LS states but also an entropy term related to the degeneracy ratio $g$ between HS and LS states with the contribution of electronic and vibrational degrees of freedom:

(3.2) $$h = -\frac{1}{2}(\Delta - k_B T \ln g), \text{ where}$$

(3.3) $$g = \frac{g_{HS}}{g_{LS}}.$$

More precisely, the above degeneracy factor takes into account the spin multiplicity and possible orbital degeneracy in material, and even changes of vibrational frequencies. This vibrational part is dominant, since $g$ is generally of the few 10s and cannot explained by the spin and electronic degeneracy's (of the order of few units). The change of vibrational frequencies is related to the changes of molecular geometry and cell volume. Actually, the above model is called an Ising – like model because the unconventional temperature dependence of the "field". So in other words, it is an effective Hamiltonian for the slow degrees of freedom of HS-LS configuration based on the integration of fast electronic and vibrational degrees of freedom. It is a physical origin of the inclusion of the entropic effect of vibrations and electronic multiplicity. For the above model we can easily define the two specific temperatures: the temperature $T_{1/2}$ where the "field" $h$ vanishes, given by the relation:

(3.4) $$T_{1/2} = \frac{\Delta}{k_B \ln g}$$

and the critical temperature $T_C$:

(3.5) $$T_C = \frac{qJ}{k_B},$$

where $J$ denotes the strength of the cooperative interaction, and $q$ is the number of first neighbours (a coordination number of the spin crossover units).

In the universal (*T*,*h*) phase diagram of the Ising model (Fig. 3.4a)), the coexistence line is located on the horizontal axis $h = 0$ and ends on the critical point characterized by the temperature $T_c$. Below $T_c$ we recognize a first order phase transition when *h(T)* crosses this horizontal axis in an oblique way. At temperatures above $T_c$ we can observe crossover phenomenon with gradual evolution of $n_{HS}$ around $T_{1/2}$, where the number of molecules in HS state is equal to the number of molecules in LS state.

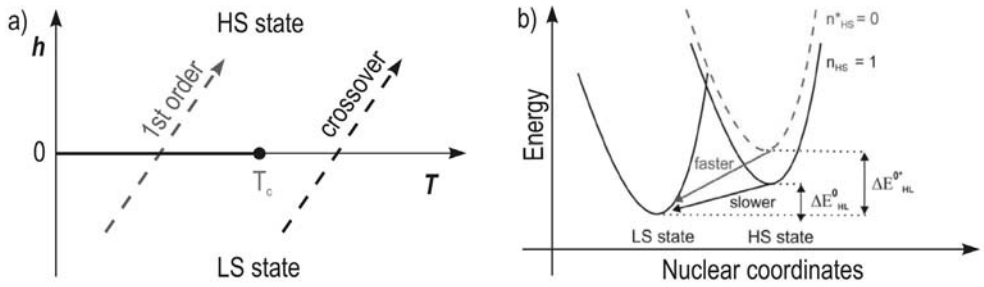


**Fig. 3.4: a)** Universal diagram (*T, h*) of the Ising model. Coexistence of the phases correspond to black line located on the horizontal axis h. **b)** Diagram of dependence between nuclear coordinates and energy correspond to them in case of LS and HS states.

By applying the Ising – like model, we can express the free energy per molecule (in an N-element system) *f* within the mean field approximation:

$$(3.6)\quad f = \frac{F}{N} = \frac{1}{2}(\Delta - kT\ln\frac{g_{HS}}{g_{LS}}\cdot(2n_{HS}-1) - [n_{HS} + \ln n_{HS} + (1-n_{HS})\ln(1-n_{HS})]\cdot k_B T + E_{int}\ ,$$

where $E_{int}$ is the intermolecular interaction energy expressed according to this approximation as:

$$(3.7)\quad E_{int} \approx -Jm^2\ ,$$

where *m* is the "net" magnetization per "spin" $m = \langle s_i \rangle$. Taking (3.6) and (3.7) we can find that average concentration of molecules in HS state, is related to *m* by $n_{HS} = 0.5 \times (m + 1)$.

An illustrative way to describe cooperative effects using mean field approach, showing well the feedback effect on each site of the active medium, is to use a Hamiltonian $H_i$ which concerns the site $i$:

(3.8) $$H_i = -h_{eff} \cdot s_i, \text{ where}$$

(3.9) $$h_{eff} = h + qJm.$$

This definition shows the dependence with $n_{HS}$ of the effective energy of the HS state (Fig. 3.4b). This is the "molecular field" approach introduced by Pierre Weiss a century ago as an explanation of origin of ferromagnetism. The evolution of the order parameter $\eta = m = 2n_{HS} - 1$ on the phase transition line ($h = 0$) can be described within the frame of phenomenological Landau theory. The Landau free energy on the horizontal axis ($h = 0$) can be presented in the form of:

(3.10) $$F(T,\eta) = F_0(T) + \frac{1}{2}A(T - T_C)\eta^2 + \frac{1}{4}B\eta^4 + \frac{1}{6}C\eta^6 + \cdots,$$

where $A$, $B$ and $C$ are constants. Off this horizontal axis a "field" term $-h\eta$ has to be added.[13-20]

### 3.1.2 Photo-excitation

Direct optical transitions from LS to HS quantum states are forbidden. To bypass this limitation, a higher lying ligand to metal charge transfer (LMCT) state is directly populated from the LS ground state, so that its relaxation opens pathway to metastable HS state (Fig. 3.4b and 3.5). Energy of a single laser photon can be 10-100 times higher than the energy difference between spin states being inter-switched. The excess energy imparted by the photon on the molecule is dissipated through incoherently excitations of the molecular and lattice vibrational modes.

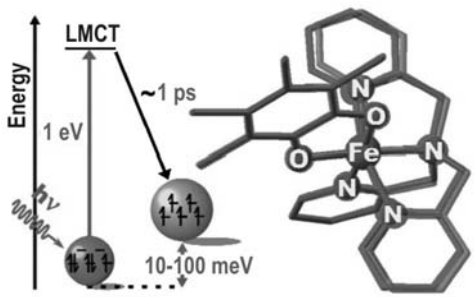


**Fig. 3.5:** Scheme of the spin-crossover relaxation due to excitation by the femtosecond pulse. Energy of the pulse is much higher than the energy difference between LS and HS states. Due to recent results we can say that relaxation time from the LMCT state is around 300 fs. Picture taken from [21].

### 3.2 Description of the [(TPA)Fe$^{III}$(TCC)]PF$_6$ crystals

In this part was presented analysis and data mostly published in [5,22], but filled by other interesting conclusions after analysis. [(TPA)Fe$^{III}$(TCC)]PF$_6$ (*Compound* ***1***) and [(TPA)Fe$^{III}$(TCC)]SbF$_6$ (*Compound* **2**), are spin crossover compounds* prototypes of molecular bistability in solid state. Both belong to a family of catecholate iron (III) complexes,[23, 24, 25] and can be synthesized in two polymorphs: monoclinic or orthorhombic form distinguishable in macroscopic scale by their shape and colour.

*Compound 1* and *Compound 2* were synthesized by the group of Marie-Laure Boillot in Orsay (Universite Paris Sud 11).[5, 26] During my Ph.D. studies we made experiments mostly on the monoclinic polymorph of *Compound 1* and several experiments on both polymorphs of *Compound 2* (monoclinic and orthorhombic form). Monoclinic polymorph[26] of both compounds, undergoes spin-crossover from a low temperature LS (S = 1/2) state to a high temperature HS (S = 5/2) state. Thermal conversion is centred at $T_{1/2}$ = 214 K and $T_{1/2}$ = 237 K, for *Compound 1* and *Compound 2*, respectively, where the HS molecular fraction $X_{HS}$ = 1/2 (Fig. 3.6).

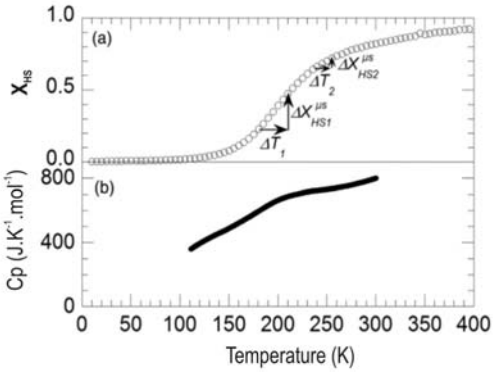


**Fig 3.6:** Magnetic measurements on [(TPA)Fe$^{III}$(TCC)]PF$_6$. **a)** SQUID – measurements, **b)** DSC studies. On the plot **a)** was also indicated changes of HS fraction due to temperature changes. Plot published in [5].

Switching between these two states occurs under external stimuli such as temperature, pressure or light.[1,27] Because the variation of $X_{HS}$ drives significant changes of magnetic susceptibility $\chi_m$ (actually $\chi_m T$), optical properties, and intramolecular structure (mainly around the central Fe ion), changes in fraction of HS and LS molecules constituting the crystal can be detected using variety of techniques. Among them: time-resolved X-ray diffraction and femtosecond optical spectroscopy, optical transmission or reflectance measurements and also steady state magnetic measurements (SQUID) – used during this work and described below.

* (TPA = tri (2-pyridyl-methyl)-amine and TCC = 3,4,5,6-tetrachlorocatecholate)

The equilibrium structures of LS and HS state and the preparation procedure of orthorhombic polymorph of *Compound 1* were described by Floquet et al.[24] Using near-IR nanosecond laser pulse Enachescu et al.,[21] have studied the photo excitation of this compound at different temperatures (Fig. 3.7). Relaxation time falls on the ms scale and is similar to other compounds of the Fe(III) family studied elsewhere[29] and this is a necessary condition for undertaking stroboscopic measuremnts.[1] First experimental evidences of HS state generation with a femtosecond pulse were recently reported for the *Com-pound 1*.[1,5,6,26] In this last study, the time course of the optical transmission on two specific wavelengths, one on either side of the isosbestic point – occur on wide spec-tral range plot, presented more detailed below, revealed the photogeneration of high-spin at $T_{1/2}$ within 300 fs following excitation. Little though could be inferred on the spectral behavior of the transient species.[5, 22]

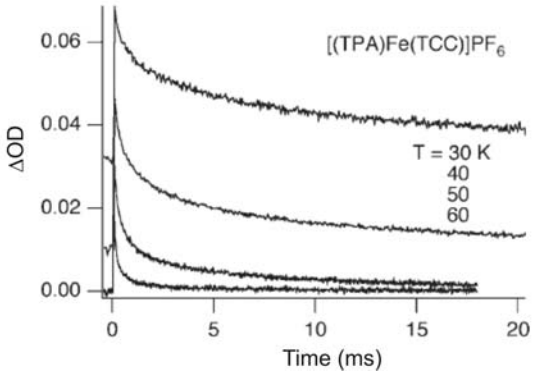


**Fig. 3.7:** Changes in OD at different temperatures, after nanosecond relaxation in spin-crossover [(TPA)Fe$^{III}$(TCC)]PF$_6$ crystal. Obtained results was published in [13,24].

### 3.2.1 SQUID measurements and DSC studies

The single crystals of the monoclinic polymorph of [(TPA)Fe$^{III}$(TCC)]PF$_6$ (*Compound* ***1***) and [(TPA)Fe$^{III}$(TCC)]SbF$_6$ (*Compound* **2**) were characterized earlier by magnetic susceptibility, optical, and – *Compound 1* – also by DSC measurements and by X-ray diffraction measurements.[5,6,26] Both of them were characterizes by a gradual spin transition showed on the SQUID measurements plot. Both HS and LS states are magnetic. The measured $\chi mT$ product of molar magnetic susceptibility $\chi m$ and temperature $T$, is consider as a sum over fractions of pure HS (defined as $X_{HS}$) and pure LS (defined as: $1 - X_{HS}$) states, changing with Temperature $T$ according to formula:

$$\chi_m T = X_{HS}(T) \times (\chi_m T)_{HS} + (1 - X_{HS}(T)) \times (\chi_m T)_{LS}. \quad (3.11)$$

Temperature dependence of $X_{HS}$ can be extracted, from the $\chi mT$ product, obtained with SQUID measurements. Fig. 3.6 confirms a gradual thermal spin-crossover from

the high temperature, HS state to the low temperature, LS state for both compounds. Temperature $T_{1/2}$ in *Compound 1* is equal to 214 K (monoclinic)[26] and in *Compound 2* $T_{1/2}$ is around 234 K.[6]

In differential scanning calorimetry (DSC) on *Compound 1* observed anomaly in heat capacity, reminiscent of weakly cooperative systems,[29] has to be due to the spin-crossover. These measurements were performed with a Thermal Analysis Q2000 type calorimeter in the temperature range from 100 K to 300 K and at different heating rates from 2 to 10 K/min. For these experiments were used single crystals, at the same size, as in time resolved optical studies. Heat capacity versus temperature dependence was shown in Fig. 3.6 and its indicate as a broad anomaly, between 140 K and 280 K with midpoint at 214 K. The temperature scan starts at $X_{HS} \approx 0$ and stops at $X_{HS} \approx 1$. The anomaly shows a hump centered around $T_{1/2}$.

Another evidence of a gradual transition due to SQUID measurements can be found on Fig. 3.8: the comparison between results obtained with different techniques: magnetic susceptibility,[24] optical reflectivity and transmission[26] and X-ray diffraction[13,21,26] – for $[(TPA)Fe^{III}(TCC)]PF_6$. This is also interesting example and good argue for optical experiments.

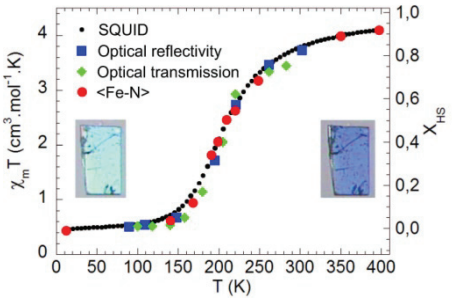


**Fig. 3.8:** Comparison between results obtained by different methods such as SQUID, optical reflectivity and transmission, X- Ray studies (bond-length). Picture published in [13, 30].

### 3.2.2 Optical steady state measurements

Using a microscope equipped with polarizers we could observe changes of OD due to temperature of the crystal and polarization of the light. OD of the material, depends on the polarization of the light with regard to the crystal axis. For instance, results from the microscope for *Compound 2* for one polarization axis were presented on Fig. 3.9.

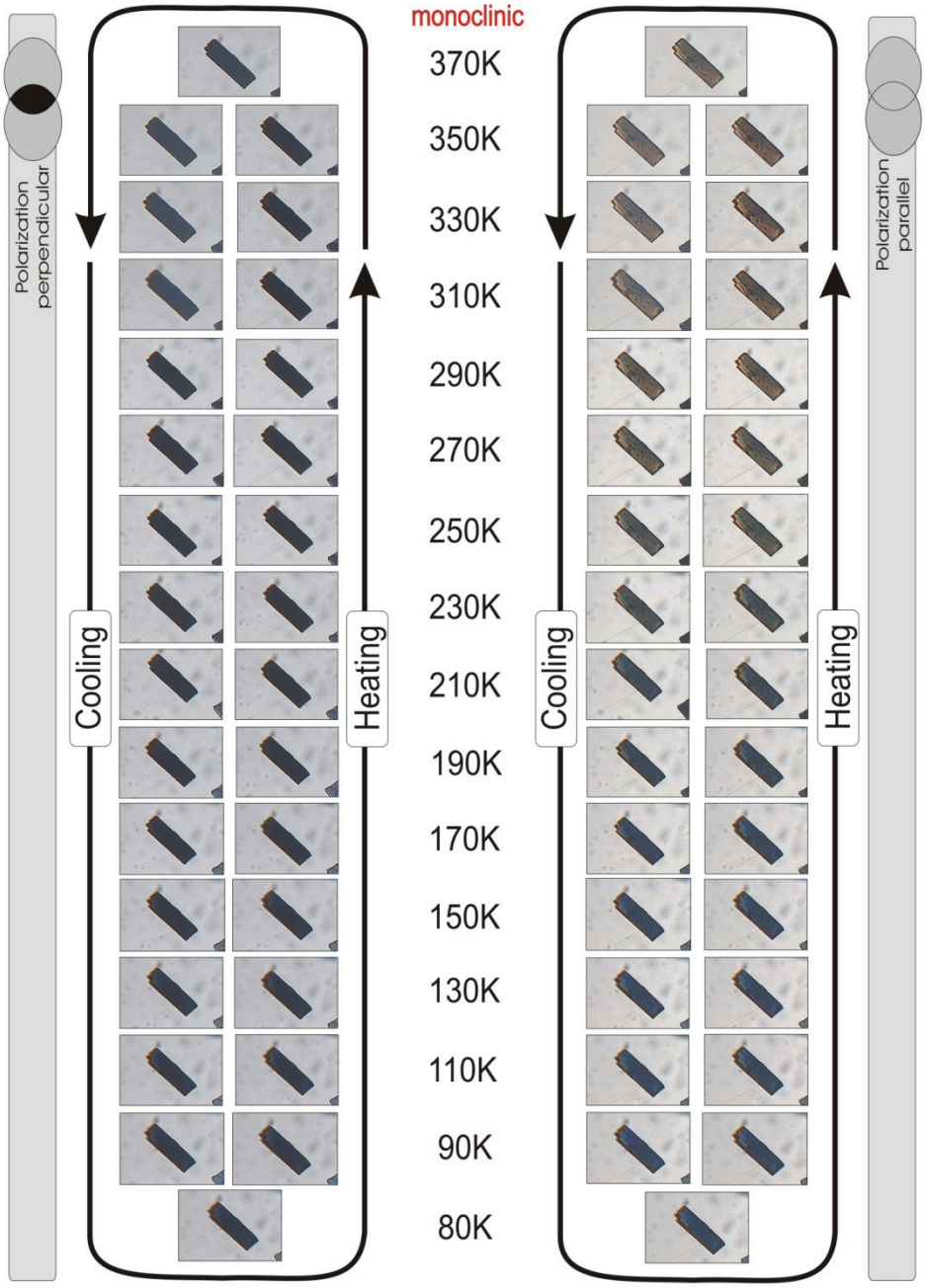


**Fig. 3.9:** Changes of the absorbance of the crystal (monoclinic form of *Compound 2*) due to temperature. Pictures were taken using polarizers parallel and perpendicular to the long crystal axis ***a***.

One of the experimental goals of my Ph.D. work was to develop a new experimental setup with broadband detection (supercontinuum), for pulsed probing on the ultrafast time scale, and complement it with a steady-state option for temperature dependence studies. This setup was useful not only for time-resolved but also for "steady state" measurements, where pump was shut down. Description of the principles of experimental setup presented below corresponds to steady state and time resolved options.

Femtosecond pulses were delivered by the laser (Mira, Coherent) directly from the amplifier (Legend Elite II, Coherent) and chopped down mechanically to 500 Hz. Supercontinuum was generated in sapphire plate and after re-collimation it was split into two beams: signal and reference. Ratio between them was checked before each experiment. Signal beam was focused on the crystal sample, and finally occur on the coupler. Typical size of the spot was around 80 x 80 μm$^2$. Reference beam was directed to second coupler. Detection system consist CCD camera (Princeton Instruments, PIXIS 100) and spectrometer (Acton Research Corp., SPECTRAPro 2500i). In "steady state" measurements we collect 10000 spectra of signal beam and reference beam. During analysis we simply divide signal beam and reference beam with respect to ratio of each wavelength recorded before experiment. In the last step of analysis, spectra were averaged. More detailed discussion about experimental setup with white light was put into chapter 6, entitled "Experimental". As a consequence, we obtain temperature dependence of optical density of the crystal:

(3.12) $$\Delta OD(\lambda,\tau) = \log\frac{I_o(\lambda)}{I(\lambda,\tau)}$$

We collect several spectra at different temperatures and compared them with observations made under microscope at the same polarization. Fig. 3.10 shows VIS spectra taken starting at 90 K up to 330 K, which means temperatures at which the fraction of HS forms varies between 0 to 0.9, respectively. According to the SQUID experiment (Fig. 3.6), almost 100% of HS should be obtained at 400 K.

Obtained spectra corresponds to gradual change of the spin-crossover evolution, and show absorption bands, characteristics for catecholato-to iron(III) charge transfer transitions observed in [6,22]. Below 530 nm, the optical density increases due to tem-perature but above 530 nm, OD exhibits the opposite behavior.

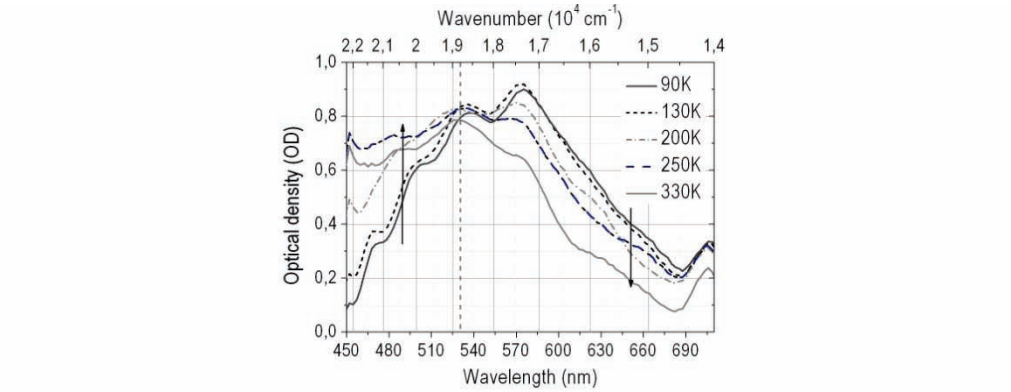


**Fig. 3.10:** Temperature dependence of the optical density of the monoclinic polymorph of the spin-cross-over crystal [(TPA)$Fe^{III}$(TCC)]$PF_6$. Results published in [22].

Using broad bandwidth spectroscopy, we could observe interesting features corresponding to the vibrational contribution riding on the electronic spectrum and clearly seen at low temperatures and gradually smeared out in higher temperatures. It becomes hardly distinguishable at 330 K. The interval between neighboring sub bands is ca. 1270-1310 cm-1 and can be tentatively attributed to a vibrational mode strongly coupled to the optical LMCT transition, very likely the CO stretching mode of the TCC ring at 1274 $cm^{-1}$.[23, 31]

During analysis we tried to apply a simple model in which we assume that the spectrum at any temperature is a sum of LS and HS spectra weighted by their respective molecular fractions. Because we couldn't obtain spectra at 400 K, we extracted HS fraction from the temperature dependence of magnetic measurements. HS spectrum is obtained from measurements at 330 K after correcting for a 0.1 contribution from LS state, directly obtained at 90 K.[22]

Presented on Fig. 3.11 the LS and HS spectra together with the spectrum at $T_{1/2}$ (lower plot) shows, that there is no such combination of HS and LS fraction, which can accurately reproduce the spectrum at the intermediate temperature. Even when fractions are hugely exaggerated for best match, what was showed at upper plots in Fig. 3.11. This suggests that spectral kinetics of electronic transitions are affected by temperature of the electronic states between which these transitions occur. Band narrowing and spectral shifts are possible consequences of thermal excitation/relaxation of vibrational modes of molecules. We touch upon this point in the following section.[5, 22]

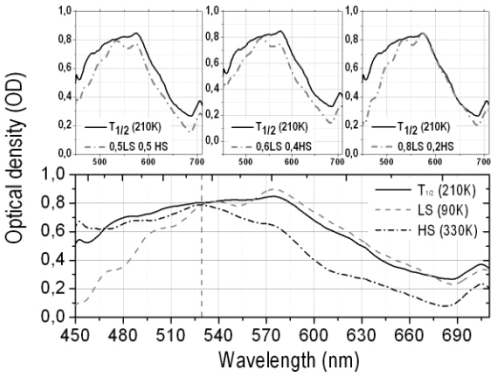


**Fig. 3.11:** Temperature dependence for three different temperatures of the optical density of the spin-crossover crystal [(TPA)$Fe^{III}$(TCC)]$PF_6$ (lower panel). Upper panel corresponds to different combinations of LS and HS states spectra. Results published in [22].

### 3.2.3 Time-resolved studies

Time resolved studies were made using a variety of combinations of pump-probe techniques. In this field we prepared standard pump-probe experimental setup with two monochromatic wavelength, experimental setup with white light as a probe beam and combination of two laser amplifiers working in synchrony to cover wide time scale of response from the sample. All experimental setup were recently reported in [5,6,22]. Detailed discussion about experimental setup was included in chapter 6, thus below I presented shortly main information about techniques, which we were using.

*Two color experimental setup*. At the beginning we prepared time resolved experimental setup with two monochromatic wavelength and Lock –In amplifier detection. As a laser source we were using femtosecond laser (Legend USP) which delivered 40 fs pulses with 1 kHz frequency. Demand wavelength was obtained due to two OPA systems (Topas C, Coherent). Pump was chopped down to 500 Hz and delayed to the probe by the optical delay line (Newport IMS linear stage). Probe beam was splitted before occurrence on the sample into two parts in a ratio 95/5. Weaker beam was triggering signal on the reference photodiode (canal B on the Lock-In). Stronger one was a signal beam (canal A on the Lock-In). In spin-crossover experiments we were measuring changes of optical density (ΔOD). Lock in detection technique allow to collect data with high sensitivity.

In our experiments we were using heterodyne configuration, A-B (described in detail in experimental section), so we manage to obtain changes with sensitivity around $10^{-5}$. Pump and probe beam were focused on the sample non-collinearly by two lenses with different focal length (probe: 200 mm, pump: 500 mm), but with similar distance between them and the sample around 200 mm. We wanted to be sure, that whole volume, where effect is induce, is covered by the probe. Typical size of the crystal was 200×150 $\mu m^2$, and the spot of the probe beam was 80 μm and 80 μm.

*Two color experimental setup in long time scale*. Dynamics of longer time delays was able to detect by two lasers working in synchrony. It means that pump beam was taken from one amplifier, but second amplifiers delivered probe beam. To change wavelength we were using two OPAs. Synchronization of both amplifiers was realizing by delay generator controls signals delivered to the amplifiers. Detection part was the same as in system described above and also some. Rest of experimental setup was the same as described experimental setup in earlier point of this paragraph.

*White light, pump-probe experimental setup*. In time resolved experiments with supercontinuum we were using setup described in 3.3.2, but in this case we add pump beam, which was part of the light inducing the white light. Femtosecond pulses were delivered from the Legend Elite II (pulse duration: 100 fs) and chopped down to 250 Hz.

Typically we were using in both kinds of experiments excitation densities of the pump beam up to 100 $\mu J/mm^2$, because of the damage threshold found at 300 $\mu J/mm^2$. First study of *Compound 1* in ultrafast time scale showed that during the thermal crossover, between 90 K and 300 K, the transmission at 600 nm increases by a factor of approximately 2[5,26] (Fig. 3.10). Using white light spectroscopy – presented above – we confirm this feature. Although $T_{1/2}$ in *Compound 1* is equal to 214 K, our optical pump-probe experiments were performed at a temperature of the cryogenic flow put up 200 K to take into account heating effects of the laser beam and to obtain in the sample fractions of HS and LS molecules close to 0.5. Using technique with monochromatic beams we were able to observe dynamics of relaxation of the spin states. White light pump-probe experimental setup complete this knowledge to whole spectra.[5,6,22]

The experimental observables in experiments with monochromatic beams are $\Delta I(t)$ and $I$, differential intensity and absolute intensity of transmitted probe light, respectively. On Fig. 3.12 we can distinguish clearly identified 3 steps. Excitation energy corresponds to 40 μJ/mm² ( ≈2 photons/100 molecules in the bulk crystal).

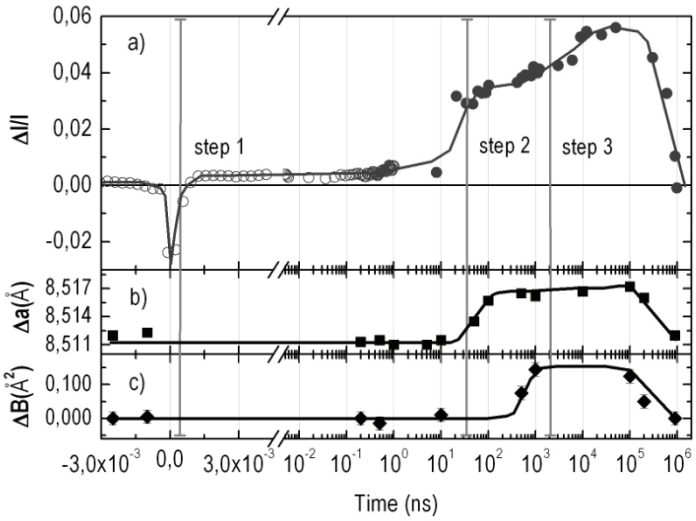


**Fig. 3.12:** Results obtained by the synchronized lasers. Plot **a)** corresponds to detected changes in optical density of the crystal. Indicated steps are explained in the text. (**b** and **c**) correspond to X-ray diffraction data obtained by 300 ps pulses from synchrotron source. Figure published in [6].

First step can be defined as the femtosecond photo-switching between molecular LS and HS states through ultra-fast population of Ligand-to-Metal Charge-Transfer (LMCT) state(s).[5,6,26] After the transient peak a long-lived increase of optical transmission is observed due to the molecular relaxation populating HS state. In nanoscale (10 s ns) a second step takes place, characterized by even bigger variation of optical transmission, while crystal volume expands as observed by time-resolved X-ray diffraction.[6,7,22] This step will be hereafter referred to as elastic step. Last, third step, associated with additional variation of optical transmission, occurs on microsecond timescale. This part, is referred to as thermal step since it is connected with heating effects discussed in [5,6].

Spectra (signal and reference) obtained from time resolved measurements were recorded independently so we had possibility to observe each "frame" from the measurement and compare it. Care was taken to avoid outliers in averaging and to ensure the correct sign of the optical density change. Typically 10 000 spectra were

collected, averaged and analysed using double reference method to improve the signal to noise ratio.[6,22] In experimental setup, pump occur every two times of probe pulses with 250 Hz and 500 Hz, respectively. To observe photo response we had to divide relative intensities of spectra from the sample with and without pump, as follows:

(3.13) $$\Delta OD = \log_{10} \frac{\frac{I^o_{pr}}{I^o_{ref}}}{\frac{I^p_{pr}}{I^p_{ref}}} = \log_{10}\left(\frac{I^o_{pr}}{I^p_{pr}} \cdot \frac{I^p_{ref}}{I^o_{ref}}\right)$$

where $I^P_{pr}$ corresponds to spectra obtained with pump, $I^0_{pr}$ – spectra obtained without pump, $I^P_{ref}$ and $I^0_{ref}$ corresponds to reference spectra collected simultaneously with $I^P_{pr}$ and $I^0_{pr}$, respectively. In brief, we can conclude that without effect induced by the pump, using double reference method the signal equals one, and the scatter around this value results from statistical noise. If pump induced effect, the signal deviates from one and the amplitude of this deviation should be directly proportional to the quantum efficiency of the photo-induced process.[6,22,32]

### 3.2.3.1 Femtosecond photo-switching step

In time-resolved experiments with two monochromatic wavelengths we were observing increase value of transmitted intensity of the probing light, what was showed on Fig. 3.12. Observed phenomena corresponds to transient absorption peak of the LMCT state.[5,6,22] Our studies of the dynamics showed, that this peak vanishes with time-constant of 300 fs, but time resolution of the experimental setup didn't allow to exclude the exponential population of the HS state from the LMCT state, or more complicated cascading relaxation of the LMCT states. Estimated value of the time decay is in good agreement with timescales reported for spin-crossover molecules in the orthorhombic polymorph[30] of the *Compound 1* and also in solution.[6, 22, 33-37] This shows that this step proceeds at the molecular scale. Fraction of photo-converted to the HS state molecules (defined as: $\Delta X_{HS}$) can be estimated according to:

(3.14) $$\Delta X_{HS} = \frac{\Delta OD(t)}{\Delta OD} \quad \text{, where}$$

(3.15) $$\Delta OD(t) = -\log\left(\frac{\Delta I(t)}{I} + 1\right) .$$

$\Delta OD(t)$ is a variation after laser excitation at a given time $t$, and $\Delta OD$ is the change of optical density between 10 K ($X_{HS} = 0$) and 400 K ($X_{HS} = 1$). Due to these considerations, after analysis of Fig. 3.12 we can calculate the fraction of molecules at HS state after excitation ($\Delta X_{HS}^{fs}$). After LMCT peak $\Delta X_{HS}^{fs} \approx 0.007$ and remains unchanged over to 1 – 10 ns, (Fig. 3.12). The time-resolved diffraction studies have demonstrated that this process occurs at constant crystalline volume.[6, 22]

Using pump – white light probe experimental setup we wanted to elicit the nature of photogenerated molecules in the metastable state observed in femtosecond photoswitching in spectral range. On the Fig. 3.13 – lower panel, was shown time-resolved spectra taken at different time delays. Spectrum of the probe light was chirped, what means, that there was a 1.6 ps time lag between the leading edge at 710 nm and the trailing edge at the 480 nm. Chirp was measured (10 fs/THz) and was consistent with the group velocity dispersion. That means also, that time zero during measurements was the coincidence with the pump of the furthermost trailing wavelength of recorded white light.[6, 22]

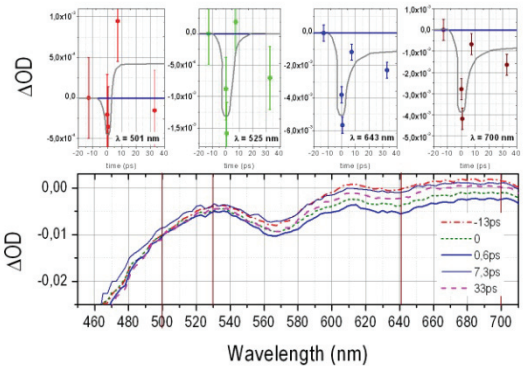


**Fig. 3.13:** Time resolved spectra at different time delays taken at 180 K was shown on the lower panel; After analysis its spectral cuts at selected wavelengths (full circles) with errors bars from experiment, solid lines drawn to help guide the eye was shown above.[22]

Spectra at negative delay (-13 ps) was taken twice to estimate the accuracy of collected data and due to chirp, we know, that probe precedes the pump in this measurements. The longest delay recorded at 33 ps ensures that the chirp (1.6 ps) has negligible effect on the spectrum, what was also demonstrated in the system which does not evolve in the 2 ps – 1 ns time window.[1, 6] It was reason why we didn't correct amplitudes due to chirp. Measurements made with 33 ps delay also ensures that the LMCT relaxation didn't affect the probed system.

On upper panel on the Fig. 3.13 was indicated wavelengths corresponds to sections, examine by the monochromatic detection. For simplicity, all plots was offset to zero for negative delays. White light spectroscopy proves resolving power to monitor even minute changes of HS state concentration (< 1%, from [1,22]). Previous measurements made with monochromatic wavelength[5,6] confirmed that at longer wavelengths, the change of OD strongly depends on increasing fraction of HS state molecules in contrary to shorter wavelengths, where the blue side of the spectrum is less conclusive than its red side. OD change stay with agreement with the change expected during thermal spin-crossover, showed on Fig. 3.10**,** where upon crossover from LS state to HS state the crystal becomes more transparent to light above 530 nm and more opaque below this wavelength. Seen of Fig. 3.10 the cut at 525 nm, was earlier identified as the isosbestic point of the spectral kinetics and shows only variations around time zero.[6, 22]

### 3.2.3.2 Nanosecond elastic step

Comparable to time resolved experiments, time-resolved X-ray diffraction revealed that at ≈ 50 ns[6,7] volume expansion of unit cell takes place, as was shown on Fig. 3.12 b,c. During nanosecond elastic step due to optical measurements we can observe, that the transmission increases again ($\Delta I/I$ between -3 ps and 100 ns, Fig. 3.12), and now the change is bigger than in the femtosecond photo-switching step. From eq. (3.14) we can calculate fraction of converted HS molecules $\Delta X_{HS}^{ns} \approx 0.042$. Excellent signal to noise ratio of the Lock-in detection allow to detect increase of HS molecules barely seen by time-resolved X-ray diffraction between 1 ns – 100 ns.[6, 22, 21]

Intensity of transmitted light can be affected by the number of HS molecules in the laser probed volume. Optical observable more accurately describes the density of HS molecules, rather than their absolute number.[6] During spin crossover transition crystalline volume expands, but the laser beam cross-section on the sample does not vary during the measurements, what means, that certain molecules should be leaving the area delimited by the beam cross-section, and as a result, it's affecting $\Delta I(t)$. Taking ratio between number of molecules in the volume probed along $\boldsymbol{b}$ in only unit cell surfaces $(\boldsymbol{a}\times\boldsymbol{c})/(\boldsymbol{a}'\times\boldsymbol{c}')$, perpendicular to $\boldsymbol{b}$, before and after excitation respectively, should be interesting.[5,6]

Data presented in [21] taken between $t < 0$ and 100 ns showed that $\boldsymbol{a}$ is changing from 8.511 Å to 8.516 Å and $\boldsymbol{c}$ changes from 9.266 Å to 9.270 Å. Dimension $\boldsymbol{b}$ changes too, but its contribution cancels out when the laser beam propagates parallel to $\boldsymbol{b}$.

Result of division $(\boldsymbol{a}\times\boldsymbol{c})/(\boldsymbol{a}'\times\boldsymbol{c}')$ has the value ≈ 0.001. The unit cell increase would lead to an HS molecular density decrease. Therefore the magnitude of $\Delta X_{HS}$ observed at 100 ns (~ 0,042), is unambiguously associated with additional conversion from LS to HS states, whose mechanism must be of elastic origin.[6,22]

### 3.2.3.3 Microsecond thermal step

In third step in microsecond time scale, we can observe the biggest value of optical transition, clearly seen on Fig. 3.12**.** Optical energy of the pump (≈ 1.55 eV) applied to switch the states from LS to HS with comparison between energy difference (10 s meV) these states is much higher. Rest of the energy transforms into non-radiative relaxation, which generates heat dissipating rapidly over the lattice vibrational modes. Pump pulse causes also gradients of local temperature due to finite penetration depth, and the temperature homogeneity in the crystal is restored only on microsecond timescale. In time-resolved X-ray studies heat diffusion through the sample is related to time dependence if the Debye-Waller[5,6] factor, which slow evolution can be seen on Fig. 3.12**.** The temperature homogenization leads to an increase of the average temperature, experimentally observed through increase of the Debye-Waller factor, $\Delta B$ between $t < 0$ and $t > 0$ (Fig. 3.12). The resulting heating drives thermal population of HS state.[6] Indeed this thermal activated process becomes efficient on a similar time-scale, as it can be extrapolated from previous optical studies to estimate the energy barrier height. From the amplitude of the signal at 1-10 μs observed in Fig. 3.12, we can conclude that the HS fraction at the microsecond step, $\Delta X_{HS}^{\mu s}$, reaches ≈ 0.09 at 200 K[5].

### 3.2.3.4 Relaxation dynamics

On Fig. 3.12 we can observe within approximately 1 ms the HS relaxation. It corresponds to the recovery of thermal equilibrium with the environment, the cryogenic flow. Before this time the sample does not exchange heat with its environment (adiabatic process). Indeed, the time scale for this exchange of heat is a macroscopic process governed by the heat capacity of the sample and the ratio of exchange be-tween its surface and the cryogenic flow. An estimation of this time scale shows it is in the range 10-100 ms, a little more than 1 ms. This explains the quasi-steady heating already discussed.[6] Previously reported structural study are in agreement with presented measurements of optical reflectance,[6] but at these study the time resolution was limited by the integration time as long as 100 μs and was sensitive only to the changes on

crystal surface only. Our study time resolution is better than 100 μs and optical transmission rather than reflectivity can in principle probe propagation and diffusion processes in all three dimensions of the crystal.[6]

### 3.2.3.4 Temperature dependence

Fig. 3.14 presents time resolved differential intensity ($\Delta I/I$) of light transmitted by the crystal at different temperatures between -50 ns to 1 ms. Within ≈ 50 ns sudden increase of transmission associated with lattice expansion is clearly seen at all temperatures, despite of the fact, that time-scan intervals of ≈ 13 ns precludes accumulating not more that several time delays between 1 ns (end of translation stage) and 13 ns. Between 100 K to 160 K, $\Delta I/I$ grows, but at 180 K and above, $\Delta I/I$ diminishes. This behaviour contrasts with the ultrafast dynamics, whose temperature dependence of $\Delta X_{HS}^{fs}(T)$ exhibits gradual decrease with temperature rising (Fig. 3.15a).[6]

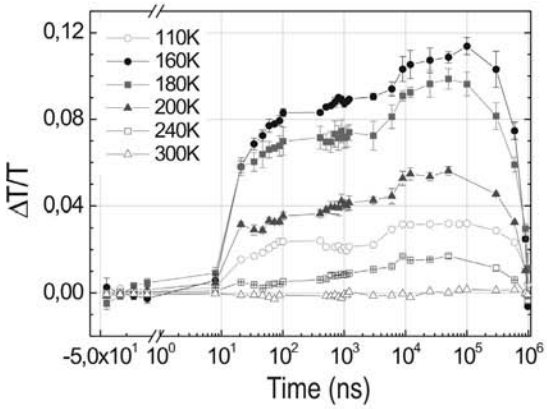


**Fig. 3.14:** Temperature dependence of the nano- and microsecond step of the spin-crossover compound – $[(TPA)Fe^{III}(TCC)]PF_6$. Sudden increase of transmission corresponds to lattice expansion – clearly seen at all temperatures. Figure published in [6].

On Fig. 3.14 at ≈ 100 μs, we can observe maximum in the thermal step. We convert using eq. 3.14 signal measured at 100 μs to $\Delta X_{HS}^{\mu s}$ and saw that conversion is particularly efficient around $T_{1/2}$, defined as 214 K due to SQUID measurements on *Compound 1* (shown on Fig. 3.6), but closer inspection of maximum show shift to temperatures below $T_{1/2}$ and under presented excitation conditions (Fig. 3.15 b).[6] Thermal conversion has its maximum around 160 K, where $\Delta X_{HS}^{\mu s} \approx 0.15$.

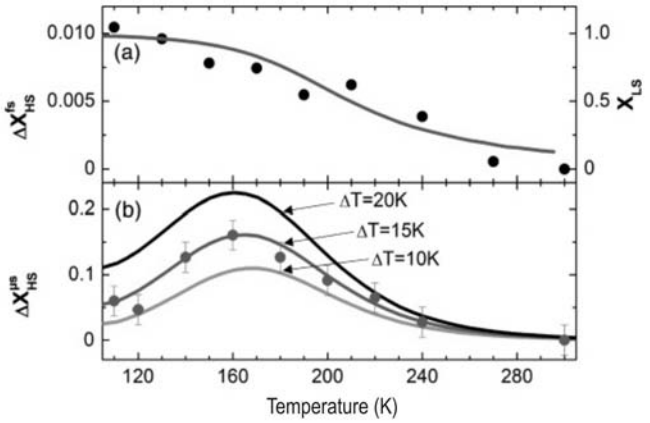


**Fig. 3.15: a)** Temperature dependence of the molecular fraction $\Delta X_{HS}^{fs}$ of the HS molecules with comparison of HS molecules switched in microsecond scale ($\Delta X_{HS}^{\mu s}$), presented on the lower panel (**b**). Discussion presented also further in § 3.3.3. Figure published in [6].

### 3.3 Discussion of the observed dynamics

Discussion about results obtained by the optical pump-probe experiments and comparable X-ray diffraction measurements was divided also in three parts corresponding to each step. A major new feature was the significant increase of switched molecules observed during elastic step. Additionally, we tried to interpret on nano- and microsecond time scale, the temperature dependencies of the switched molecular fraction of HS molecules (showed on Fig. 3.15).

#### 3.3.1 Femtosecond step

Optical studies showed on Fig. 3.15 a, shows that fraction of the photo-induced HS state molecules ($\Delta X_{HS}^{fs}$) decreases when temperature increases. This suggests that number of molecules follows with out of the temperature dependence of the LS fraction $X_{LS}$ ($X_{LS} = 1\text{-}X_{HS}$), in agreement with the fact that pump laser photons were absorbed mainly by LS molecules. Relaxation to HS state can go on different relaxation pathways, which are possible quantum mechanically. Oscillator strength between transient states corresponds to the efficiency of a given pathway. What is worth to say, although possibly complex ultrafast pathway, there is still proportional dependence the fraction of photo-switched HS molecules to $X_{LS}(T)$. Description of those results is a prove, the observed spin switching in femtosecond time scale takes place at the molecular scale via intra-molecular processes.[6]

In white light studies in femtosecond step major goal was to obtain a snapshot of a pure photo-generated HS state, and see difference between them and HS state of the 100% HS crystal converted thermally. On Fig. 3.16 was shown comparison between optical density spectrum of the thermally populated HS state put on the spectrum taken 33 ps following excitation. Optical density spectrum was scaled down by a factor of 171 (Fig. 3.16 a). Under the spectra we put residual signal taken from the difference between of pairs of photo-induced and thermally generated HS state. Both spectra have very similar shapes but their spectral weight is not exactly the same throughout the VIS range.[6,22] To better understanding this phenomena, we compared two spectra of a crystal in 100% LS state, but at different temperatures. We did it, because the fraction of LS molecules at 90 K and 130 K are practically the same and almost 1[22] due to magnetic measurements (SQUID). The comparison between those spectra shown some difference which cannot be explained only by intensity fluctuations. Superimposed spectra are also not affected by the molecular concentration. Between 90 K and 130 K of LS state spectra shows similar deviation as those of photo-induced HS state at 180 K from thermally converted HS state at 330 K – except region between 610 – 660 nm.[22]

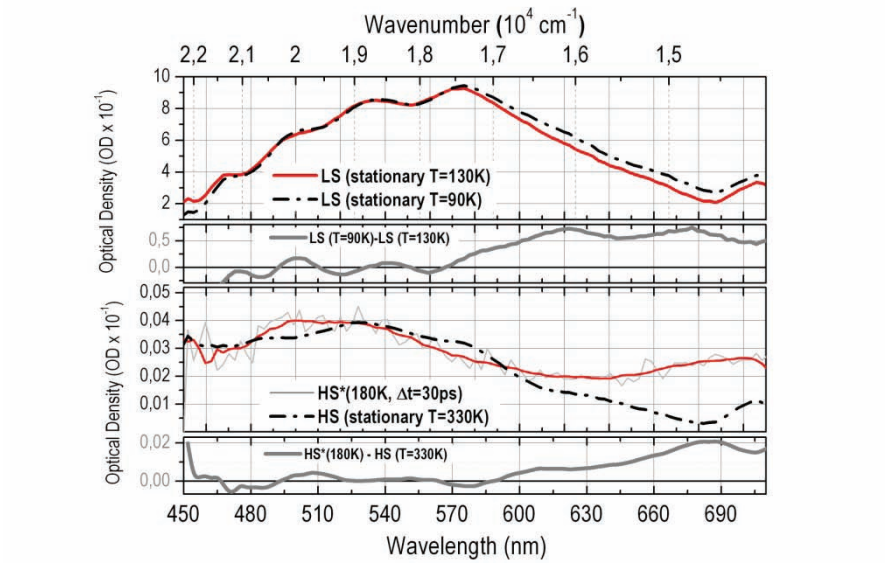


**Fig. 3.16: a)** Superposition of LS spectra taken at 90 K (black dashed) and 130 K (red solid), the residual difference signal is shown as a black curve below; **b)** Time-resolved spectrum taken at 180 K and 30 ps after laser excitation (red solid line) superimposed on HS spectrum at 330 K (black dashed), the residue shown below b). Figure published in [22].

Explanation, which we believe, is supported by the deviations, due to thermal population of vibrational levels of the electronic potentials of the HS and LS states. Answer for this hypothesis could be solved by dedicated studies using far-IR techniques. We conjecture that the HS state generated at 180 K by a laser pulse can be vibrationally cooled within 30 ps. In the photo-induced state, "cold" HS molecules are has got less thermal energy than when the crystal is 100% HS at temperatures above 330 K.[22]

### 3.3.2 Nanosecond elastic step

Elastic step observed during spin state transformations driven by a light pulse has already been explained by experimental[1,6] and theoretical works dedicated to such systems.[33,34] LS and HS states are characterized by different molecular volumes (in the HS state, volume is bigger than in LS) and elastic nature of cooperative interactions between them are supported by this fact.[6,22] After excitation nonradiative energy from the relaxed molecules is dissipating during femtosecond step, but crystal will expand because of the swelling of photo-switched molecules. The volume expansion process involves propagation over relatively long distances, so it is not instantaneous and can be described in two steps. In the first one occurs at constant volume and as a result we can defined the increase of pressure, which will relax due to volume expand in step two. During volume expansion a nonlinear propagation of the pressure front over macroscopic dimensions occur, with the speed similar to sound velocity in solids.[21] Simple picture of this idea can be presented as a shock-wave fashion, which limits the propagation of the relaxed pressure and force molecules to swell and so to switch from LS to HS states. What is more, this phenomena of the propagation of molecular volume expansion in real-time was demonstrated in liquids with picoseconds X-ray pulses.[35] Therefore if we take crystal dimensions, we can calculate, that described above phenomena should occur in timescale to few nanoseconds – what is in agreement with Fig. 3.12. At the nanosecond and microsecond steps, we can also observe maximum at 160 K of the evolution of $\Delta I/I$ – showed on Fig. 3.14. In this elastic step we can precise velocity (a few km/s) of the collective response in the dynamical out-of-equilibrium process – leading to self-amplified switching between spin states, which is very different, a few orders of magnitude faster, to the diffusive dynamics of the phase front propagation during the thermal transformation in similar systems which is measured in the μm/s range.[36]

### 3.3.3 Microsecond thermal step

Occurrence of significant thermal switching was supported by the results presented in § 3.2.3.3 and already discussed in previous works.[37-39] We want to compare the temperature dependence of $\Delta X_{HS}^{\mu s}$ obtained in § 3.2.3.3 with the values calculated from a simple model based on both heat capacity, $C_p$(T) and $X_{LS}(T)$. We start with evaluation of energy – $E_a$, deposited on the crystal by the laser pump which is mainly absorbed by the LS molecules (that's what we consider in § 3.3.1) and can be expressed by:

(3.16) $$E_a \propto X_{LS} \times E$$

We have to remember, that most of $E_a$ is redistributed over internal vibration modes and phonons during the relaxation process from the LMCT states to the lower lying HS state. Present heat at this stage will cause, that at macroscopic scale crystal's temperature $\Delta T$ will arise. Heat will be diffused on a timescale determined by diffusivity (typically $10^{-6}\,m^2s^{-1}$). Relates between $C_p$ to $E_a$ express the following formula:

(3.17) $$E_a(T) = \int_T^{T+\Delta T} C_p(T)dT$$

Taking eqs. (3.16) and (3.17), and assuming by a small temperature increase $\Delta T$, the following we can express $E_a(T)$:

(3.18) $$E_a(T) = C_p(T) \times \Delta T = A \times X_{LS}(T)$$

where $A$ factors in all temperature independent quantities, including $E$. To calculate the temperature dependence ΔT, we can take it from (3.18):

(3.19) $$\Delta T = A \times X_{LS}(T)/C_p(T)$$

This temperature increase $\Delta T$ is directly at the origin to the increase of the HS fraction $\Delta X_{HS}^{\mu s}(T)$ on the microsecond timescale. Expression for $\Delta X_{HS}^{\mu s}(T)$ is as follows:

(3.20) $$\Delta X_{HS}^{\mu s}(T) = X_{HS}(T+\Delta T) - X_{HS}(T) = X_{HS}(T + A \times X_{LS}(T)/C_p(T)) - X_{HS}(T)$$

The temperature dependencies of $C_p$, $X_{LS}$ and $X_{HS}$, are known from experiment (Fig. 3.6), so from eq. (3.20) we can take the temperature dependence of $\Delta X_{HS}^{\mu s}$. For the discussion we took three values of factor A (which determined the temperature $\Delta T$).

We chose arbitrarily temperature at 180 K, where we make three trials for $\Delta T$ of 10 K, 15 K and 20 K. Temperature dependence of $\Delta X_{HS}^{\mu s}(T)$ is plotted in Fig. 3.15b. The best experimental data match of $\Delta X_{HS}^{\mu s}(T)$ is obtained with $A$ scaled to $\Delta T$ of 15 K. Results of $\Delta X_{HS}^{\mu s}$ showed on Fig. 3.15b, with chosen $A$, agree with the experimental data. $\Delta X_{HS}^{\mu s}$ has got at 165 K with a value of 0.15. Comparable time resolved with similar excitation conditions and $A$ factor, yielded $\Delta X_{HS}^{\mu s} \approx 0.1$ at 180 K, which agrees with our model calculation too.[6]

An interesting aspect of this model is that it also explains why the maximum of $\Delta X_{HS}^{\mu s}$ does not occur at $T_{1/2}$. On Fig. 3.6a we showed schematically (by small vectors), that different temperature increase, $\Delta T_1$ and $\Delta T_2$, in the same pump energy, $E$, depend on the initial temperature. If we look at the relationship between $T_1$, $T_2$, and $\Delta T_1$ and $\Delta T_2$, we can see that $T_1 < T_2$ the overall temperature effect can be opposite with $\Delta T_1 > \Delta T_2$. $C_p(T)$ value increasing with temperature and $X_{LS}$ decreasing with temperature is a consequence of counteracting contributions from this latter. That's why $\Delta X_{HS}^{\mu s}$ (the magnitude of the thermal switch at $T_1$), can be greater than $\Delta X_{HS}^{\mu s}$ at $T_2$. Energy, when it is increasing, it is magnifying the effect. Fig. 3.15 shows also this effect.

If we would like to set a threshold or some limitation $\Delta X_{HS}^{\mu s}$ it might be hard to verify, because of the damage of the crystal. What is possible, if we decrease the temperature we prolong the lifetime of photo-excited HS molecules. This last feature is also limited when lifetime becomes longer than the period of laser excitation. For circumventing these limitations time-resolved single shot experiments hold big promise – and we tried to develop such system for this kind of compounds.[6, 22]

### 3.4 Conclusions

In this chapter we have presented optical time-resolved measurements of a Fe(III) spin-crossover crystal, where several experimental innovations were applied. During measurements we monitored the optical transmission of the crystal, which was triggered by ultra-short light pulse. To study long time delays we used synchronized two laser amplifiers due to which we could extend our investigation of this compound over a very large range of time scales. Earlier optical studies on the

ultrafast timescale exhibited only the femtosecond photo-induced step. Now we can also discuss about processes associated with elastic propagation and heat diffusion across the crystal.[6] As a general conclusion we can say that the transformation pathway is multistep and complex (see Fig. 3.17).

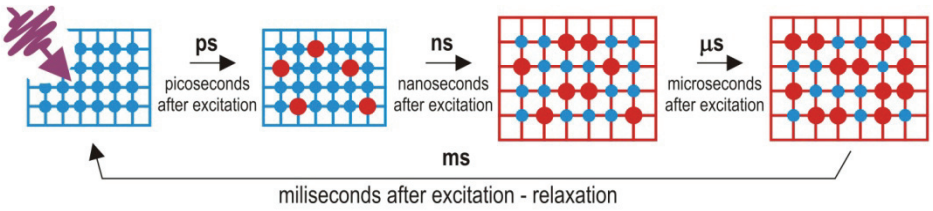


**Fig. 3.17:** Idea corresponds to relaxation of the HS molecules in the lattice of spin-crossover compound. Figure published in [21].

After excitation the pump laser pulse initiates purely photo-induced molecular process leading to an increase of $X_{HS}$, complete within 300 fs. Femtosecond step we can observe plateau after the molecular relaxation towards the HS state, accompanied by heat releases by every photo-excited molecule through the incoherent excitation of phonons and intra-molecular vibrations. However, the process where a large amount of energy coming from the absorbed photon spreads out to neighbouring molecules is not well known. Next step, completed in less than 1 ns was defined as the elastic one, where volumes of the unit cells are changing rapidly through the crystal. In this step we can consider elastic interactions caused by both the swelling of photo-excited molecules and the lattice heating discussed just before, the two causes leading to an increase of pressure inside the crystal. Thermal processes leading to the thermal equilibrium of the crystal, which remains adiabatically isolated from its cryogenic environment, takes place over the microsecond timescale after the laser excitation. Experiments of photo-active materials on nanosecond to microsecond timescales are essential to deeply understand the mechanism of the transformation in particular inside the thermal hysteresis.[11-14] Naturally new experiments would be required to observe coherent elastic switching over the picosecond timescale and control it[40] and additionally capturing local clustering.[41] This is also true for a deep investigation of shock-wave effects.[34] Until now different models of elastic interactions are discussed to describe the transformation of a spin-crossover in contact with a thermal bath,[4,27-29] so investigating slow thermal processes. But still fast and ultra-fast photo-induced phenomena in bistable molecular system needs to be further investigated from the theoretical view-point. Studies

during my Ph.D. work in ultrafast time scale present new clues for designing efficient photo-active devices, taking into account shock-wave driven transformation with light, where also macroscopic descriptions are required.[6] We should also underline, that in nano-particles or object with smaller size than ours crystal elastic switching should be faster and more efficient due to low $C_p$ of such systems.

**References:**

[1] P. Gütlich et al., *Top. Curr. Chem*. **233**, (2004)
[2] M. Rini et al., *Nature* **449**, 72 (2007)
[3] M. Chollet et al., *Science* **307**, 86 (2003)
[4] A. Bousseksou et at., *Chem. Soc. Rev*., **40**, 3310 (2011)
[5] M. Lorenc et al., *Phys. Rev. Lett*. **103**, 028301 (2009)
[6] M. Lorenc et al., *Phys. Rev. B* **85**, 054302 (2012)
[7] S. Koshihara et al., *J. Phys. Soc. Jpn*. **75**, 011001 (2006)
[8] L. Cambi et al., *Chem. Ber. Dtsch. Ges*. **64** (10), 2591 (1931)
[9] E. Koenig et al., *Inorg. Chem*. **6** (1), 48 (1967)
[10] M. Marchivie et al., *Acta Cryst. B* **61**, 25 (2005)
[11] S. Blundell, *Magnetism in condensed matter*, Oxford 2001
[12] K. Nasu (Ed.), "*Relaxation of Excited State and Photo-Induced phase Transitions*", Spr. (1997)
[13] E. Trzop, *Ph.D. Thesis*, Wrocław - Rennes 2009
[14] M. Nishino et al., *Phys. Rev. Lett*. **98**, 247203 (2007)
[15] J. Wajnflash, *J. Phys. Status Solidi*, **40**, 537
[16] A. Bousseksou et al., *J. Phys. I France* **2**, 1381 (1992)
[17] A. Bousseksou et al., *J. Phys. I France* **3**, 1463 (1993)
[18] A. Bousseksou et al., *J. Phys. I France* **5**, 747(1995)
[19] A. Bousseksou et al., *Coord. Chem. Rev*. **251**, 1822 (2007)
[20] H.-B. Chernyshov et al., *Phys. Rev. B* **70**, 094116 (2004)
[21] H. Cailleau et al., *Acta Cryst. A* **66**, 189 (2010).
[22] W. Kaszub et al., *Acta Phys. Pol.. **A*** **121**, 325 (2012)
[23] C.Enachescu et al., *Chem. Phys. Chem.* **7**, 1127, 2006
[24] S. Floquet et al., *Dalton Trans*., 1734 (2005)
[25] A.J. Simaan et al., *Chem. Eur. J*. **11**, 1779 (2005)
[26] E. Collet et al., *Acta Cryst. B* **65**, 474 (2009)
[27] P. Gutlich et al., *Angew. Chem. Int. Ed*., **33**, 2024 (1994)
[28] P. Gütlich et al., *Top. Curr. Chem*. **234**, **235** (2004)
[29] T. Nakamoto et al., *Inorg. Chem*. **40**, 3805 (2001)
[30] N. Moisan et al., *C. R. Chimie* **11**, 1235 (2008)
[31] N. Bréfuel et al., *Angew. Chem. Int. Ed*. **48**, 9304 (2009)
[32] R. Naskręcki - *Femtosecond transient absorption spectroscopy. Photophysical study of the excited states of molecules and short - living individua*, Wydawnictwo Naukowe UAM, Poznan 2000

[33] W. Gawelda et al., *Phys. Rev. Lett*. **98**, 057401 (2007)
[34] C. Bressler et al., *Science* **323**, 489 (2009)
[35] M. Khalil et al., *J. Phys. Chem. A*. **110**, 38 (2006)
[36] C. Brady et al., *Top. Curr. Chem*. **235**, 1 (2004)
[37] A. Cannizzo et al., *Angew. Chem. Int. Ed*. **45**, 3174 (2006)
[38] G. Galle et al., *Chem. Phys. Lett*. **500**, 18 (2010)
[39] M. Lorenc et al., *Phys. Rev. Lett*. **103**, 028301 (2009)
[40] T. Feurer et al., *Science* **299**, 374 (2003)
[41] L. Guérin et al., *Phys. Rev. Lett*. **105**, 246101 (2010)

Chapter 4:

# Photo-induced phenomena in $(EDO\text{-}TTF)_2SbF_6$

# 4 Photo-induced phenomena in $(EDO\text{-}TTF)_2SbF_6$

The organic crystal, $(EDO\text{-}TTF)_2PF_6$ belongs to the $(EDO\text{-}TTF)_2XF_6$ family of molecular-based charge transfer salts.[1,2] These quasi-one-dimensional salts present an insulating to metal phase transition at thermal equilibrium. $(EDO\text{-}TTF)_2PF_6$ was also a first organic crystal, where giant ultrafast photo-response accompanied by coherent oscillations was observed.[3] This was considered as a new step in photo-induced phase transitions science, with regard to previous studied cases such as the ionic to neutral phase transition in TTF-CA.[4] This new molecular-based system also became a candidate for ultrafast photo switchable device. Since then, in other systems from the same family of molecular materials, the photo-response and its dynamics have been observed and studied.[1]

During my Ph.D. studies we made and compared response from complementary time-resolved and steady state optical experiments on the $(EDO\text{-}TTF)_2SbF_6$ crystalline compound, which is another member of $(EDO\text{-}TTF)_2XF_6$ family. It is isostructural to $(EDO\text{-}TTF)_2PF_6$ crystal but with bigger anion. This time the aim of research on $(EDO\text{-}TTF)_2SbF_6$ was focused on the observation of dynamics of the coherent phonons induced by a light pulse and specific properties of the photo-induced state.

## 4.1 $(EDO\text{-}TTF)_2XF_6$ family of compounds

### 4.1.1 Description of $(EDO\text{-}TTF)_2XF_6$ compounds

The tetrathiafulvalene (TTF) salts are well known as one-dimensional conductors since 1970 when a high conductive metallic phase was discovered.[2] Associated with one ethylenedioxy group, say EDO, it forms the ethylenedioxy–tetrathiafulvalene salts – EDO-TTF. A schematic drawing of the neutral EDO-TTF molecule is presented on Fig. 4.1. These compounds exhibit a non metallic ground state at low temperatures.[2]


**Fig. 4.1:** Structure (**a**) and structural formula (**b**) of the neutral EDO-TTF donor molecule. Picture was published in [7].

Up to now in the (EDO-TTF)$_2$XF$_6$ family of isostructural crystals, different compounds were synthesized, each with different size of anion, among them: (EDO-TTF)$_2$SbF$_6$, (EDO-TTF)$_2$AsF$_6$ and finally (EDO-TTF)$_2$PF$_6$. All these compounds undergo first order, abrupt, metal – insulator phase transition at thermal equilibrium. They differ by different temperatures of transition and wideness of the thermal hysteresis observed by on static magnetic susceptibility measurements versus temperature (Fig. 4.2).[5] The bigger the ion is, the smaller the transition temperature $T_0$ and the wider the hysteresis – summary presented in Table 1.

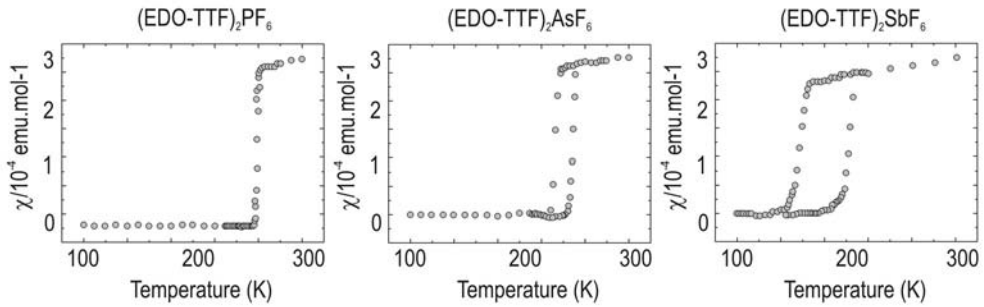


**Fig 4.2**: Comparison between static magnetic susceptibility of different (EDO-TTF)$_2$XF$_6$ family of compounds – comparable with Table 1. Data presented in [5].

In (EDO-TTF)$_2$PF$_6$, the M-I phase transition occurs at 280 K[3] (278 K[5]) and is characterized by a small hysteresis of about 1 – 2.5 K. The bigger anion molecules in (EDO-TTF)$_2$SbF$_6$ causes that the phase transition is observed around 240 K and with an hysteresis wideness of about 22 K.[5] The comparison between the hysteresis of three different crystals of the family, observed on the static magnetic susceptibility versus temperature, is shown on Fig. 4.2 and breakdown on Table 1.[3,5] Additional measurements in (EDO-TTF)$_2$PF$_6$ shows that the temperature of the phase transition is shifted to higher temperatures when the number of cycles passing through the transition temperature increases, but without change of its hysteresis wideness.[6]

**Table 1:** Comparison between different temperatures and width of hysteresis of transition in (EDO-TTF)$_2$XF6 family of compounds.[6]

| | **$T_c$ (K)** | **Hysteresis width (K)** |
|---|---|---|
| $PF_6$ | 278 - 280 | 1-2.5 |
| $AsF_6$ | 270 | 8 |
| $SbF_6$ | 240 | 22 |

### 4.1.2 Structural aspects

In these quasi-one-dimensional ¼ or ¾ filled (¼ in terms of holes) band salts the EDO-TTF donors form columns where molecules are stacked by head to tail and the acceptor molecules are located in cavities between donor layers.[2] Structure of both phases was shown on Fig. 4.3.[7]

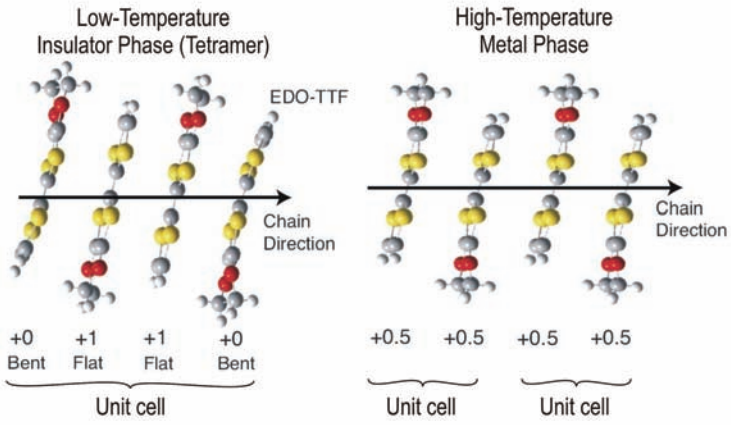


**Fig. 4.3:** Two thermally induced states: insulating in low temperature; cell doubling (tetramerization), and metallic one in high temperature. Picture published in [7].

At room temperatures, when the crystal is in the metallic phase, the periodic unit along the chain axis is composed of two slightly bent donor molecules which are equivalent by an inversion center. Electrons are delocalized and uniformly spread on all donor molecules. The equivalence of charge density on each donor molecule can be described as (½, ½). In the insulating phase donor molecules are alternatively bent or flat. These molecular deformations are the signature of a charge ordering, where, approximatively the charge in bent molecules corresponds to a 0 value in contrary to flat donors with a 1 value.[7] In such systems, two types of charge ordering may be considered: (1010) or (0110).[3] In EDO-TTF salts, in the low temperature phase, exist the second type of ordering (0110) which is observed instead of (1010) one, generally expected with regard to the nearest-neighboring electronic repulsion.[8] During metal to insulator transition, the periodic unit along the stacking axis has doubled – leading to tetramerization. The tetramers formed finally consist in two pairs of one bent and one flat molecule.[7]

In addition to these structural features, a significant increase of thermal vibrations, i.e. rotational oscillations of acceptor molecules (anions) are observed in the metallic phase. In summary, the (EDO-TTF)$_2$XF$_6$ family phase transition from metal to insulator provides a complex physics due to interplay among electron-lattice, electron-correlation (charge ordering) and anion thermal disorder.[6,8] Fig. 4.4 presents a schematic view of the charge density of donor molecules (cations) in metal and insulator phase with the different structural features associated to molecular deformations, as well as thermal disorder between acceptor molecules (anions).

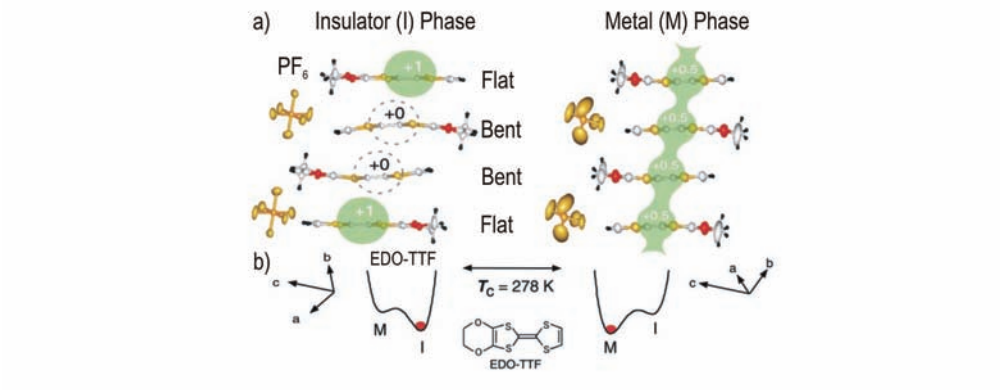


**Fig 4.4**: **a)** Charge density and structure of (EDO-TTF)$_2$PF$_6$ in both phases with comparison of molecular deformations for donors and thermal disorder for acceptors – observed in X-ray crystallographic studies. **b)** Schematic thermodynamic potential change. Picture taken from [3].

## 4.2 Metal to insulator phase transition in (EDO-TTF)$_2$PF$_6$

### 4.2.1 Symmetry breaking analysis

Investigation of the thermal induced phase transition by X-Ray diffraction on a single crystal allowed to measure the temperature dependency of unit-cell parameters and an hysteresis is observed between 276 K and 280.5 K.[8] The large jump of unit-cell parameter between M and I phases made it possible to observe Bragg peak coexistence inside the hysteresis related to long range ordered M phase coexisting with long range ordered I one. In order to express the symmetry-breaking keeping the same crystallographic axis, the space group of the high-temperature M phase is not the conventional $P_{4}$ space group but the face centered $C_{4}$ one. With that convention, the symmetry-breaking between M and I phases manifests by the appearance of (hkl) h+k odd reflections in the low temperature I phase. These observations are consistent with magnetic susceptibility measurements and DSC studies.[8]

### 4.2.2 An ultrafast giant photoresponse

The giant photoresponse of $(EDO\text{-}TTF)_2PF_6$ to a 800 nm (1.55 eV) laser pulse of 120 fs has been observed a few years ago using time resolved optical reflectivity experiments.[3] This wavelength is near the charge transfer band from $D^{2+}D^0$ to $D^+D^+$, related to the charge ordering process. The probe light covered a wide region from IR and VIS avoiding wavelengths around 800 nm, because the strong scattered light from the pump would have been detected like being the probe beam. Large reflectivity changes were observed in less than 1.5 ps.[3] The different electronic configuration of donor molecules between I and M phases are at the origin of these changes in reflectivity spectra which were detected – see Fig. 4.5a. Fig. 4.5b presents curves, corresponding to the reflectivity spectra at t = -10 ps and before t = 3 ps after excitation. This was done for two different temperatures: 180 K (insulating phase) and 265 K (metallic phase).

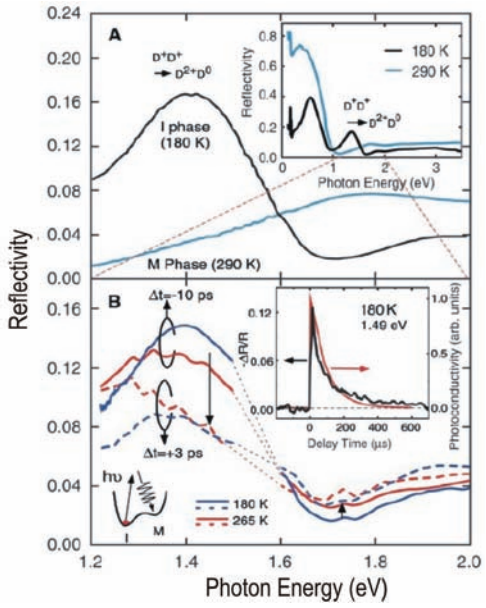


**Fig. 4.5 a):** (Plot A) Reflectivity of the crystal in two phases: metal and insulating one in two temperatures: 290K and 180K respectively [3].

**Fig. 4.5 b):** (Plot B) Time resolved reflectivity spectra taken at two different temperatures and two different time delays. Information about colors of the curves was put in lower panel [3].

**Fig. 4.5 c):** (Plot on the top of figure B) Comparison of results on time evolution obtained by two independent methods: photo-response from the optical experimental setup (black line) and photoconductivity measurements (red line). Plot taken from [3].

Changes after excitation at 180 K indicated that a broad band, which could be characteristic of the M phase, has appeared. This was interpreted as a metallization process occurring in less than 3 ps after the excitation.[3] In order to have one more proof that the obtained phase corresponded to the metallic induced one, transient reflectivity measurements from optical pump–probe experiment at the microsecond time scale (more than 600 μs) were compared to photoconductivity measurements after excitation. The results presented on Fig. 4.5c show that both curves exhibit a

similar time decays around 500 μs. It was calculated that around 50% of donor molecules were converted from low to high temperature phase and that one photon was able to transform 500 molecules. In this work, Chollet et al., also made experiments with different photon flux in pump beam. They concluded that the transformation occurred only after the critical absorbed photon density of $2\times10^{18}$ $cm^{-3}$, exhibiting a cooperative nonlinear amplification of the photo-response.

### 4.2.3 A difference between the photo- and thermally-induced metallic phase

Onda et al., [9] presented in 2008 measurements of the reflectivity change in the photo-induced phase of $(EDO\text{-}TTF)_2PF_6$ over a wider photon-energy range, largely extended over the infrared one. Thus in this work, they cover the range from 69 meV to 2.1 eV, instead of the limited 1.2-2.0 eV range previously investigated in [3]. In the photo-induced phase just after photo-excitation ($\Delta t = 0.1$ ps), a charge band, not present in the metallic thermal phase, appears. This reveals that the laser pulse induces a new type of state different from the metallic phase at thermal equilibrium.

Using a theoretical model incorporating electron-electron and electron-phonon interactions, respectively described by the neighbour Coulomb repulsion term V and the electron-phonon coupling term γ, they performed numerical calculations of the (V,γ) phase diagram for the insulating ground state. The coupling γ makes the (0110) charge order state favouring and the repulsion V makes the (1010) charge order state favouring. The optical conductivity spectrum assigned to the CT excitation have been calculated for the two charge order states, three bands for the (0110) state and one band for the (1010) state. This seems indicate that the photo-induced state is this (1010) charge-disproportionate state. It was also observed that the phonon oscillation became incoherent in the mid-infrared region Fig. 4.6.[9]

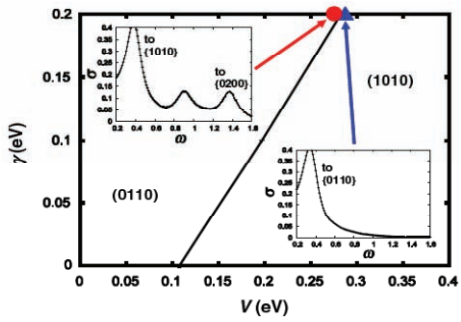


**Fig. 4.6**: Theoretical calculations of the metastable phase presented on (V, γ) plot. Small plots inside presents typical spectra in the near the phase separation line. Plot taken from [9].

### 4.2.4 Intra-molecular mode observed by 10 fs pulses

Higher time resolution and new pump probe experimental setup using 10 fs pulses in measurements is now challenging. This opens new possibility to observed photo-induced transformations, which can be useful to explore early dynamics. With this ultrafast technique new problems appear. For example, 100 fs pulse is quasi monochromatic. Shorter 10 fs pulse covers almost 200 nm of the spectrum. Therefore, such wide pulses can cover not only one charge transfer band but more.

However those measurements allow to observe in reflected light evolution of the spectral dependence, which agrees quantitatively to the case of thermally induced transition. In low energy part, sign, amplitude location of isosbestic point stay with agreement to reflected light obtained earlier by different groups. In higher energy part only amplitude doesn't have the same value. 10 fs pulses gives an idea of processes governs photo induced phase transition in this compound and we can say about bottleneck on pure excitation.[10, 11]

## 4.3 The case of $(EDO\text{-}TTF)_2SbF_6$

### 4.3.1 Description of $(EDO\text{-}TTF)_2SbF_6$ properties

Opaque crystals are crystallized as single needles of typical size around 0,1 x 0,5 x 1 $mm^3$. They are prepared by electro crystallization method, using a room temperature ionic liquid $EMI^*SbF_6$ as electrolyte, where EMI denotes 1-ethyl-3-methylimidazolium.[5] During phase transition, which occurs at T = 240 K, structural changes of structure are large and crystal can be easily damaged and broken. Comparison of hysteresis shown on Fig. 4.2 for the EDO-TTF family, show that $(EDO\text{-}TTF)_2SbF_6$ has got the biggest wideness range – 22 K.

In general, the penetration depth of laser beam is less than the micron, so for observations of the dynamics of the photo-induced phenomena time resolved reflectivity spectroscopy is more suitable than transmission.

Then, it is possible to observe the thermal phase transition by performing measurements of the reflectivity of a crystalline sample, which is sensitive to changes in electronic structure. Such an experiment was performed in Rennes before my thesis work (Fig. 4.7a).[12] The laser light used in this experiment was provided by continuous laser diode at wavelength 635 nm. The detection was ensured by a photodiode associated with an oscilloscope. The critical temperature and hysteresis wideness

observed are comparable the one observed by magnetic susceptibility measurements (see Fig. 4.2) and shows also, that after phase transition, reflectivity of the sample changed. This confirms that optical reflectivity measurement is a good tool to probe the sample state.

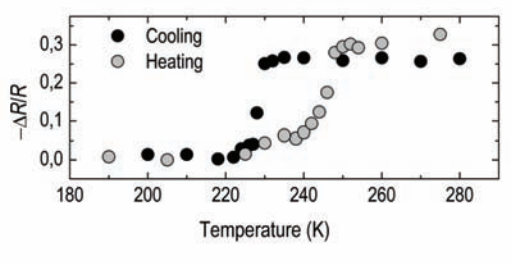


**Fig. 4.7a:** Changes of optical reflectivity of the (EDO-TTF)2SbF6 crystal with temperature. Measurements were prepared on the single crystal and with continuous laser-diode. Optical data are comparable to magnetic measurements – presented on Fig. 4.2. Picture presented in [12].

Experiments on (EDO-TTF)2SbF6 under high pressure at room temperature were also performed in Rennes in collaboration with Japanese colleagues. Raman measurements exhibit two types of spectra corresponding to two different phases (Fig. 4.7b). At low (below to 2000 bar) and high (above 5030 bar) pressure, peaks at around 1592, 1517 and 1471 cm $^{-1}$ appear. They can be interpreted as C=C stretching modes of the metal phase, and have already been seen in another compounds with TTF molecules. Spectra in the medium pressure range (2100 – 4030 bar), change suddenly giving a proof of a 1st order MI transition. The occurrence of a metal phase above 5 kBar pressure remains however a matter of debate.[13]

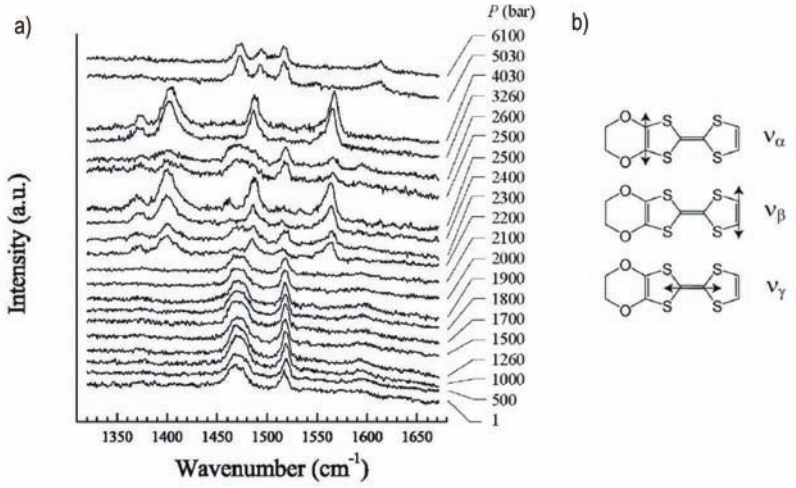


**Fig 4.7b:** a) Raman spectra versus pressure in room temparature.b) stretching modes corresponds to C=C oscillations bond in EDO-TTF molecules. Plot taken from [10].

### 4.3.2 Experimental details

As was mentioned at the beginning of this chapter, steady state and time-resolved methods were applied during experiments on $(EDO\text{-}TTF)_2SbF_6$. Using femtosecond, time-resolved experimental setup, we could observe changes of the reflected light due to collective motions occur after excitation. Relative change of the reflected light was also indication that new photo-induced phase generated in crystal, had different dielectric function than in insulating phase. After analysis, when frequencies of coherent phonons were extracted from time-resolved signal, we could find out if those modes can be observed in different phases by stationary Raman spectroscopy in thermal equilibrium.

#### 4.3.2.1 Raman measurements

Raman spectra were obtained using an XY DILOR Raman spectrometer with a triple monochromator equipped by a CCD camera. The laser system (SPECTRA PHYSICS) contains an argon gas laser used to pump a Ti:Sa laser delivering a continuous wave from 700 nm to 850 nm. In our own experimental setup, we used a laser line cantered at 747,2 nm. At each temperature, the back-scattered signal is collected in 30 minutes by the CCD camera. The triple monochromator used in subtractive Stoke-Anti-Stoke configuration is able to detect frequencies from $\pm 20\ cm^{-1}$ to $\pm$ 0,6 THz from the excitation beam. This property is crucial because only frequencies of oscillations between 0,5 to 6 THz are seen in time-resolved experiments.

The crystal was cooled in a close cryostat at ambient pressure. The temperature precision was around 1 K but incertitude exists on the sample temperature due to the possible heating by the laser beam focussed on the surface. This experimental setup was described in details in [13].

#### 4.3.2.2 Time-resolved measurements

General idea of the experimental setup used in measurements was described shortly in chapter 3 (“Spin-crossover transformation…”), because we were using for these measurements the same experimental setup (historically it was first one). Details can be found in chapter 6 (“Experimental”). Difference relied mainly on the reflectivity configuration of the setup, because $(EDO\text{-}TTF)_2XF_6$ crystals are non transparent for the light (the penetration depth is approximately some few nanometers). In these measurements both, pump and probe beams, were collinearly focused on the sur-

face, thanks to $2^0$ wedge put near the sample. Pump fluency was below threshold of super continuum generation inside the wedge (what was observed with pump fluence used in spin-crossover measurements). Typically we were using two pair of wavelengths for pump/probe: 850/720 nm and 800/1500 nm respectively.

We prepared experiments on $(EDO\text{-}TTF)_2SbF_6$ with different conditions presented graphically on Fig. 4.8, to improve and correlate, dynamics of occurrence of the photo-response.

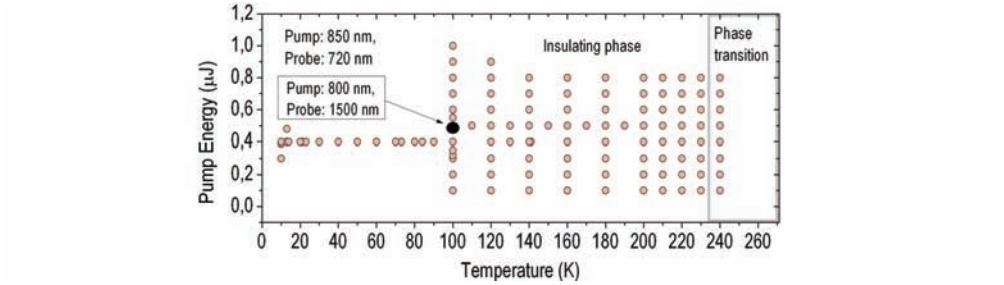


**Fig. 4.8**: Scheme of experimental conditions during measurements. Grey dot corresponds to spectra obtained using two different wavelength used only in one measurement series. Rest of time resolved spectra were obtained using pump near charge transfer band – optical conductivity. Temperature studies from 10 K to 90 K were done using helium as a cooling media, rest of them – using liquid nitrogen.

*Temperature range.* On the plot can be seen two groups of measurements. First one, where as cooling medium we were using liquid nitrogen (100 K – 240 K, open and close cryostat), in second case – liquid helium (10 K – 100 K, close cryostat). At 100 K in this compound we could observe long time coherent oscillations. Above 240 K occurred the phase transition with temperature hysteresis. Lower temperatures we chose to verify, how much, thermal motions affects the oscillations and that's why we prepared measurements only with one energy value.

*Energy range.* Energies of pump excitation was chosen due to material response from the crystal. Energies of the pump, above 0,8 μJ was destructive for the sample. In low energy range we prepared measurements, mostly up to 0,1 μJ, and also an extra low excitations to observe occurrence of the threshold of photo-induced response.

*Wavelength of the pump and probe beam.* Color of the beams was chosen due to optical conductivity spectrum made at the beginning. We chose wavelength near the charge transfer band. One measurement was done with different pairs of the pump, probe wavelength on both sides of the charge transfer band.

### 4.3.3 Analysis method

The experimental data were analyzed in term of non-oscillating and oscillating part of the photo-induced response. Here we put in details the methods used to study the coherent phonons involved. The oscillating part of the signal is extracted by subtracting an exponential decay (Fig 4.9) from the time resolved photo-response of $(EDO\text{-}TTF)_2SbF_6$ which contains several additional phenomena, like excitation peak and plateau. In description of the program inventors noticed, that some signals treated by Fast Fourier Transform (FFT) module give inadequate results because of leakage sometimes occur in the initial signal. That's why special care was taken to preparation of the results before FFT.

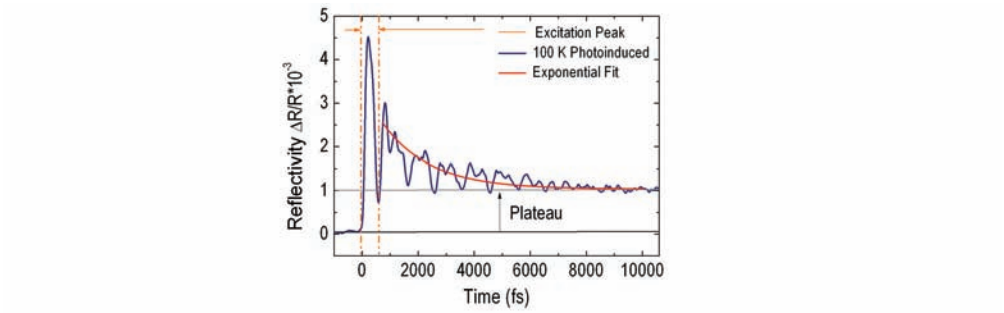


**Fig. 4.9:** Example of the obtained results after experiment. Clearly observed oscillations and plateau showed on the plot.

The oscillating part is then analyzed by several methods. First, a simply (FFT) is performed and principally used to obtain the frequencies of the modes. Secondly, we tried to characterize the dynamics of the phonons and use two different methods: Short Time Fourier Transform and fitting of the oscillations. On Fig. 4.9, a typical photo-response detected from the reflected light can be seen. The plateau may be a signature of photo-induced phase different from the insulating one – because of changes in intensity of reflected light. The value of this plateau can be positive or negative depending of the used probe wavelength – this information is carrying by steady state reflectivity spectra in different phases. For example, if relative change in reflectivity has got positive values – plateau is this same as shown on Fig. 4.9.

#### 4.3.3.1 FFT – **F**ast **F**ourier **T**ransform

The term FFT designs algorithms performing Discrete Fourier Transform (DFT) in a way faster than the one using simply the formula:

$$X_k = \sum_{n=0}^{N-1} x_n \cdot e^{-i2\pi \frac{k}{N} n} \tag{4.1}$$

The complexity of an FFT algorithm varies indeed like *O (n*ln n)* instead like *O (n²)* and the time needed can be 100 times faster.[14] This tool is a standard method available in Origin software.

During analysis we were using two types of windows: rectangular and Hanning windows, to be sure that peaks corresponds to frequencies really occurring in the signal and not artefacts. The rectangular window was specially adapted to distinguish two frequencies close to each other. The Hanning window was more dedicated to signals containing several sinus functions. In our analysis we took both and compared the results to each other.

We used also *zero padding* to increase the number of points calculated in the frequency spectra and as a consequence, we could increase the precision of obtained data. It is important to underline that, when we add zero padding, width of the peaks in FFT stays the same, but precision in better (we could observed "structure" of the peaks).

#### 4.3.3.2 STFT - **S**hort **T**ime **F**ourier **T**ransform

Short Time Fourier Transform was prepared using MatLab programming environment. The main idea of this data treatment relies on multiplying several times curve from experiment by a Gaussian function $\omega(t - r)$– each time with a different delay $r$ between the beginning of the scan and the beginning of the Gaussian window. After each multiplication, a FFT was performed in order to obtain the frequency spectra during the time of the window. The general formula for STFT due to its definition is:

$$STFT\{x(t)\} \equiv X(r, \omega) = \int_{-\infty}^{\infty} x(t)\omega(t - r)e^{-j\omega t}dt \tag{4.2}$$

After such operation we obtained a time resolved Fourier transformation. These results were traduced in 3D plots on which we had time – frequency plane and amplitude as a Z axis. Using this kind of data treatment we could observe the dynamics of the frequencies of the photo-induced phase. A scheme of this idea is presented on the simple scheme shown below:

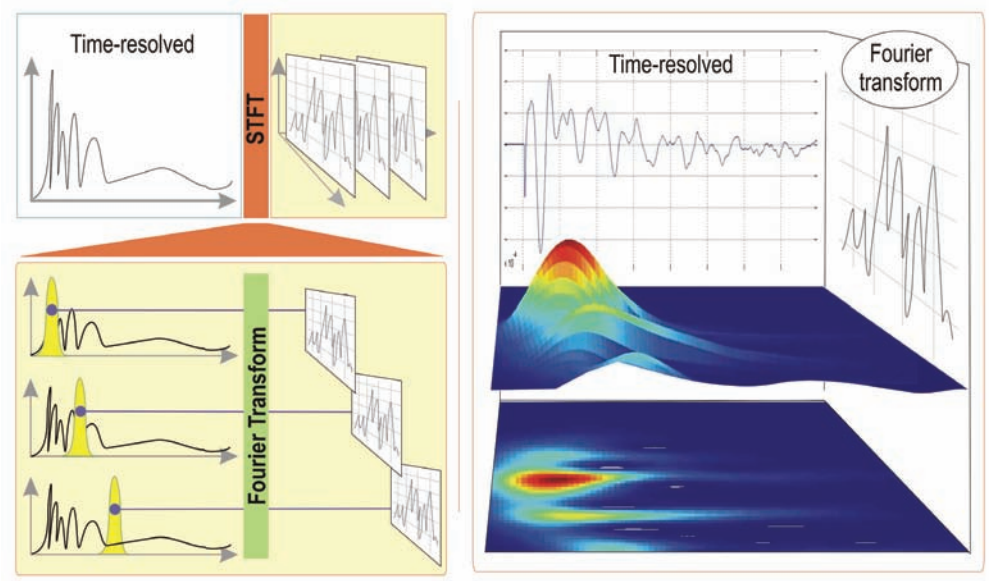


4.3.3.3 Artifacts of STFT method

*"Zero" frequency.* Such kind of artifacts came from the procedure used to remove the exponential decay (Fig. 4.10a).

*Wrong position of maximum amplitude*. On STFT plots, the maximum of the frequency on the time scale near the excitation peak is more shifted than it is suppose to be from the experiment. It results from the multiplication process between the beginning of the part of the analyzed curve with the Gaussian window. Zero Padding caused zero values at this moment. After multiplication, values from the beginning were affected by the "zero" and as a consequence, the amplitude of the FFT at this time was lower than for the bigger decays.

*Initial "bridge" between different modes at the beginning of the signal.* The second artifact occurred on the plots, was connected with "bridges", which appeared between neighboring modes at the beginning of the plot (Fig. 4.10b). This is attributed to the

brutal jump from a zero signal of the Zero-Padding to the initial value of the oscillating part. Such kind of feature corresponds to the pulse which contains a lot of frequencies.

*"Bridge" between different modes*. The same kind of artifacts occurred along the whole time of the scan with neighboring frequencies (Fig. 4.10b). It was related to the fact, that the presence of two near frequencies in a signal corresponds to the modulation without carrier wave. In the global FFT, the carrier frequency which is the mean between the two frequencies doesn't appear, but the finite windowing of the signal performed during the operation of the STFT led to be sensitive to this mode. Knowledge about those artifacts was helpful in interpretation of obtained results, because this method was useful, but with interpretation of the results we had to be careful.

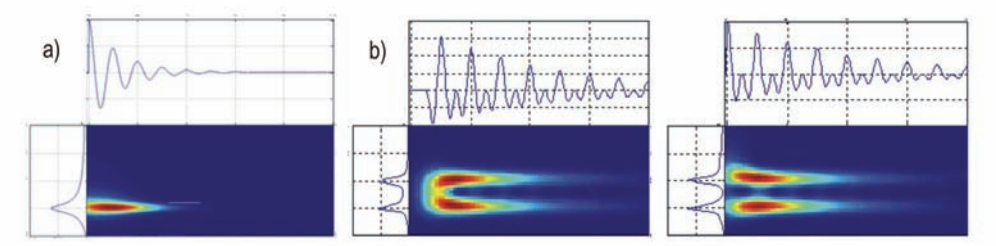


**Fig 4.10**: Typical artifacts observed in Short Time Fourier Transform (STFT): **a)** *Zero frequency* and false *maximum* amplitude position, **b)** Initial bridge accompanying to maximum frequency and between two frequencies.

#### 4.3.3.4 Function fit with three sinus components

Important part during analysis was fitting to obtained data function with three oscillation components and suppression. For each curve, we applied different fitting curves and several results exhibited clear three components of oscillations. After fitting process, obtained curve was also analyzed by FFT module and compared with frequency spectrum from experimental data.

## 4.4 Raman spectroscopy results of (EDO-TTF)2SbF6

Results obtained using Raman spectroscopy at different temperatures was presented on Fig. 4.11. The most interesting range for us (as was mentioned above) was covering between 0,5 to 4 THz, because of frequencies observed in time-resolved experi-

ments. In literature temperature dependence of Raman spectra was published only on $(EDO\text{-}TTF)_2PF_6$ crystals[2,6] and we knew that $(EDO\text{-}TTF)_2SbF_6$ ought to have slightly different phonon spectrum.

Obtained Raman spectra in two thermally induced phases were quite different. The metal phase exhibits two main peaks with relatively large FHWM. In insulating phase, six frequencies at 1 THz; 2 THz; 2,5 THz; 2,9 THz, 3,1 THz and 3,4 THz were clearly distinguishable. Difference between both phases is clear.

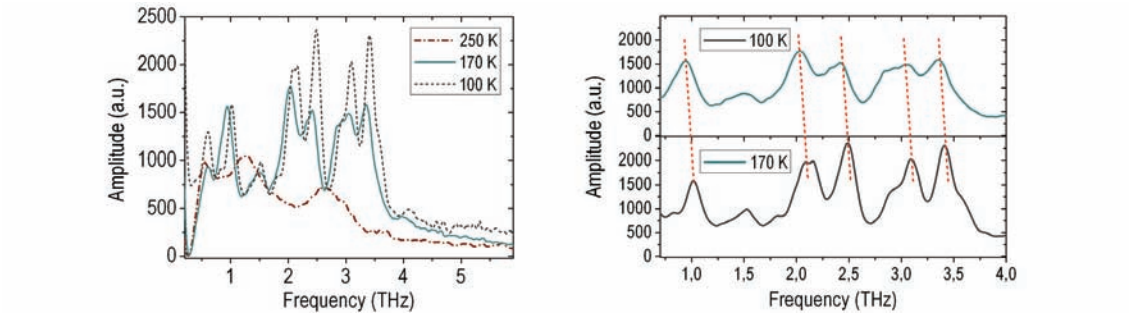


**Fig. 4.11:** Spectra obtained from Raman scattering in $(EDO\text{-}TTF)_2SbF_6$: Left plot presents comparison between spectra obtained in high and low temperature phase. Right plot show frequency shift in insulating phase.[15]

In insulating phase, two spectra at different temperatures were made. After analysis of the obtained results, we can see a frequency shift, constantly affected all $(EDO\text{-}TTF)_2SbF_6$ modes, moving to shorter frequency values when temperature arise. This kind of feature is common due to thermal anharmonic effects.[15]

### 4.5 Time-resolved results of $(EDO\text{-}TTF)_2SbF_6$

On Fig. 4.12 (next page) was presented results obtained at 100 K, 170 K and 230 K. First column show the spectra taken directly from the experiment. Second column shows oscillation part, extracted from the original signal by removing plateau, excitation peak and exponential decay. Third column shows results of the FFT – for the simplicity, we presented here analysis only from the one defined window.

Comparing obtained results with those from the Raman spectra, we can observe three main modes, at: 1 THz; 2 THz; 2,5 THz; which appear on frequency spectra at all temperatures. At 100 K we can also detect three other, rather smaller at: 2,9 THz,

3,1 THz and 3,4 THz. This stays in good agreement with Raman spectra in thermal equilibrium, so we can say, that observed in time resolved studies frequencies correspond to coherent phonons detected in insulating phase.

In next paragraphs we tried to extract several aspects of the photo-induced transformations in (EDO-TTF)2SbF6 thanks to analysis tools presented above. Those features correspond to electronic excitation, nature of photoinduced transformation and dynamics of the phonons in general, but are also related to the different temperatures.

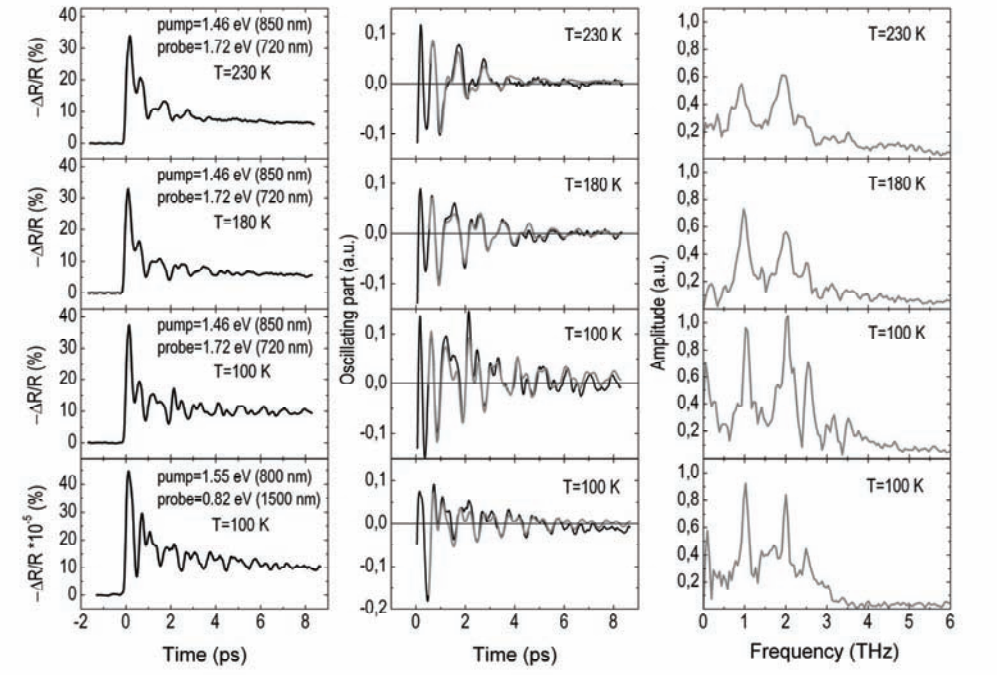


**Fig. 4.12:** Photo-response from the (EDO-TTF)2SbF6 compound in different temperatures and energies of the pump and probe. Plots were formed to columns correspond to each step made during analysis: response from the crystal, extracted oscillation part and its FT part, respectively.[15]

### 4.5.1 Electronic excitation

Experiments with different excitation desities, with number of photons per laser pulse, allow to observe how the density of photoexcited molecules may to infulence the bahaviour of phonon modes. As a consequence, some information on the nature

of the photoexcited electronic states can be deduced. The variation of the three main frequencies with the energy of excitation was presented on Fig. 4.13. As we can see there is no excitation density dependancy. This is in contrary to the mode softening observed in Bi[16] and Te[16]. In this compounds, the collective delocalized excited state induces a significant change of the lattice potential. As a consequence, the strength between atoms decreases and phonon frequencies decrease. As such phenomenon is not observed in $(EDO\text{-}TTF)_2SbF_6$, it probably essentialy localized on the molecule (self trapping).

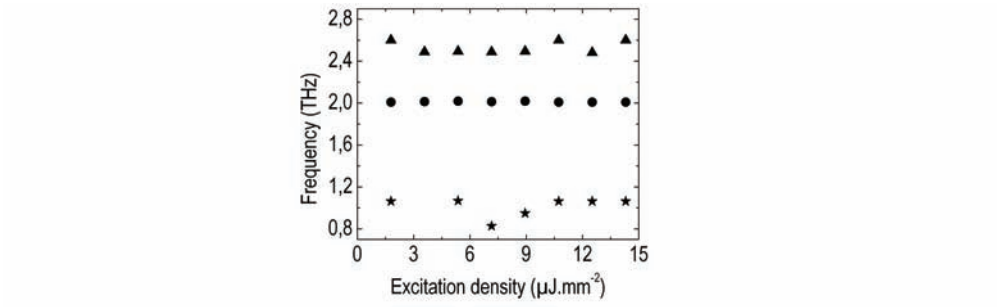


**Fig. 4.13:** Plot presents frequency of the modes with the temperature changes. As we can see there is no excitation density dependancy of the amplitude for three modes.[15]

### 4.5.2 Nature of photoinduced state

We tried to establish if a phase transition was induced by the laser pulse and see if the photoinduced state is the same as the thermal phase at high temperature. We performed experiments at 230 K, which were inside the thermal hysteresis – results of those measurements were presented on Fig. 4.12. We knew, that in hysteriesis, both, metallic and insulating phase, are stable, and by applying train of femtosecond pulses we should switch the low temperature phase to high temperature phase during the first pulse of the train. As a result we should see on the signal that matter is not relaxing to initial state. In our measurements it would be seen as a signal without plateau – because if the crystal didn't relax, there is no difference between state before and after excitation. Obtained data we are interpretating, as a different state, induced from the insulating one, but not the same state as in the metallic phase.

Fig. 4.14a presented the initial peak signal and integrated signal of $\Delta R/R$ and phonon amplitude between 6.5 ps and 8.5 ps versus excitation density. No threshold can be detected. Measurements with long time acquisition and specially calibrated pho-

todiode at excitation densities under 100 nJ.mm$^{-2}$ was presented as on Fig. 4.14b and again, no threshold appeared. Phase transition requires interaction and cooperativity between molecules. This phenomenon induces the presence of non-linearity with the density of excitation and especially such as a threshold. New photoinduced state, observed by Chollet et al., in (EDO-TTF)$_2$PF$_6$ shown existence of such a threshold in the photo-induced effect.[3]

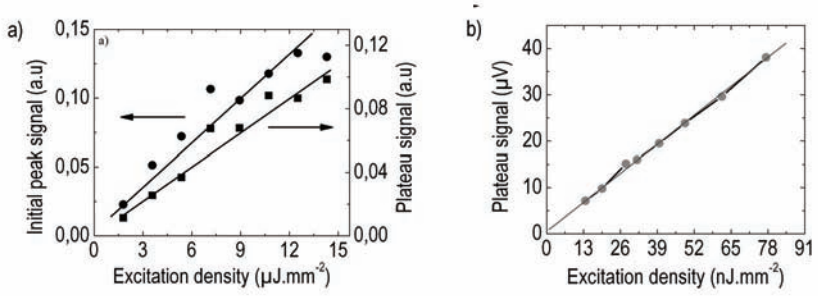


**Fig. 4.14: a)** Threshold measurements on (EDO-TTF)$_2$SbF$_6$. **b)** Measurements made with excitation energies in nano-Joule, obtained using special photodiode.[15]

Differences between those two compounds, i.e. no phase transition is performed in (EDO-TTF)$_2$SbF$_6$, could be relied to the size of the XF$_6$ molecule. Possibly, the wavelength of the pump beam, could also play important role in interaction between constituents. At low temperatures, despite of long time scale observations of coherent phonon (described below), we learnt that plateau vanish at 10 K. That means we applied the same electric field and excited optical phonons but we didn't induce the metastable photo-induced state. Comparing reflectivity data on Fig. 4.15 we conclude that at 10 K charge transfer band should be different than at 100 K.

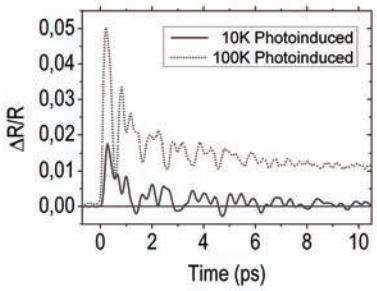


**Fig. 4.15:** Comparison of two photo-induced spectra at different temperatures: 10 K and 100 K, respectively, induced by the pump pulse at the same excitation energy. At 10 K plateau vanish, what means that we didn't induce metastable photo-induce phase.

### 4.5.3 Phonon dynamics

During analysis we compared frequency values of coherent phonons at different temperatures obtained by time-resolved measurements with those, observed by Raman spectroscopy in thermal equilibrium at 100 K and 170 K (Fig. 4.16a). Observed frequencies in both experiments in the low temperature phase are comparable and mode softening of the frequencies can be observed. Three main modes at 1 THz, 2 THz and 2,5 THz are present in Raman spectra at insulating phase, but only first two show clear temperature softening around 16% and 6% respectively. Third mode at 2,5 THz was not so visible and from 190 K and we didn't need it to perform the fit. Time decays coherent oscillations, compared on Fig. 4.16b, take place at the picosecond time scale. However the mode at 2 THz has a shorter life time. Due to this results we can also say that no bond softening takes place with time.

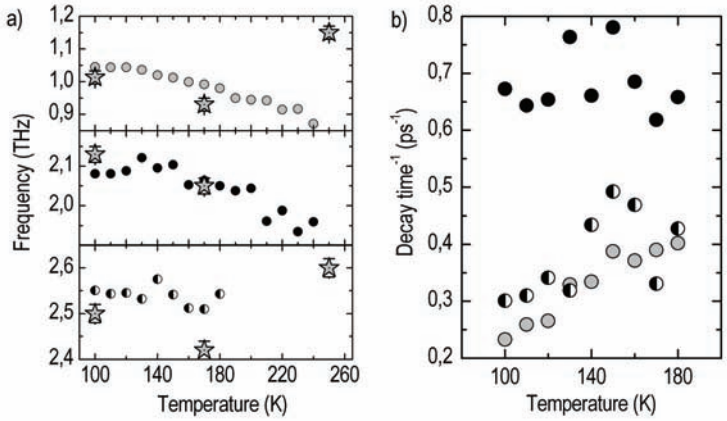


**Fig. 4.16**: Comparison between frequencies obtain in Raman spectroscopy and time-resolved studies in different temperatures. **a)** Mode softening of the phonons can be clearly observed. **b)** Decay time of mode softening in different temperatures.[15]

In order to increase the lifetime of the phonon and perform a better observation of its dynamics, we performed experiments at lower temperature range between 10 K and 100 K. On reflectivity spectra – shown on Fig. 4.17, intensity of reflected light is changing between both, metal and insulator phases, but also at low temperatures some changes in the visible region can be observed. The optical conductivity is slightly different between 100 K and 10 K, so we apply the same laser condition to find out, what kind of dynamics change happen between these temperatures.

At 10 K, thermal motions which can affect dynamics of optical phonons at 100 K are frozen. Fig. 4.18 presents oscillations at 10 K and 100 K at the same density of energy 5,5 μJ.mm$^2$. At 100 K, we can observe optical phonons which decay rapidly in contrary to second case at 10 K, where optical phonons are present at a very long time scale.

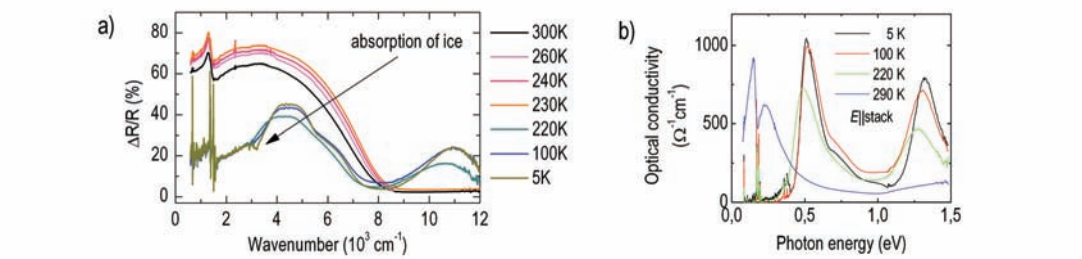


**FIG 4.17:** Reflectivity spectra of (EDO-TTF)2SbF6: **a)** Reflectivity spectra in different temperatures. Plot published in [13], **b)** Optical conductivity spectrum made from reflectivity spectra (thanks to Y. Maesato).

The same effect was observed between 100 K and 210 K.[5] This is due to the fact that thermal motion induces decoherence of the phonon at higher temperatures. During analysis, we paid attention to normalize curves on Fig. 4.18 using the same factor, which means that at lower temperatures excitation peak is smaller. The same situation we can observe on Fig. 4.15. In this case we compared different curves from 10 K and 100 K, at the same excitation energy and without normalizing – only ΔR/R values.

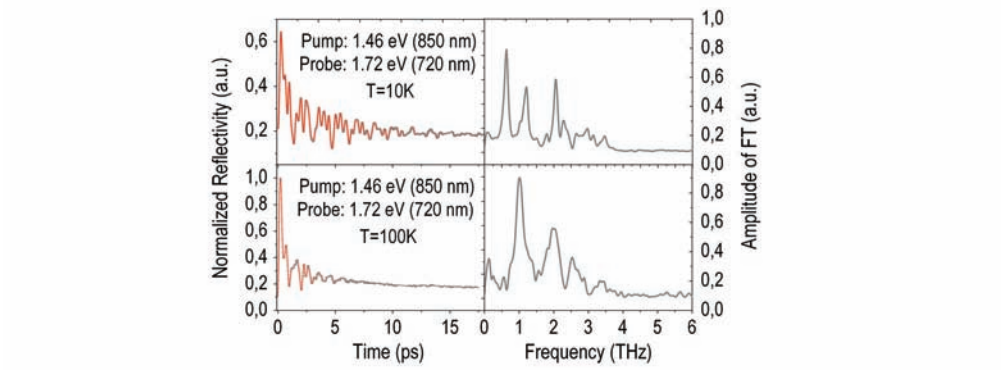


**Fig. 4.18:** Coherent phonons induced by the laser light in two temperatures: 10 K and 100 K. Left plots correspond to data obtained from the experiment. On the right – its FFT.

According to reflectivity spectra shown on Fig. 4.19, we selected two different pairs of pump and probe wavelength and compare results to each other. The three main frequencies can be observed in both cases, but, also a different shape of the oscillations can be observed. This might be due to the fact that two different probe wavelength have a different sensitivity to the three phonons and also different pump pulses can interact differentially with the sample.

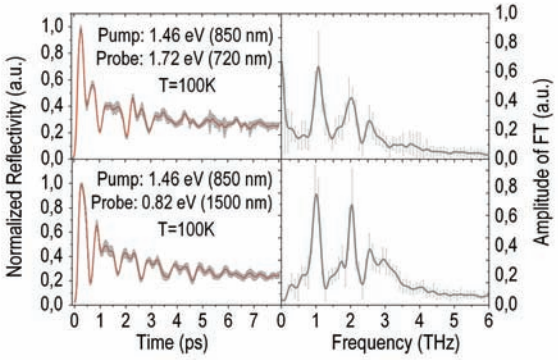


**Fig. 4.19:** Oscillations obtained by different wavelength of probe light. Left plots corresponds to time-resolved spectra. Right plots corresponds to FFT results from those spectra. Red curves show average value taken from 5 – 10 scans. In grey was shown error bars on a both plots.

### 4.6 Comparison between stationary and time resolved results - conclusions

During analysis of experimental data for the new compound of the $(EDO\text{-}TTF)_2XF_6$ family, $(EDO\text{-}TTF)_2SbF_6$, we made interesting observations by pump-probe optical measurements. This results presents some difference with the reported giant photoresponse in the prototype $(EDO\text{-}TTF)_2PF_6$.[3]

We conclude as follows:

- In this compound femtosecond laser pulse at 850 nm induces a mainly localized transformation which can imply several molecules but without the establishment of a new long range order. In other words, it is not a complete phase transition, in contrary to those at thermal equilibrium. This conclusion is also supported by the analysis of the data collected inside the hysteresis and the absence of nonlinearity of the response.
- The photo-induced ultra-fast dynamics implies several coherent optical phonon modes, not observed until now in this family of compounds. In obtained

results we can distinguish superposed response from the photo-induced metastable state and several coherent phonons excited by the laser pulse.

- Comparison of the frequencies of the collected data due to temperature, show a weak but significant softening with temperature of the three main phonon modes in frequency domain, but not with the excitation density. This is again in favour of the localized picture.

**References:**

[1] F. Shao et al. *Science* **405**, 75 (2010)
[2] G.-J. Linker et al. *Chem. Phys. Lett*. **487**, 220 (2010)
[3] M. Chollet et al. *Science* **307**, 89 (2005)
[4] H. Okamoto et al. *Phys. Rev*. *B* **70,** 165202 (2004)
[5] N. Moisan, *PhD Thesis*, Rennes 2008, France
[6] A. Ota et al., *J. of Mat. Chem*. **12,** 2600 (2002)
[7] K. Iwano et al., *Phys. Rev*. *B* **77,** 12 (2008)
[8] L. Guerin et al *J. Phys. Conf. Series* **21**, 149 (2005)
[9] K. Onda et al., *Phys. Rev*. Lett. **101,** 067403 (2008)
[10] J. Itatani et al., *Sci. and Tech*. **185,** (2006)
[11] J. Itatani et al., *Ultrafast Phenomena XV: Springer Ser. Chem. Phys.*, Springer, Berlin **88**, (2007)
[12] M. Lorenc et al., *J. Phys. Conf. Series* **148** 012001 (2009)
[13] M. Maesato et al., *J. Phys. Conf. Series* **148** 012004 (2009)
[14] Origin 8.1, help software
[15] M. Servol, in preparation
[16] S. Johnson et al., *Phys. Rev. Lett*. **100** 155501 (2008)

Chapter 5:

# Single shot spectroscopy

# 5 Single shot spectroscopy

In Landau's Phenomenological Theory of Phase Transitions we can distinguish two kinds of states: discontinuous and continuous. In the first case we can observe abrupt change of order parameter. In the second case, during a phase transition the order parameter fluctuates and two different phases coexist simultaneously. This situation is interesting, because an adequate external stimuli can switch the phase or favor some values of the order parameter. Therefore "one shot" could preferentially switch one phase to a still, and detecting the phenomena underlying such switching would too have to be achieved in only "one shot". Single shot techniques seem to be the unique solution for this kind of experiments.

## 5.1 The dream of single shot

Single shot experiments are typically required to monitor ultrafast dynamics, when sample depletion, or damage, and product accumulation restrict the range of substrates, structural environments, excitation conditions amenable to study.[1] The femtosecond pulses have extremely high intensity, often causing ablation or non-thermal melting of studied material, both of which evidently preclude common stroboscopic measurements. For circumventing these limitations time-resolved single shot experiments hold big promise, and the first attempts have proven successful in diverse applications utilizating single pulse of laser,[1] X-rays,[2] or electrons.[3,4]

An interesting aspect related to the phase transitions is the occurrence of hysteresis.[5] Studying transitions inside hysteresis loop also requires single shot methods. In a recent experiment spin-state relaxation triggered by the single laser pulse was observed on the nanosecond time scale.[5]

Yet another aspect is related to the highly excited molecules and irreversible processes in condensed matter. After strong excitation using one shot we should be able to record a signal from the sample before it disintegrates, that is when energy contained in a molecular system cannot dissipate quickly enough to the environment. Only single shot technique can detect such irreversible processes.[1,3,4]

### 5.1.1 Real-life limitations

Single shot is not a common technique. Also, the definition of "single shot" experiments is not very exact. Any technique capable of collecting the sought information on the sample can be thus called.

Single record of the response from the sample is usually hampered by very poor statistics, so the adequate experimental setups for such signals should provide sufficient signal to noise ratio for interpretation of obtained data. In a conventional femtosecond pump-probe experiment this problem is solved because typically a huge number of shots is averaged, and the noise on the response will essentially be dictated by Poisson statistics.[6] In addition, by applying normalization routines, in transient absorption spectroscopy for example the sensitivity can be increased to $10^{-5}$ ΔOD![6] In single shot spectroscopy, prohibiting this strategy, detectors with high dynamic range at least partially solve the problem of the signal to noise.

## 5.2 From imagination to application

### 5.2.1 Single shot with single wavelength

An interesting method was proposed by Poulin and Nelson.[1] In their experimental setup, a monochromatic beam was used to induce and detect changes in time. Dynamics of the process was monitored by delayed small parts of the beam, generated by echelons. The scheme of this system is presented in Fig. 5.1. In their experiment Poulin and Nelson monitored crystalline reaction dynamics of triiodine ion $I_3^-$ before the buildup of permanent photoproducts. Resolution of the experimental setup was determined by the step of the echelon and the total window for temporal observation by the dispersion of the echelon. The results of that experiment allowed for the confirmation of theoretical studies made on this compound.

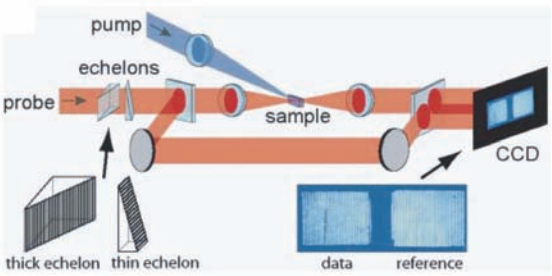


**Fig. 5.1:** Single shot experimental setup presented in [1]. Beam from the femtosecond laser was split in two. An echelon pair encodes time delay to each pixel on an imaging CCD.

### 5.2.2 Single shot with femtosecond white light probe

The scheme of the experimental setup based on chirped white light built and used during my Ph.D. study was described in chapter 6 ("Experimental"). Conceptual difference of this setup from that used in chapter 3 ("Spin-crossover transformation…"), on which essentially it is based, relied on the modifications which we made to make it work in the single shot regime rely on customizing the CCD for fast readout and implementing a shutter mounted on the pump path.

From the data recorded with the camera, we could extract each frame corresponding to a single acquisition of signal and reference pulse. Placing a shutter before the sample allowed opening the pump pulses at a desired instant, for instance after accumulation of a certain number of frames of an unexcited sample. Those pulses would typically serve for determining the baseline. Shutter was not synchronized with the laser and would open in 1 ms, and care was taken to disregard those spectra that were affected by an occasional and weaker pre-pulse. Those unwanted pre-pulses were removed during analysis due to shape of the affected spectra.

The shutter's open-close cycle was too long to prevent many more shots hitting the sample, hence we could not take postmortem "one shot" images using standard methods, i.e. microscope or standard camera.

#### 5.2.2.1 Detection system

Detection system was described shortly in chapter 3 and in details in chapter 6. In single shot measurements recorded frames were processed one-by-one and then indexed around the first pump pulse. Sensitivity of the single-shot experimental setup was better than 2% of change of the absolute signal. The dynamic range of the CCD was increased by cooling the chip to -75$^0$C, thereby limiting the dark current.

#### 5.2.2.2 Double reference method

Fig. 5.2 illustrates the sequence of pulses recorded in the experiment. For the signal analysis we used double reference method – described in chapter 3. The sequence of probe pulses before the pump was recorded to provide "baseline" for the response from the material, that is before the occurrence of the first pump pulse. Pulses after the occurrence of the pump are indexed for easier analysis.

The probe and reference pulses are indexed odd and even, respectively, with numbers 1 and 0 corresponding to the first shot coinciding with the pump. This drawing will be helpful for further description of the results from experiments, described below.

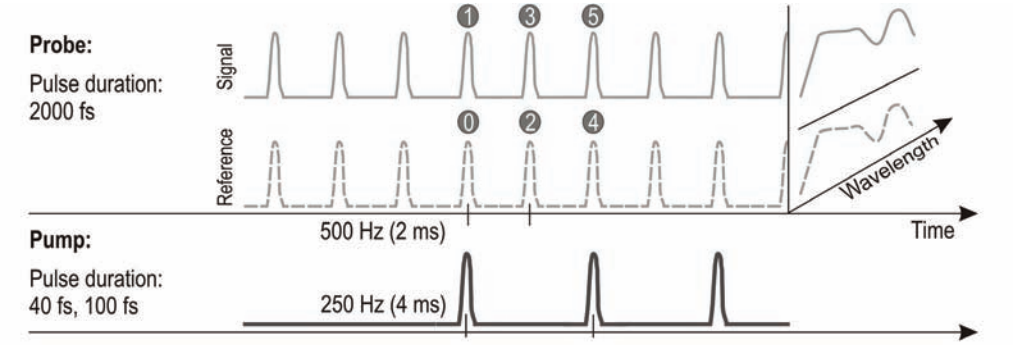


**Fig. 5.2:** Train of pulses enumerated in the single shot set-up. Red is the probe, green is the reference. Pump is shown at the bottom in blue.

### 5.3 "Dummy" experiment on a gold layer

For benchmarking single shot experimental setup, we carried out measurements on a 300 nm thick gold layer deposited on a dielectric substrate made of fused silica glass. We chose a metal, because laser induced reflectivity changes in the case of metals are expected to be spectacular, and the goal was to test the abilities of the experimental setup by detecting such changes. Gold was a perfect candidate because of its optical transitions in VIS region, resulting from the band structure – described further in the text. Also, by using a dielectric substrate, weakly reflecting VIS light, we had an excellent surface sensitive diagnostic for probing the physical state of the surface. Measurements made on a thin foil[4] would otherwise give a discrete information on the induced changes: 1 – reflectivity before and 0 – after the intense laser pulse impacts the metal.

Dielectric substrate was mounted on a rotation stage, to allow accurate determination of the angle between initial and reflected probe beam. Pump was directed parallel to the normal of the surface. Pump and probe were focused and overlaid on the sample, but the beam-waist of the pump beam was bigger. The idea was as follows: depending on the pump intensity, we observed either of the two cases defined as stroboscopic and irreversible.

The first case corresponds to the observation of reversible transitions on the gold layer, described in [7,8], induced by the pump pulse. After excitation, the energy of the pulse is transferred into the gold layer thereby increasing the electronic temperature of the metal. Hot electrons very quickly thermalize with the lattice through electron-phonon coupling. Both effects strongly modify the reflectivity spectra.

In this chapter we chose to use a double abscissa – energy and wavelength, because experiments are compared mostly with works from high energy physics and plasma physics. In this section photon energies are more adequate than wavelengths.

### 5.3.1 Interaction between metals and light

Metals are one of the best natural conductors of current and heat and are also characterized by high reflectivity coefficient. Theory explaining these features was introduced by Drude and then modified over the years. Main consideration was based on the free electron model, which means an electron plasma of valence electrons behaving like an „electron gas" between positively charged atoms of the crystalline lattice. This theory has for long satisfactorily explained the properties of metals. Further experiments revealed novel properties resulting from the differences between semimetals, semiconductors and insulators or materials with positive values of the Hall coefficient[9] – as a consequence, this model became insufficient.

New concepts took advantage of quantum mechanics and the dependence of the energy levels on the metal structure. That laid foundations for the "band structure" theory, where metals, semimetals and insulators have different representations on the energy diagram. This theory has also introduced the definitions of the valence band, the conduction band and the band gap between them, corresponding to forbidden values of electron energies, characteristic for each type of material.

To describe the number of states for the electrons per energy interval of each energy level, the density of states (DOS) was introduced. DOS diagram can be narrow or wide – depending on the material, and corresponds to the probability of absorption by an electron. The energy level of the highest occupied quantum state in the system at absolute zero temperature is called the Fermi level. At finite temperatures this value is changing and cause small changes in the absorption spectra of metals.

Strong absorption in metals, in most cases in far UV region of the spectrum,– is caused by a resonance with the electron plasma and that's also why metals exhibit good reflectivity in IR-VIS regions, but not in UV.[10] The plasma frequency in gold is equal 2.18 x $10^3$ THz, which translates to the absorption of photons carrying energy equal or higher than 8.98 eV.

Noble metals, like gold or cooper exhibit additional features in the absorption spectra. Namely they are coloured, which is the consequence of the inter-band transitions, called optical transitions, falling in the VIS region. It is shown schematically in Fig. 5.3a.[10]

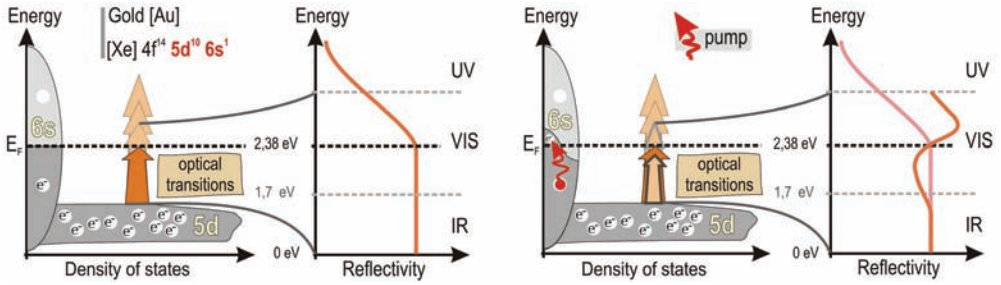


**Fig. 5.3:** A simplified schematic describing reflectivity of gold, based on the density of states (DOS) contributing to the inter-band transitions.

If we apply strong electric field in a short enough time, with a an intense femtosecond laser pulse for example, we will transfer a lot of energy to the electrons and consequently cause the electronic temperature to increase and thus modify the density of states around the Fermi level. Absorption spectra corresponding to this region will automatically differ from a stationary state, as shown in Fig. 5.3b. Modified DOS in the vicinity of Fermi level will cause changes of reflectance spectra of gold around 2,38 eV, , as indicated in Fig. 5.3b.[10,11]

### 5.3.2 Reflectivity spectra of the gold layer and the dielectric substrate

In order to better understand the results from the time resolved experiments we conducted stationary measurements to collect spectra from the gold layer and the dielectric substrate. Using a halogen lamp with monochromator as a light source, and a Lock-In amplifier we collected reflectivity spectra of the gold surface and the bare dielectric, for a set angle. The experimental setup is sketched in Fig. 5.4. The monochromatized beam was modulated with a mechanical chopper and collimated

with a lens. Modulation of the beam was required for the detection system (phase sensitive). The incidence angle of the beam in this experiment was equal to 45 deg to the normal of the gold surface, meaning it was the same as in the single-shot experiment. Obtained results were compared after analysis with the theory based on Fresnel equations. Each wavelength was detected independently. The automated measurement, controlling the monochromator and the Lock-In detector were realized with a LabView interface.

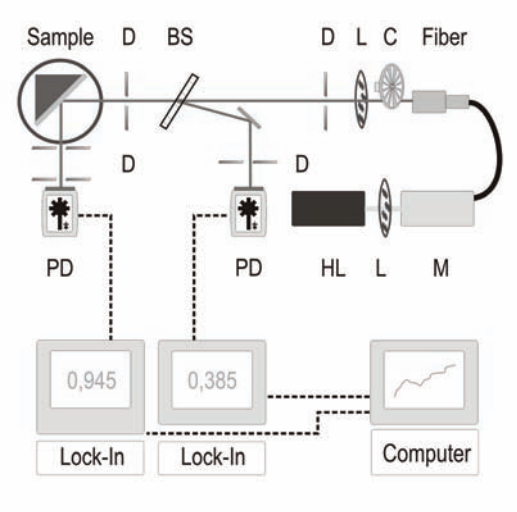


**Fig. 5.4:** Scheme of steady state experimental setup:

D – diaphragm
BS – beam splitter
L – lens
C – chopper
PD – photodiode
HL – halogen lamp
M – monochromator

The angle between the beam splitter, sampling off a fraction of the incidence beam for normalization purposes, and the incident beam was small enough, below 10 deg, to obtain a non-modified intensity of the whole spectrum irrespective of the polarization. Lock-In detection used here was described in details in chapter 6 ("Experimental").

#### 5.3.2.1 Results from steady state measurements

Fig. 5.5 shows, reflectivity spectra of the gold layer deposited on the dielectric substrate, as well as the reflectivity of the substrate itself for different polarizations of the incident beam. Symbols represent the theoretical data points expected for the substrate.

The small changes of the intensity near 1.7 eV observed in Fig. 5.5 are due to sudden drop of the extinction coefficient of the Polaroid we used to polarize the light from the source.

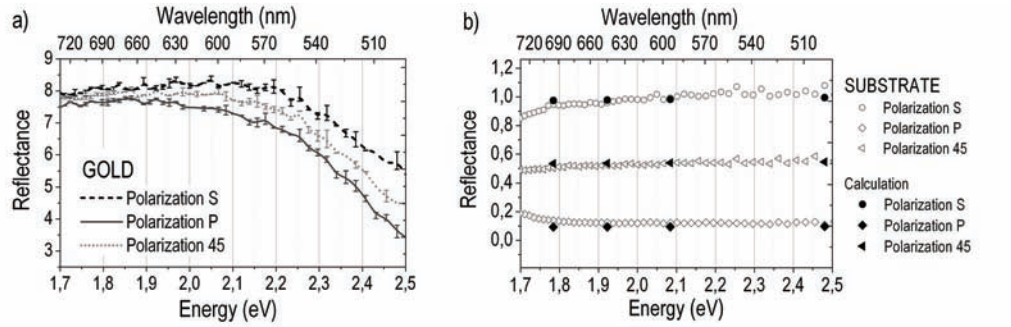


**Fig. 5.5:** Stationary reflectance of **a)** substrate and **b)** gold

Fig. 5.6 shows a comparison of results obtained from reflectance of white light (solid line) with steady state data points obtained by independent methods: steady state measurements (open circles), and Fresnel equation (full circles). As for the reflectance of white light, we normally applied double reference to determine the spectra. In this case we took only 20 frames from a time resolved experiment, when no pump occurs on the gold layer (shutter closed), which we averaged by using single reference, according to eq. (3.12). Spectra thus obtained were scaled to the values calculated using theoretical model, and the scaling factor was equal 0,117.

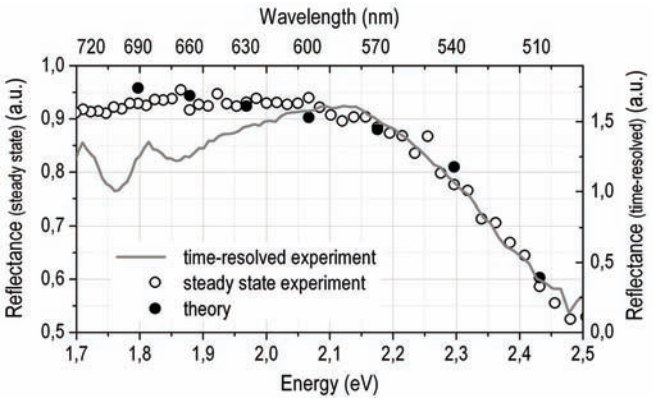


**Fig. 5.6:** White light experiment and steady state results. Plot is presenting changes in reflectivity of gold without excitation monitored by three methods: stationary spectra, theoretical calculations and time resolved without pump – analysis described in the text.

## 5.4 Laser induced effects on the gold layer, the stroboscopic regime

Time-resolved stroboscopic experiments were typically carried out with the energy of the pump around 12 μJ. Fig. 5.7a we shows a typical plot of raw data obtained directly from the camera, before the analysis. Two distinguishable bundles of curves correspond to the probe and the reference spectra. Because the pump and the super-continuum chirped probe have distinctly different pulse durations, 100 fs and 2000 fs respectively, we had to define "zero time" between the pump and each wavelength component of the probe.

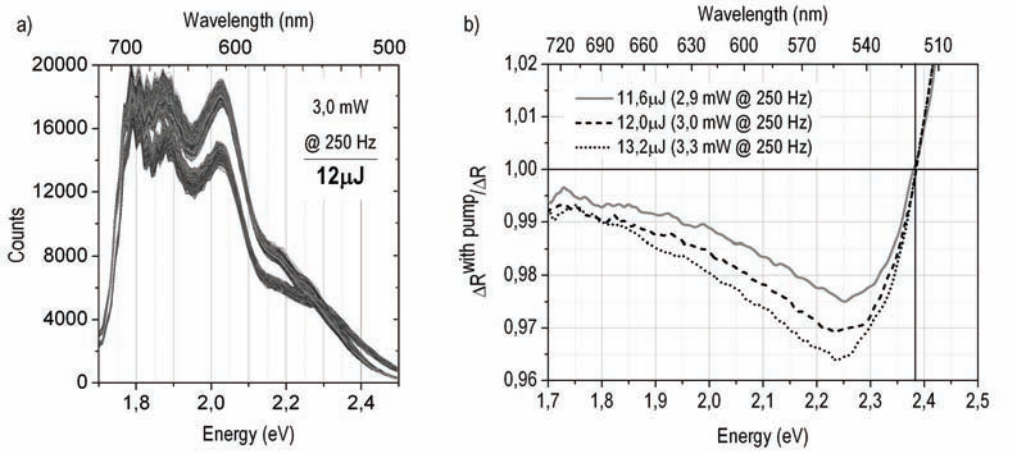


**Fig. 5.7: a) S**pectra taken directly from the CCD camera. Two family of curves corresponds to signal and reflectance. **b)** Monitored changes of reflectivity due to energy of the pump (energy induced reversible processes).

Fig. 5.7b presents the spectra from Fig. 5.7a after analysis and averaged over 10000 frames. This figure shows a snapshot of modified reflectance 6 ps after excitation, reversible at these energy levels. If we compare theoretical and experimental studies from literature,[2,12] we can conclude, that the observed signals correspond to the cooling of electronic temperature, inflicted by of the laser pump. Fermi level of gold is around 2,38 eV,–which Fig. 5.8 and Fig. 5.9 illustrate clearly.[5,8] The figures show the electronic occupancy about the Fermi level at different temperatures, as well as the corresponding reflectivity spectra. Earlier studies[7,8] suggest that during initial 10 ps following the excitation during the first 10 ps photon energy is transferred into electronic temperature.[7] According to the two temperature model, the electrons cool down by releasing heat to the lattice, which causes the observed transient reflectivity change.

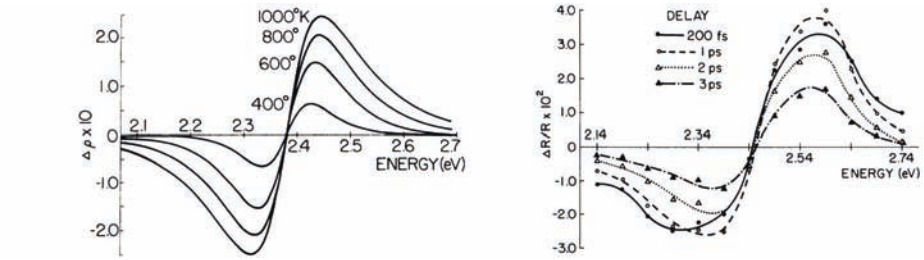


**Fig. 5.8:** Left, calculated changes of electronic occupancy about the Fermi energy for different electronic temperatures. Right, change of reflectivity from the gold surface versus energy for different delays between pump and probe, taken from [8].

Because the probe pulse is chirped, it is possible to monitor relaxation process during 2 ps window allowed by the chirp. These changes were monitored across a broad spectral range. Fig. 5.9 shows also DOS of *d* and *s*/*p* electrons, directly comparable with Fig. 5.3, and the two together relate the electronic temperature to the laser excitation. Using this comparison, the electronic temperature after excitation could be roughly estimated to around 1000 K.

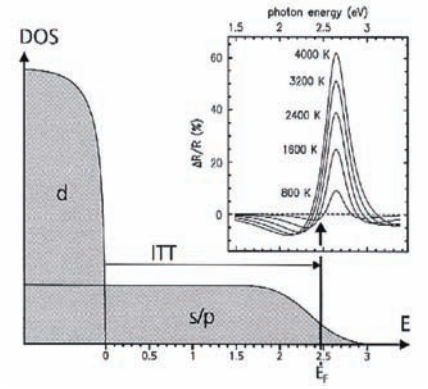


**Fig. 5.9:** DOS (Density of States) and changes of relative reflectivity due increased temperature of gold[7] after excitation. ITT – inter-band transition threshold.

## 5.5 Single Shot on the gold layer, the irreversible regime

In this part of work we discuss a feasibility of measuring irreversible reflectivity changes after just one laser shot. Photographs taken after the experiment testify the irreversible damage on the gold layer, however no information on the number of shots necessary to inflict such damage is available with the imaging method. The laser shutter operated only in an off-on o mode: closed-without the pump and open-with the pump. The shortest open-time imposed by the shutter's inertia did not allow shutting down after one shot. The surface state seen under microscope was

that after several hundreds of shots. Fig. 5.10 shows comparison between two kinds of single shot experiments the only difference being the energy of the pump, 0.022 W and 0.23 W. Detailed description of this experimental setup is given in chapter 6 ("Experimental"). The reflectivity spectra from this experiment are presented on Fig. 5.11.

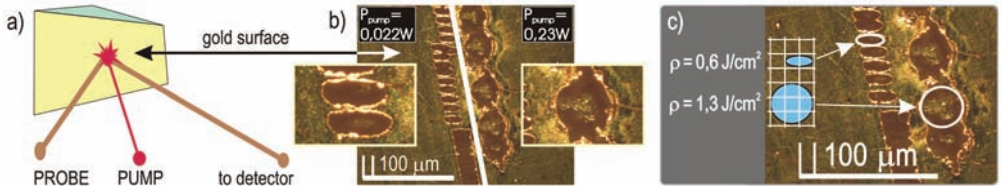


**Fig. 5.10:** Photo of the gold surface taken under the microscope. **a)** View of the prism with pump and probe beams. **b)** Photographs of the holes made by the two different energy pulses. **c)** Calculation of the excitation density at two different energies of pulses.

The excitation density in both cases was calculated assuming a Gaussian beam on the surface. The calculated values were enough to melt the gold layer. In second case the energy was much higher, and permanent changes to the substrate could also be observed.

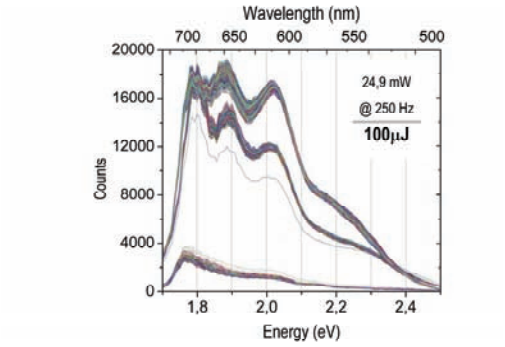


**Fig. 5.11:** Typical plot obtained from the single shot experiment within the chirped probe spectrum. Power of the pump was equal 0.025 W. Note the sudden change coinciding with the first pump pulse.

A graphical analysis of the spectra is shown in Fig. 5.12. As was mentioned at the beginning of this chapter, the camera records every single frame (shot) separately. The analysis of the results from the second part of the record, that is when pump was present on the sample, reveals that changes are seen but only between curves 1 and 5 (3 shots). Spectrum 1 corresponds to the first probe pulse after the impact of first pump pulse. The pump pulse hits the sample within the temporal envelope of the chirped probe, and the probe wavelength coinciding with the pump in this particular shot was equal 680 nm. Spectrum 3 is that of a sample surface 2 ms after the impact of the first pump, and shows a huge drop in reflectivity. Spectrum 5

shows the reflectivity of the surface during the impact of the second pump pulse, and reveals a slight increase compared to 3. The following spectra show no more change. We tentatively describe the above observations in the next section.

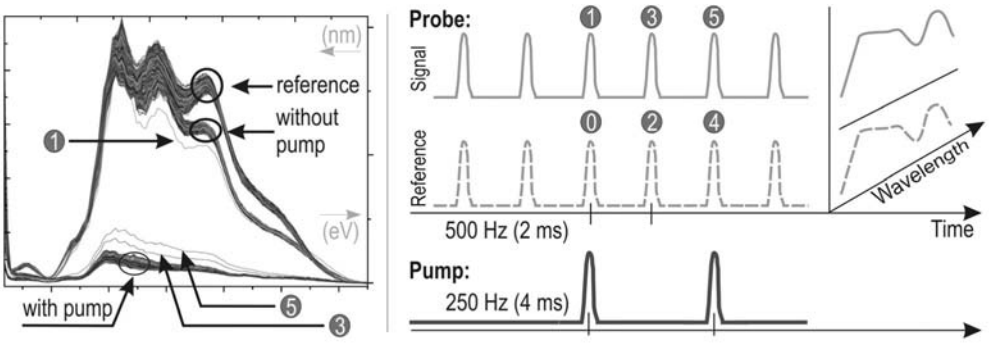


**Fig. 5.12:** Left, typical raw spectra obtained from the camera in the single shot experiment, description provided on the curves. Right, "translates" the left plot in terms of the pulse sequence.

### 5.5.1 Single shot or not?

As for the interpretation of the recorded physical phenomenon, at this stage we can only speculate on the mechanisms causing the observed dramatic changes in reflectivity. However, we can be certain of the removal of gold layer following a single intense laser shot, as demonstrated below. After an intense laser pulse, the electronic temperature on the gold surface reaches temperatures exceeding critical values for melting or even ablation, and the densities we used in this experiment fall in that critical range. Spectrum 1 is a histogram of this event by mapping wavelength-to-time, and in this sense is very similar to a by Lindenberg et al.[2] In that study, the authors mapped space-to-time, by creating a temporal sweep with beam-crossing the pump and the probe on a crystal surface. They were able to record a topological histogram of a molten InSb crystal, and argued that the material for the first few hundred femtoseconds is in an intermediate phase between solid and liquid. In our study on gold the temporal sweep is given by the chirp, and the making of the femtosecond histogram is described in the following section. At this stage, we shall not speculate beyond saying that the Spectrum 1 is that of gold with a potential softened to the points where atoms are free to move. This suspected softening has a dramatic effect we recorded with the spectrum 3, which is a lot simpler to model. We expect this spectrum be the reflectivity of the dielectric substrate stripped of the gold layer by the intense laser pulse. We prove the above it two ways. The first

approach, consisted in dividing the spectrum of the second probe pulse (3), that is after the impact of the first pump pulse by the spectrum from the pulse preceding the pump. The exact procedure is illustrated in Fig. 5.13, which essentially is the double-reference method described earlier.

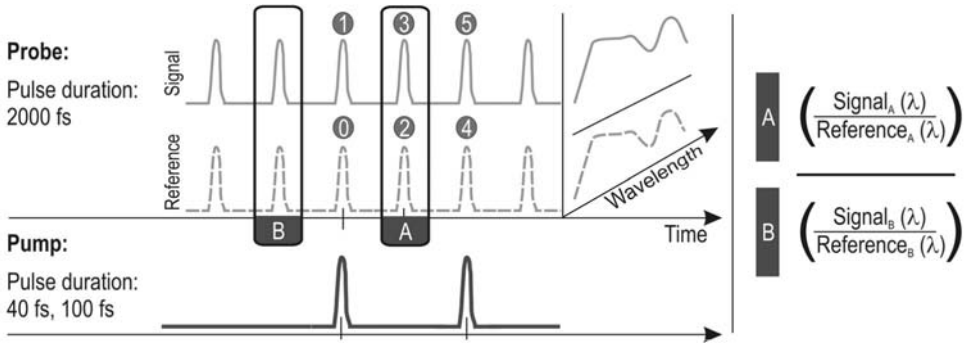


**Fig. 5.13:** A schematic of the analyzing method: to obtain information about the reflectance after the pump pulse, the spectra after a single shot (frame A) were divided by the spectra preceding that shot (frame B).

Obtained relative spectral change was compared with the expected relative change calculated for the hypothesis when dielectric substrate replaces gold – see Fig. 5.14 (right-hand panel). In the second approach, the relative reflectivity change recorded by pulse (3) was compared to the steady state measurements of the reflectivity change between the substrate and gold, of exactly the same sample as used in the single shot experiment, Fig. 5.14 (left-hand panel). This doubly verified hypothesis supports the feasibility of a single shot detection of irreversible processes with the current setup. We emphasize that such demonstration was the prime goal of this study. For the sake of thoroughness, we have to comment on spectrum 5, which in view of the earlier conclusion, is that of the dielectric under intense a laser pulse. In such a case, it is expected that the intense laser generates plasma on the surface of the dielectric, thereby increasing the reflectivity of such surface. The Drude model describes this phenomenon from first principles. To round off the observations in Fig. 5.12 we can rather safely assume that all spectra following 5 are those of laser damaged dielectric surface, therefore diffusive reflectivity of the incident light, rather than Fresnel reflectivity, contribute to the recorded spectra. In support of this argument, we observe almost no further spectral evolution after the impact of two consecutive intense laser pulses.

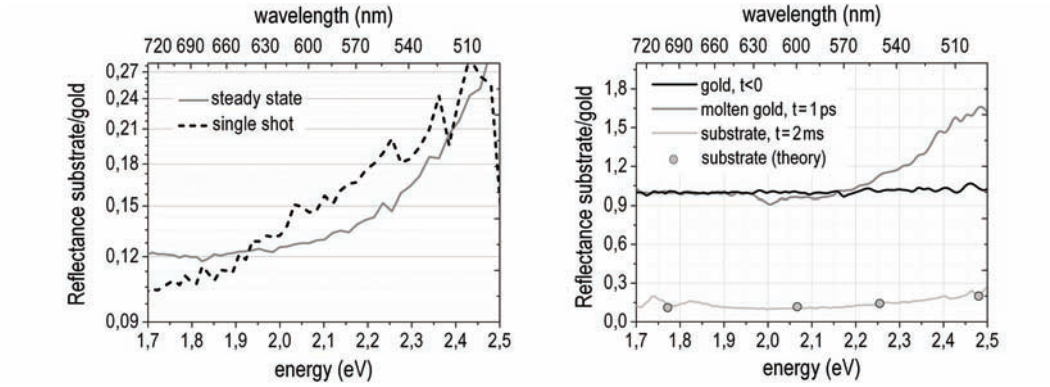


**Fig. 5.14:** Left, comparison between the spectra obtained from the steady state measurements and the spectra from time-resolved measurements. Right, comparison between the spectra time-resolved measurements at different time delays with calculations (symbols).

### 5.5.2 Ultrafast dynamics under intense pulse

In Fig. 5.15, we focus on retrieving the histogram of the potential softening of solid gold under critically high fluency, by mapping the energy of the incoming photon to time. The probe spectrum is chirped, meaning the photons of different energies hit the surface at slightly different times.

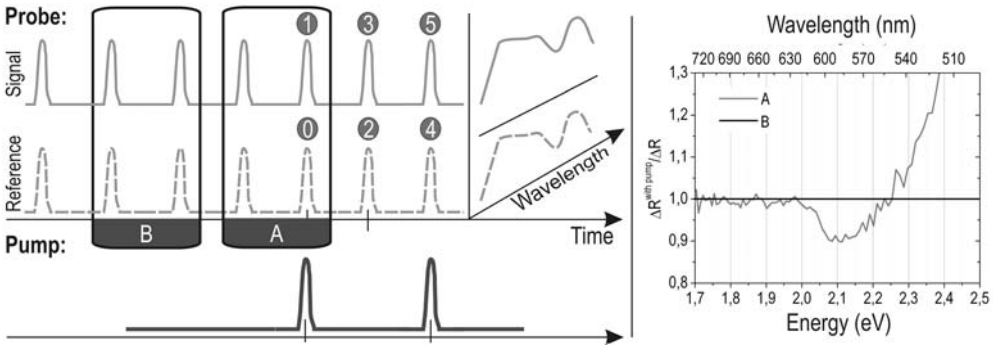


**Fig. 5.15:** Double reference between response from the pulses before pump occurrence (frame B) and from single shot measurements (frame A). For simplicity on the plot we consider that results from the frame B will be approximately equal to 1 (black curve on the plot).

We determined this chirp in a separate experiment by following the cross-phase modulation in a thin glass window (chapter 6: "Experimental"). Thus obtained chirp is shown in Fig. 5.16a with blue symbols. We recorded a series of single-shot frames, each at a slightly different pump-probe delay. Fig. 5.16b. This figures shows clearly

the onset of time-resolved signal move towards low energy photons (or red-shifts) as time passes. This onset can be very accurately overlaid with the chirp of the white light probe. Fig. 5.16, thereby illustrating that the recorded single-shot data reflect the ultrafast dynamics of strongly modified band structure of gold, possibly molten already despite a very short time-scale.[2] We believe that the observed dynamics are precursor to the irreversible collapse of solid gold structure, proven in the previous section. Further claims without support from theory would be unfounded, nevertheless we would like to point to strong features revealed by our data. Namely, the band gap at 100s fs time-scale seems significantly narrowed, from 2.38 eV expected for solid gold to ~ 2.2 eV in our measurement.

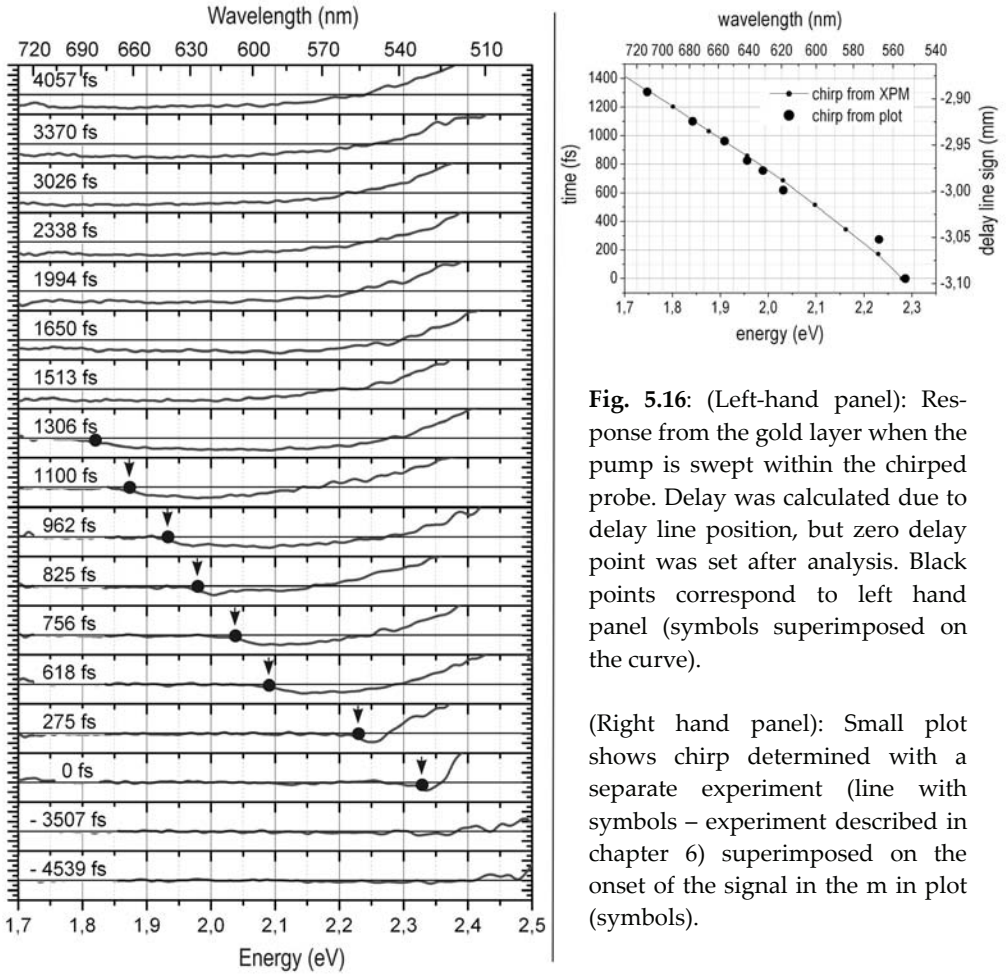


**Fig. 5.16**: (Left-hand panel): Response from the gold layer when the pump is swept within the chirped probe. Delay was calculated due to delay line position, but zero delay point was set after analysis. Black points correspond to left hand panel (symbols superimposed on the curve).

(Right hand panel): Small plot shows chirp determined with a separate experiment (line with symbols – experiment described in chapter 6) superimposed on the onset of the signal in the m in plot (symbols).

Let us remind that the reflectivity with low fluency, Fig. 5.7b, shows exactly 2.38 eV therefore any systematic error can be excluded in our band gap determination. Secondly, the reflectivity of gold under high fluency reveals a uniform distribution of depleted DOS below the Fermi level, rather than resembling a Gaussian expected from thermal distribution of DOS around the Fermi level. All spectra in Fig. 5.16, recorded at times later than 1500 fs unambiguously reveal this strongly perturbed DOS.

## 5.6 Conclusions

The single shot experimental with our setup based on chirped white light proved feasible and allowed recording a temporal sequence of an irreversible process. We observed that a single laser pulse of high fluency strips a dielectric surface of its gold layer. However, the interpretation of collected data from single shot measurements requires more analysis and certainly a valid theoretical model. Fig. 5.17 (next page) illustrates some of the hypothesis put forward at this early stage of analysis. The single-shot setup presented here promises new insights into the physics of phase transitions, and the first attempts on molecular solids have been undertaken.

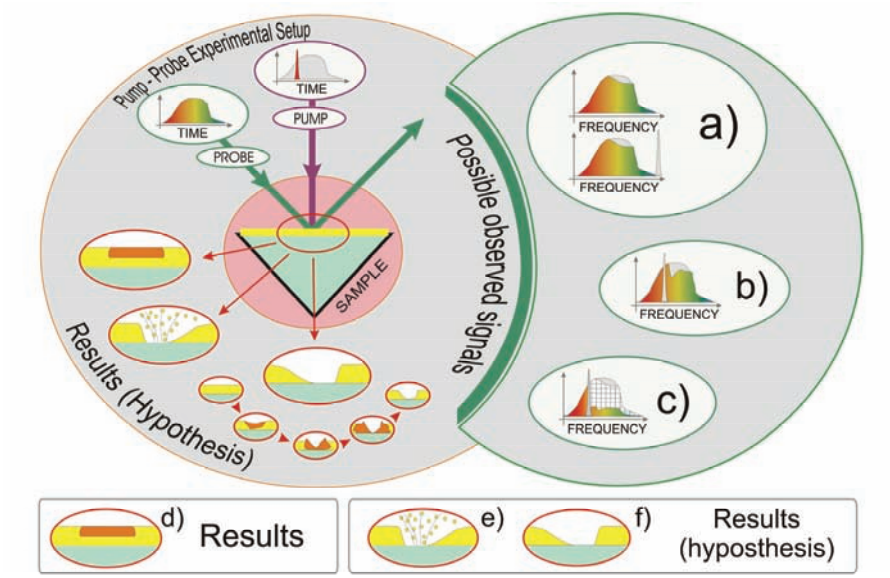


**Fig. 5.17:** Pump – probe experimental setup with supercontinuum light as a probe is schematically shown on the left side. Spectra of the probe and pump pulses were exceptionally presented versus time, because probe light was chirped and with comparison with the pump it was almost 20 times longer – see grey shape of the probe light with comparison with pump pulse. Second plane – on the right - corresponds to spectra (in frequency domain!) of reflected light in different observations.

**a)** On the plot we can see comparison between reflected light and initial pulse – indicated here as a colorful and grey shape. Spectra are different, because gold has got yellowish color, due to its band structure – explained in the text. Situation on the plot a) occur when: no pump occur on the sample or delay between pump and probe is big enough that relaxation processes in the gold after excitation are finished.

**b)** Different spectra between initial pulse and reflected light were observed after reversibly gold excitation by the pump. Lattice was very hot but able to relax (shape of reflected light also explained in next paragraph due to band theory of solids). What happened with gold layer is schematically shown on **d)** – matter became hot, but able to cool down without changes of its structure.

**c)** Single shot measurements. Grey shape corresponds to initial probe pulse. Crossed background corresponds to spectra, which would be seen in situation b), but energy was high enough, and lattice hadn't relax. What happened with gold layer trying explain part **e** and **f**. Situation is complex, that's why this is only hypothesis.

**e)** *Hypothesis 1:* ablation process, observed as a consequence of interaction between femtosecond pulse and matter. Gold particles are pulled out from the layer.

**f)** *Hypothesis 2:* corresponds to non-thermal melting, when layer is very hot, it start to melt and due to pressure occur at the center of the beam it starts to create a crater.

**References:**

[1] P. Poulin et al., *Science* **313**, 1756 (2006)
[2] I. Lindberg, *Science* **310**, 5750 (2005)
[3] P. Musumeci, *J. Appl. Phys*. **108**, 114513 (2010)
[4] R. Li. Chuang et al., *Rev. Sci. Instrum*. **81**, 036110 (2010)
[5] G. Galle et al., *Appl. Phys. Lett*. **96**, 041907 (2010)
[6] R. Naskręcki - *Femtosecond transient absorption spectroscopy. Photophysical study of the excited states of molecules and short - living individua*, Wydawnictwo Naukowe UAM, Poznan (2000)
[7] J. Hohfeld et al., *Chem. Phys* **251**, 237 (2000)
[8] R.W. Schoenlein et al., *Phys. Rev. Lett*. **58**, 1680 (1987)
[9] C. Kittel, *Introduction to solid state physics*, PWN, Warszawa (2001)
[10] M. Fox, *Optical properties of solids*, OXFORD (2001)
[11] J. Singleton, *Band Theory and Electronic Properties of Solids*, OXFORD (2001)
[12] R. Ernstorfer et al., *Science* **323**, 1033 (2009)

Chapter 6:
# Experimental

# 6 Experimental

This chapter was devoted to detailed description of the experiments made during my Ph.D. study. Intentionally it was put at the end of this thesis despite the essential part of work being dedicated to the experimental developments, aimed at time-resolved studies of the photo-induced phase transitions. Our intention was to bring out the science first, and leave for the end the complexity of technical solutions. The single shot experiment (chapter 5) was set up for new applications, which began after my Ph.D. work. They are primarily concerned with new spin-crossover compounds, and are a subject of an ongoing project.

In this chapter was presented all instrumental developments used during this work, such as two detection systems (monochromatic and polychromatic), synchronized amplifiers delivering pulses at programmable delays covering 10 decades on the time scale, as well as the single shot technique.

## 6.1 Laser source used in experiments

Scheme of the complete laser source, including the electronic trigger signals was presented in Fig. 6.1 (next page). This laser setup consists of a femtosecond oscillator (Mira, Coherent), two regenerative amplifiers (Legend USP, Legend Elite II), and four OPA's (Topas, Positive Light, Coherent) delivering wavelengths "on call" from IR to UV region. To avoid dust and instabilities due to temperature fluctuations, the source was placed in a dedicated hutch with clean air.

### 6.1.1 Birth of a femtosecond laser pulse

The idea of a femtosecond experimental setup, such as ours, was introduced in 1980's,[1] and since the components have been continually improved for stability and power. Pulses in our experimental setup were produced by the femtosecond oscillator Mira Seed (Coherent), in Ti:Sapphire crystal, pumped by a cw laser Verdi (Coherent). Ti:Sapphire crystal exhibiting broad absorption and emission spectra was a revolution almost 30 years ago for the ultrafast laser systems.[2,3,4] When such material is put inside a laser cavity, thanks to mode-locking it starts generating trains of pulses, of which the time duration is as short as femtoseconds. Interpretation of this phenomenon came from nonlinear optics. Due to Optical Kerr Effect (OKE), induced in a small volume delimited by the propagating laser beam in

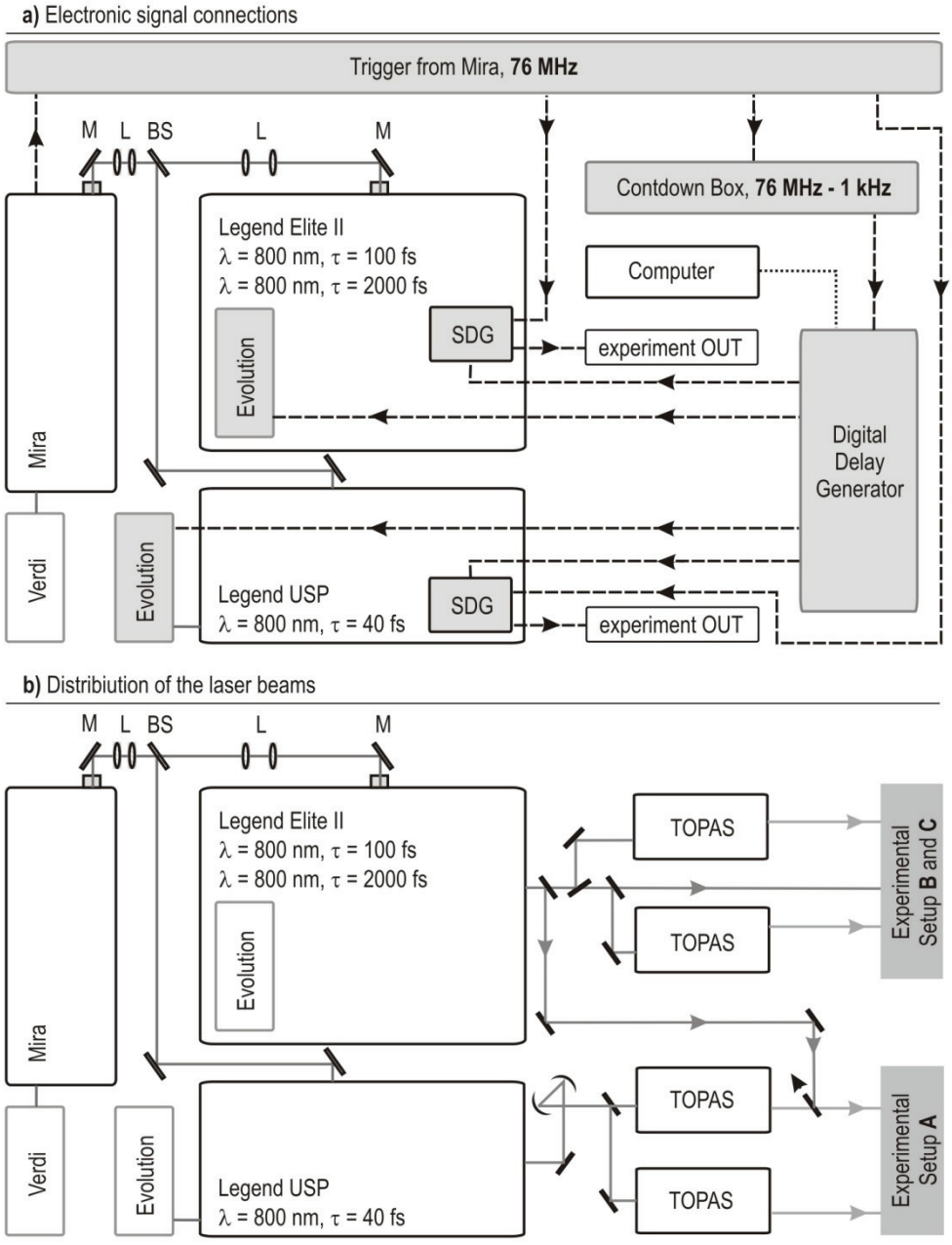


**Fig. 6.1:** General scheme of the laser source working in synchrony: a) electronic connections and triggering signals synchronized with seed laser (Mira) and Regenerative Amplifiers (RGA). Detailed discussion about synchronization process was presented in § 6.2.1.2.

the crystal, the intensity is strong enough to change the value of the refractive index.[5] In a consequence, the beam self focuses, and the cavity can be designed such that the gain will be preferentially saturated with a narrow beam. For example, by placing slits at the focus of OKE the mode-locking can be maintained for a long a and stable operation. Mira delivers laser pulses with frequency 76MHz, on the wavelength around 800 nm (40 nm FHWM), and pulse duration 35 fs.[6]

### 6.1.2 Amplification of the femtosecond pulse

Regenerative amplifiers (RGA) have also been known for many years now.[7] In amplification of a femtosecond pulse we can distinguish three processes: stretching the spectrum of the pulse, its amplification and finally compressing. Fig 6.2 illustrates the birth of a femtosecond laser pulse.

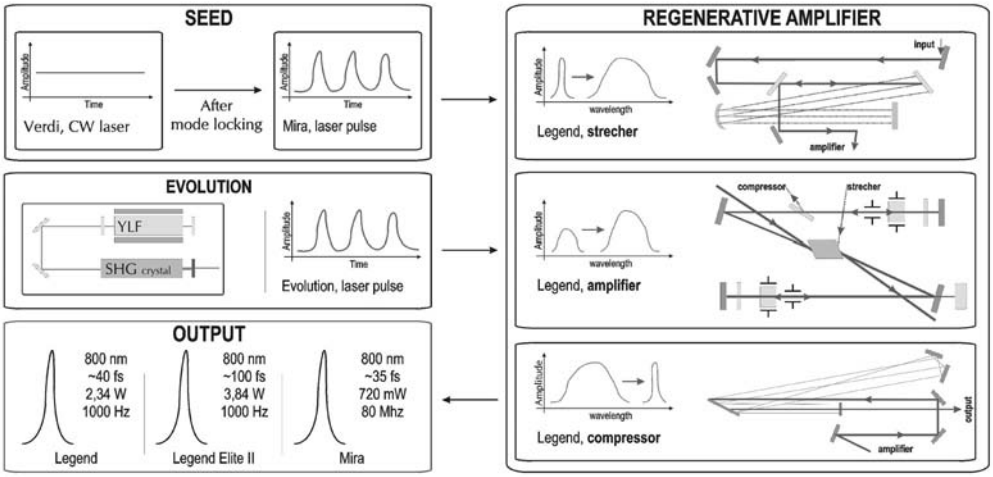


**Fig. 6.2:** Main idea of the femtosecond laser setup used in experiments. Left part corresponds to laser beam characteristics: from seed laser (Verdi) and Evolution which amplifies weak femtosecond laser pulses from the femtosecond oscillator. Right part corresponds to physical aspects mentioned in the text: from stretching the spectrum, amplification process and finally, compressing part. Each of them was shortly described in the text.

*Stretcher.* If we were to amplify a femtosecond laser pulse directly from the oscillator, the peak power would damage the optics. That's why in the first step we have to stretch the pulse spectrally using gratings and only than amplify it. The gratings cause one edge of the pulse travel ahead of the opposite edge due to dispersion of the gratings.

*Amplifier.* Amplification process inside the cavity is essentially realized with two Pockels cells, and a gain medium (crystal pumped by the pulse laser – Evolution (Coherent)). Pockels cells are a kind of gate, which are open and close at a well defined time. The cells and the pumping laser are controlled by synchronizing unit (SDG – compare to Fig. 6.1). The pulse makes around twenty round trips in the cavity to saturate the gain. Temperature of the depends on the output power of the laser. In Legend USP the temperature is 0°C, but in Legend Elite II – it's lower, equal to -10°C.[8,9]

*Compressor.* Amplified pulse is compressed in a compressor, of which the operation principle is similar to that of the stretcher, except that it reverses its action. Output power and time duration of the pulses from the RGAs were different. In Legend USP we obtained 40 fs pulses with average power around 2 W.[8] Second laser (Legend Elite II) delivered 100 fs pulses with 3.5 W[9] output power. Repetition rate of the pulses is 1 kHz, but there is possibility to divide this value with the SDG unit. Otherwise, the optical choppers are used to slow down the repetition rate.

*Idea of lasers in synchrony.* In a standard femtosecond laser system the SDG unit controlling amplification process is triggered by 1 kHz signal from the pump laser in phase with the pulses at 76 MHz from the oscillator. In our experimental setup, we installed an external delay generator unit controlling both SDG's, to obtain synchronization between lasers, described below. Fig. 6.1 depicts the signal (electronic) connections in our experimental setup.

### 6.1.3 OPA – "wavelength on call"

For tuning the wavelength to optimize the excitation, we were using Optical Parameter Amplifiers (OPA), from Light Conversion (Topas C) from which we could obtain any color of the beam, between near-IR up to UV light by mixing signal, idler and fundamental beams. To filter unwanted beams propagating through the OPA, we were using band pass filters (CVI, Melles Griot or ThorLabs). To reduce the power of the beams we were using neutral filters (Melles Griot).

## 6.2 Detection systems

During my Ph.D. work we were using two kind of detection systems: Lock-In detection system was based on two-color experiment (pump and probe), whereas the broad bandwidth detection (one color for the pump and white light for the

probe) was based on a CCD camera and a monochromator. Second type of detection system was also employed to single shot measurements.[10] Description of detection systems corresponds to measurements made during studies.

### 6.2.1 Monochromatic detection

In two color pump - probe experimental setup we were using photodiodes (InGas, Si-silica, from ThorLabs, depending on the probe wavelength) feeding photocurrent directly to the Lock-In Amplifier. Excellent S/N ratio, with the noise floor $10^{-5}$ of the absolute signal[10,11,12] allowed measurements of changes of optical density in spin-crossover compounds (see chapter 3, "Spin-crossover transformation…"), and modulation in reflectivity in $(EDO\text{-}TTF)_2SbF_6$ (see chapter 4, "Photo-induced phenomena…").

#### 6.2.1.1 Lock-In Amplifier detection system

Lock-In amplifier is a phase sensitive detection system requiring that the analyzed signal be in phase with a reference signal. We were using Stanford research Lock-In amplifier, model SR 830, triggered by the frequency of 500 Hz from a divider box (countdown signal from the laser at 1 kHz).

*Idea of the Lock-In detection*. In a good amplifier signal from the measurement can be filtered from the noise with 100 Hz gain. Lock-in amplifier can bring this value down to 0.01 Hz, which is crucial when the sought signal changes are very weak riding on top of a strong signal. Lock-In provides a reference frequency phase-locked to the signal from the experiment. Fig. 6.3 depicts the idea of dual phase locking allowing to demodulate the amplitude of the absolute signal, R (eq. 6.1). In brief, Lock-In generates a sine reference from the reference provided by the experiment. Then the signal from the experiment is modulated by this internal reference. As a result, we obtain AC signals with the two different frequencies ($\omega_{ref}+\omega_{sig}$, $\omega_{ref}-\omega_{sig}$). Those signals are removed by the low pass filter, as a result only DC signal is amplified, provided the signal and internal reference have the same frequency. In reality, the signal is affected by the noise, and the lock–in will amplify signal components of frequencies close to the reference. The time constant of the low pass filter will determine the bandwidth of the filter. That's why it is important that the signal from experiment be in phase with the reference, because if the phase varies continually, the RC filter will stop the AC signal rather than passing it for amplification.[12,13,14]

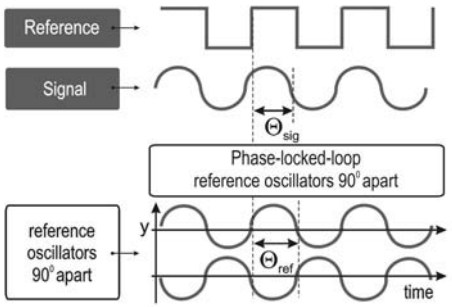


**Fig. 6.3:** Scheme of the signals in Lock-in amplifier technique. Green curves correspond to experiment, blue one – to internal signals of the Lock-in's oscillator. Phase between signal and reference is setup by phase-looked-loop (PLL).

Fig. 6.5 shows an example of cw light, modulated with a mechanical chopper at different frequencies. We simulate the Lock-In amplification process by Fourier Transform (FT) analysis of the frequency content of thus modulated real signal. We plot the resulting frequency spectra and different low pass filters used. The effect of attenuating the noise and amplifying the signal's fundamental component is thus graphically explained. The degree of noise attenuation clearly depends on the time constant of the RC filter.

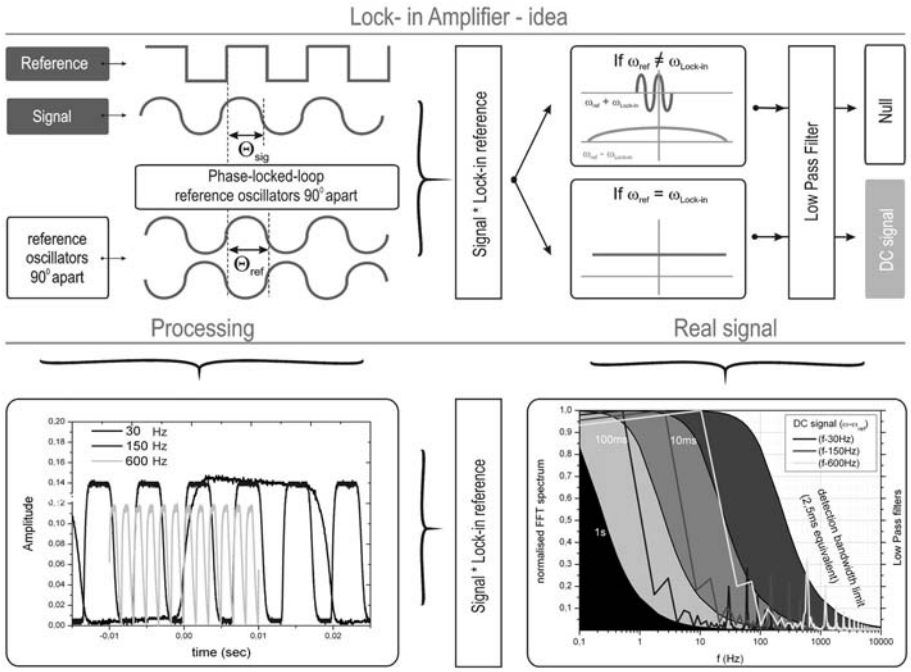


**Fig. 6.5:** Idea and scheme of the signals in Lock-in amplifier detection technique and idea of analysis. Signals in lower part of the scheme correspond to signals obtained in real experiment and analyzed by methods adequate to Lock-In procedures.

The most important part of this amplifier is the phase sensitive detector, PSD, which uses phase locked loop (PLL) fixing frequency of the internal oscillator to the reference frequency. Model SR830 is a "dual phase lock-in", generating two outputs, proportional to $\cos(\theta_{sig} - \theta_{ref})$ and $\sin(\theta_{sig} - \theta_{ref})$ whereby phase independent amplitude of the signal can be measured according to:

(6.1) $$R = (X^2+Y^2) = v_{sig},$$

where $X = v_{sig} \cos\theta + v_{sig} \sin\theta$. In addition, for our time-resolved measurements we chose to heterodyne the signal, schematically illustrated in Fig. 6.5. The signal from the photodiode has 1 kHz frequency, the same as the probe light, but the photo-induced signal has the frequency of the pump light, 500 Hz. The Lock-In, as well as the mechanical chopper of the laser pump, were triggered by the common signal from a divider box (500 Hz), itself triggered by the 1 kHz laser. To subtract the noise from laser fluctuations (typically 1-3 % RMS) , which contributes equally to the fundamental and the harmonics of the signal's Fourier spectrum, we worked with two balanced photodiodes (A from the probe beam, B from the reference beam) and set the lock-in input to A-B mode. During the experiments we recorded the photo-induced differential signal (ΔR or ΔOD), but also the absolute signal (R and OD). In the first mode, A-B, we obtained signals on the order of 1 mV with noise below μV. In the second mode, A, typical signals were around 10s of mV with noise at mV level, reflecting the RMS fluctuations of the laser mentioned above and measured with a thermopile detector.[11,16]

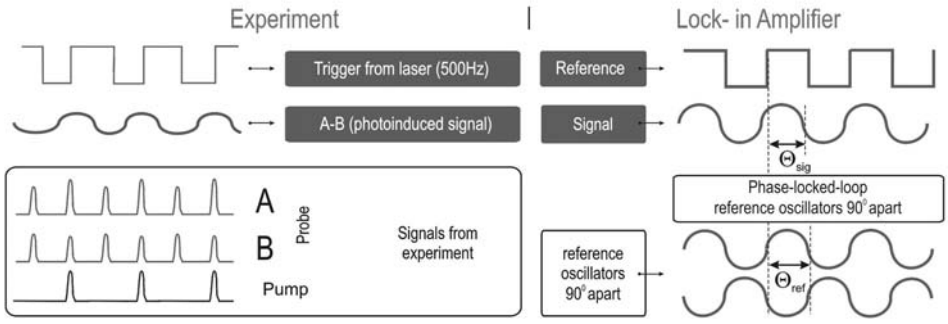


**Fig 6.5:** Idea of heterodyne detection exploit in our experimental setup. Left part corresponds to signals obtained from the experiment. Right part corresponds to Lock-In simple idea of detection.

6.2.1.2 Experimental setup used in measurements

*$(EDO\text{-}TTF)_2SbF_6$ measurements.* Pump-probe experimental setup used in the measurements with two colors was shown in Fig. 6.6. Beams from the OPAs were steered onto the two optical delay lines. First one for the probe was fixed, and the second one was variable. The fixed delay line compensated the optical path difference between pump and probe. The second delay line, Newport M-ILS 250CCHA,[16] was additionally equipped with a hollow corner cube. Maximum time delay available by this mechanical delay line was 1.6 ns with a single round-trip, and the shortest mechanical step equivalent to around 1 fs. The Pump was modulated by a chopper at 500 Hz and its power continuously variable with a neutral filter. Metallic or dielectric mirrors (Thorlabs, CVI) were used for beam steering. The probe beam was split in two with a ratio of 95/5. The weaker of the beams was used as reference. The stronger one, was used as signal. Pump and probe were polarized parallel to the long crystal axis and spatially overlaid on the sample surface with the aid of a microscope objective (InFocus, model KC, Infinity, NA = 0,05).[10] Final resolution of the experiment was determined by the pump and probe cross-correlation and was equal 80 fs at FWHM.

Pump and probe beams were focused by the lenses of 500 mm and 200 mm focal lengths, respectively. At the focal plane, that is on the crystal, the probe was smaller than the pump. As mentioned in chapter 4, a collinear geometry between pump and probe beams was used with a $2^0$ wedged to window to avoid ghosting on the sample. Crystals in temperature range between 100 K and 240 K were cooled down by an open jet cryostream, described at the end of this chapter. For experiments requiring temperature range from 10 K to 100 K, we used a close cryostat filled with helium gas.

The signal from the sample was focused on the signal photodiode by a lens with 50 mm focal length. The scattered or reflected residual pump light was stopped by band-pass filters (CVI) or color filters (Melles Griot). Change of the reflectivity was detected by the phase sensitive Lock-In amplified described above. The repetition rate of the laser pump was 500 Hz, and the probe's was 1 kHz, thereby allowing to heterodyne the laser pump induced signal.[16]

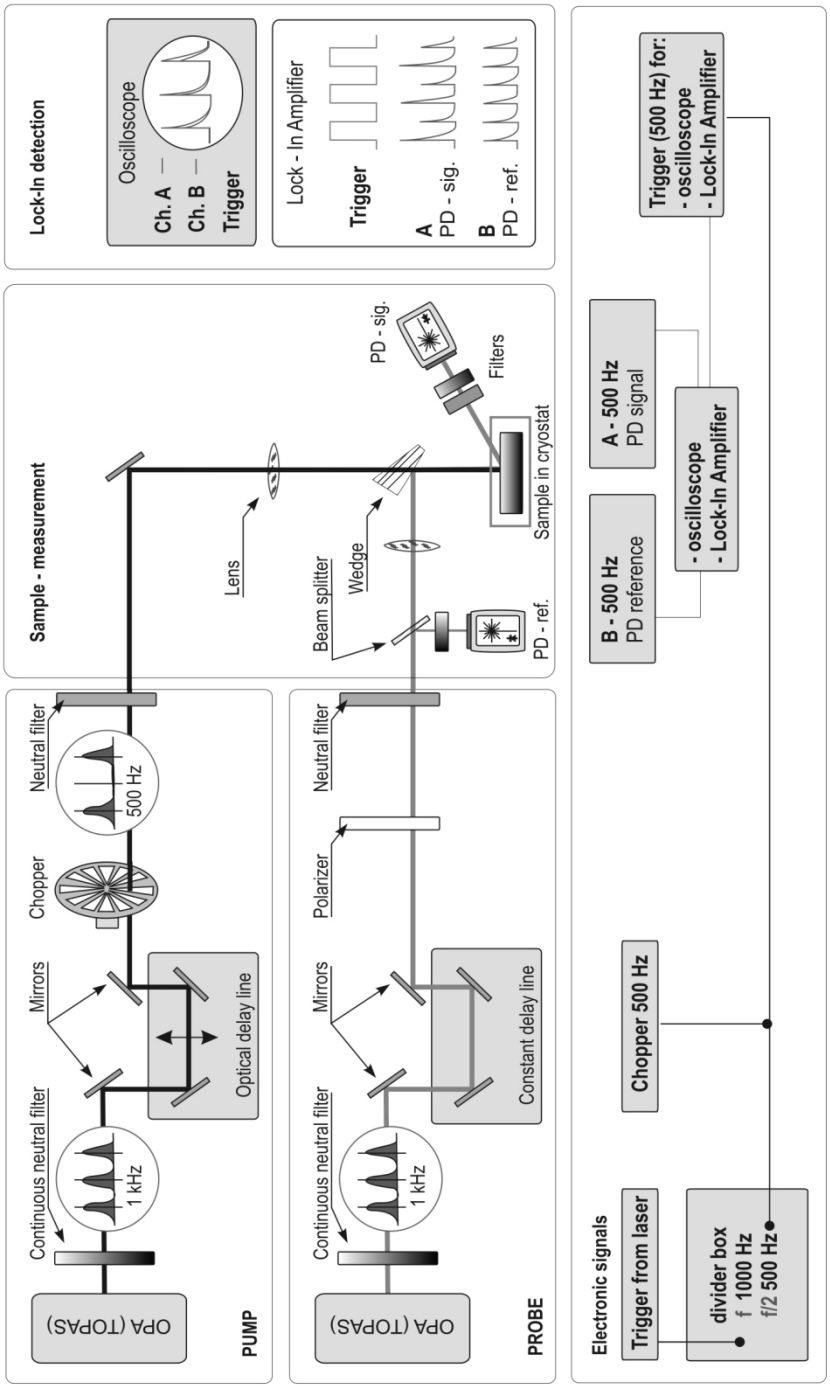


**Fig 6.6:** Pump-probe experimental setup used with $(EDO\text{-}TTF)_2SbF_6$ experiments. Pump and probe beams from the OPAs were directed to delay lines (in probe case it was constant delay line with fixed delay time). Pump beam was chopped down by mechanical chopper, synchronized with the laser (detailed description of the frequencies was included in the text). Probe beam was split up into two beams: reference and signal one. Before sample, pump and probe beams were focused on the crystal's surface.

*[(TPA)Fe$^{III}$(TCC)]-$PF_6$ and -$SbF_6$ measurements on short time scale.* The scheme of this experimental setup was similar to that presented in 6.2.1.1,[17] but here we worked in transmission mode, so some modifications concerned beam focusing on the sample and on the signal photodiode – see Fig. 6.7 (next page). For example, the wedged window ensuring parallel propagation of the beams was removed. Temporal resolution was slightly worse than in previous case, and amounted to around 100 fs. The angle between pump and probe was nevertheless maintained at less than $7^0$.

Polarization of the pump and probe beams were parallel to each other and to the long crystal axis ***a***, along which the laser penetrates deepest.[17,18,19] Pump beam was propagating parallel to the crystal axis ***b***. Because typically, the crystals were 5 – 10 μm thick, we were setting the optical density (OD) for VIS probing light to a value within 1 – 1.5 at 100 K (LS state).[18] This thickness strikes good compromise between laser penetration length (3 – 5 μm at 800 nm) and the number of excited molecules in the probed bulk. Crystals were cooled down by the open cryostat with nitrogen gas flow (Oxford Instruments).

*[(TPA)Fe$^{III}$(TCC)]-$PF_6$ and -$SbF_6$ measurements on long time scale – synchronized lasers.* The idea of this experimental setup was shown in Fig. 6.8. Pump beam was provided from the direct output of the femtosecond regenerative amplifier (Legend USP, Coherent, pulse duration 40 fs), so samples were excited at 800 nm. The probe beam, was provided by the second femtosecond regenerative amplifier (Legend Elite II, Coherent, pulse duration 100 fs). Wavelength of the probe light was tuned with an optical parametric amplifier (TOPAS, Light Conversion). Probing light at 600 nm, was identified as most sensitive in the VIS range[18] to the spin transition [(TPA)Fe$^{III}$(TCC)]$PF_6$. The temporal resolution of this experimental setup was equal 110 fs.[18]

The most important modifications concern the timing of the setup (shown on Fig. 6.1), which requires that several sources operate in synchrony: the femtosecond oscillator (Ti:sa), the amplification pump lasers (Evolution from Legend USP and Legend Elite II) used to power the amplification stages, and the regenerative amplifiers (Legend USP and Legend Elite II).[18] To clock the synchronization the digital synchronization electronics were employed. As indicated in Fig. 6.8, that train of femtosecond pulses from Ti:sa oscillator is split in two by a beam splitter. Than twinned pairs with zero temporal jitter were trapped and amplified by the regenerative amplifiers which operate at 1 kHz each. Because "free-running" oscillator operated at frequency around 76 MHz, but amplifiers at 1 kHz, signal from the

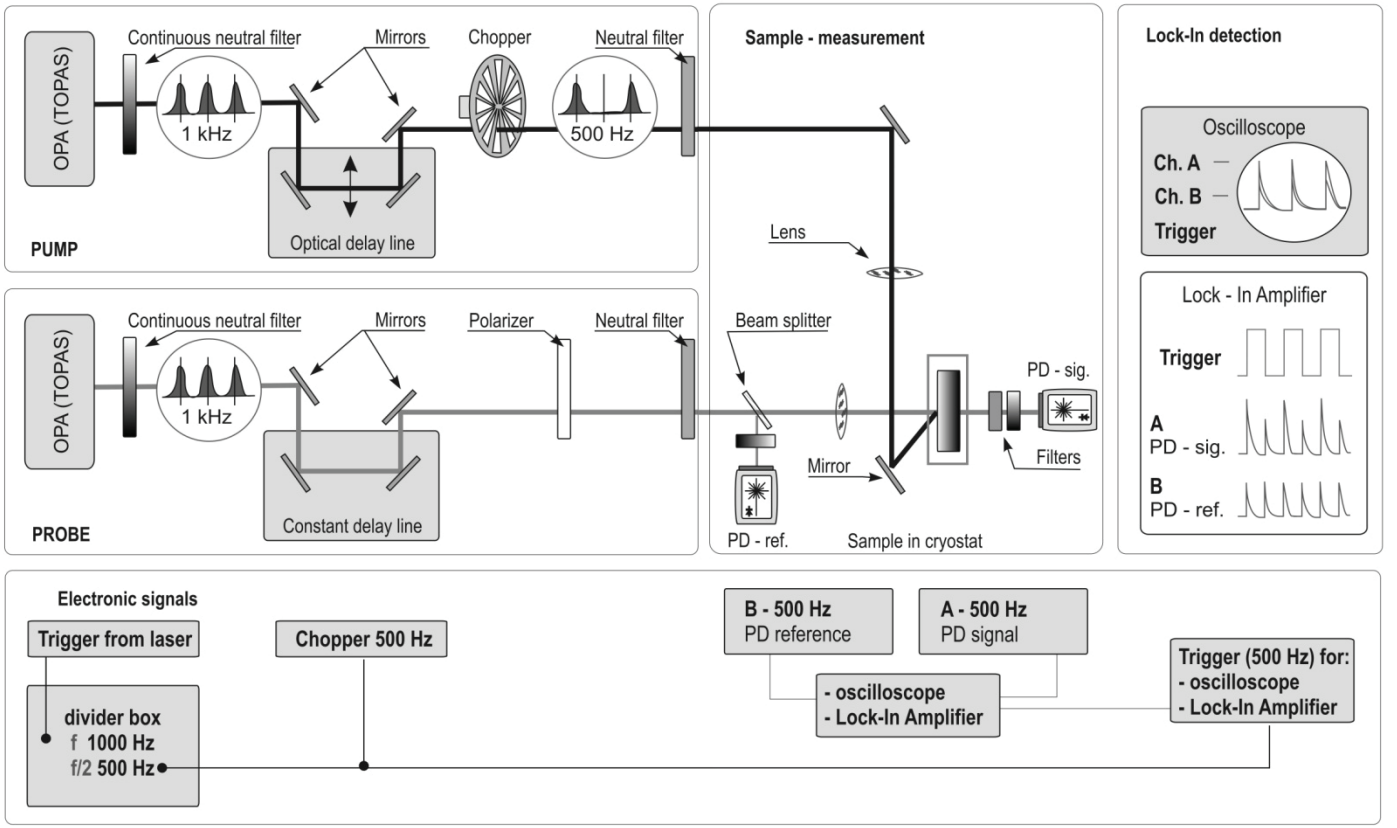


**Fig 6.7:** Pump-probe experimental setup used with [(TPA)$Fe^{III}$(TCC)]-$PF_6$ and -$SbF_6$ experiments. Description of the experimental setup is similar to that shown on Fig. 6.6. Some modifications in detection system appear (we were working in transmission mode) and instead of the wedge, we were using moon mirror.

Mira seed was divided to 1 kHz by the countdown box (Coherent). This frequency was fed to a 4 channel digital delay pulse generator (DDPG, model 9524 Quantum Composers) – compare to Fig. 6.1 – delivering phase-locked trigger signals at 1 kHz to two regenerative amplifiers. As was mentioned at the beginning of this chapter, each amplifier requires two such signals, one for Q-switching the amplification laser (Evolution, Coherent), and one for triggering the Pockels cells, responsible for trapping only one pulse from the RF train.[18]

In a typical regenerative amplifier, the SDG (Coherent) unit compares triggering 1 kHz signal for Pockels cells with the 76 MHz of the oscillator. In our setup we synchronized both amplifiers with an external delay generator (DDPG, Quantum). Thereby delaying the Pockels cells of the Legend USP, and the Q-switch driver of its Evolution laser, a later pulse from the RF train is trapped and amplified with respect to that trapped in the Legend Elite II. Pulses from the RF (Mira) were electronically enumerated by the delay generator, owing to a common time origin. So if we consider, that $i$ and $j$ were the pulses from Legend USP and Elite II, respectively, the pulses could be fired at well defined instants :

(6.2) $$t_1(i) = PL_1 + t(0)_1 + i/f_{RF}$$

(6.3) $$t_2(j) = PL_2 + t(0)_2 + j/f_{RF}$$

where $f_{RF}$=76 MHz, $t(0)$ is the time offset for gating DDPG channels, and $PL_1$ and $PL_2$ define the optical path length from Legend USP and Elite to the sample. The time offset was constant during the gating process, so the delay between gated pulses, expressed directly from (6.2) and (6.3) was as follows:

(6.4) $$t(j,i) = \Delta PL + (j-i)/f_{RF}$$

where $\Delta PL = (PL_2 - PL_1)$. It follows from equation (6.4), that any delay between the two lasers being a multiple number of 13 ns (inverse of 76 MHz) can be thus obtained.

By combining the optical and electronic gating on short and long time scales, respectively, we could monitor the dynamical response to a laser excitation from 100 fs to 1 ms under constant excitation conditions.[18]

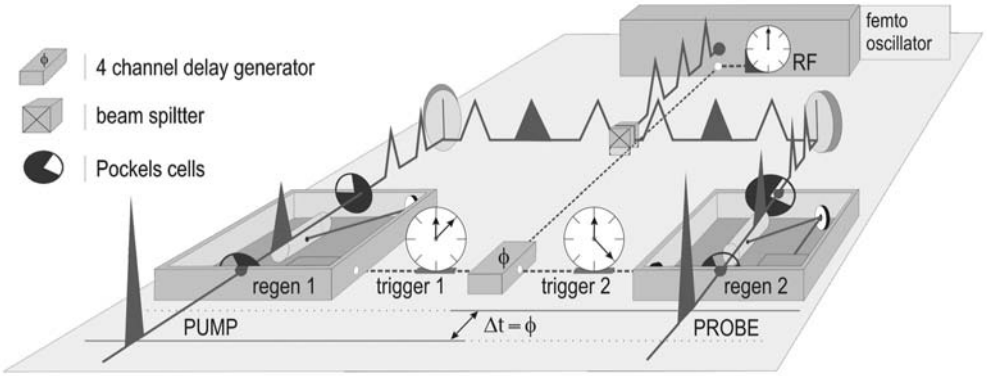


**Fig 6.8:** Experimental setup used on $[(TPA)Fe^{III}(TCC)]SbF_6$ experiments with synchronized lasers. Detailed discussion was included in § 6.2.1.2 and also in chapter 3 ("Spin-crossover…").

### 6.2.2 Polychromatic detection

In experiments with polychromatic detection a spectrometer (Acton Research Corp., SPECTRAPro 2500i) and a CCD camera (Princeton Instruments, PIXIS 100) were used. Light from the signal and reference beams were transferred by the two multi-mode fibers to the spectrometer's slits, dispersed with a grating and imaged onto a CCD chip. To minimize the dark current and so to increase the dynamic range of the camera, the CCD chip was cooled down to $-75^0$C.[10,20,21]

The principle of the CCD array readout (Charge Coupled Device) was presented in Fig. 6.9 The image area is divided to sectors (pixels) resembling a chessboard, with rows and columns. The readout relies on transferring the pixels from the columns to the register shift, one by one from each row. When charge in register shift is accumulated it is then shifted into the output node and output amplifier. Capacity of the pixels in the register shift is twice as big that of a normal pixel. In the output amplifier electrons accumulated in the pixels are grouped and counted. The result is transferred to the preamplifier, where gain is applied.

The readout time can be made shorter by binning the pixels. The scheme of the binning process was showed in Fig. 6.9. In our case after binning, we obtained 4 rows (25 lines each) and 134 columns (10 pixels each). Fast analog to digital converter (ADC), with 2 MHz module, vertical and horizontal shift times allowed the readout at 500 Hz rate. The maximum number of counts per pixel was equal 60 000, but for the stable operation, we never exceeded 40 000 counts.

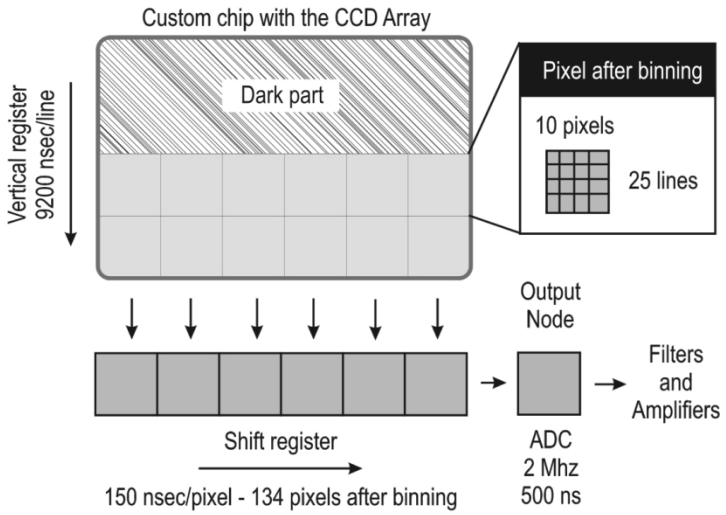


Fig. 6.9: Principles of CCD readout customize to the experiment. Current from the pixels is transferred to register shift and than to the via ADC to the amplifier. Pixels after binning (software) consist 10 x 25 pixels, that decrease the readout time. To increase the speed of the detection system – CCD chip was divided in two parts, what was indicated in the picture (description further in the text).

The camera was synchronized to the laser by an external trigger at 500 Hz provided from the divider box described earlier. The "logic out" signal from the camera was monitored on a digital scope and compared with the pulse from the photodiode sampling the probe beam pulses. Because camera typically needed one trigger period to get synchronized, first two pulses were discarded from the analysis.

Data collected by the software was exported to ASCII. Because 10000 spectra were typically collected, fast averaging procedure was executed by MatLab and immediately displayed in Origin.

#### 6.2.2.1 Dynamics of the CCD chip

The CCD chip was customized such that only half was shifted to the register (see Fig. 6.9) whereas the other half was used a dark buffer for the following exposure. Two stripes on the camera correspond to dispersed spectra from the signal and the reference beams (pixels from 0-25 and 26-50 respectively). The dark buffer (pixels 51-100) is shown in Fig. 6.10.

During acquisition the exposed and pixels shifted to the register were replace by the dark ones from the upper part of the chip. Such customizing of the camera chip permitted recording the spectra at the rate of 500 Hz.

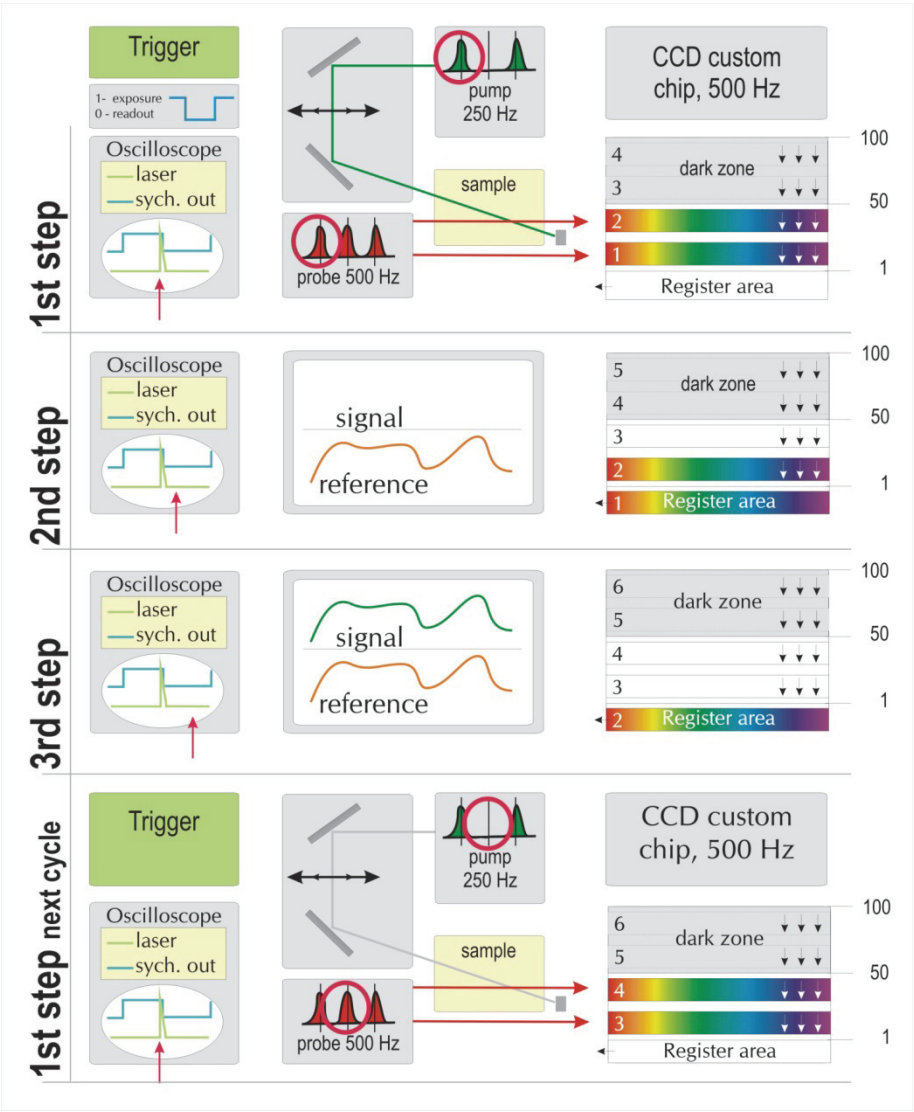


**Fig. 6.10:** Dynamics of the CCD chip. Picture presents 4 steps of the camera readout. From the left to right was shown schematically: "logic out" signal observed on the oscilloscope simultaneously during measurement and compared with signal from the photodiode registering occurrence of the probe beam in time (red arrow); sequence of the procedure with delay line, sample and computer register; idea of the "fast" readout of the camera.

The exact readout time after binning was equal 1,34 msec. The speed of the vertical shift was around 9200 nsec/row and the speed of horizontal shift from the register around 150 nsec/row. The following formula gives the readout time of a binned CCD:

$$t_R = \left[N_x \cdot N_y \cdot \left(\frac{t_{sr}}{n_x} + \frac{t_v}{n_x \cdot n_y}\right)\right] + (N_x \cdot t_i) \tag{6.4}$$

where $N_x$ is a smaller dimension of the CCD, $N_y$ is its larger dimension, $t_{sr}$ is the time needed to shift one pixel out of the shift register, $t_v$ is the time needed to digitize the pixel, $t_i$ is the time to shift one line into the shift register, $n_y$ is a number of binned pixels, $n_x$ is the number of binned lines.[21]

6.2.2.2 Experimental setup used in [(TPA)$Fe^{III}$(TCC)]-$PF_6$ and -$SbF_6$ measurements

Our laser source delivered femtosecond pulses with frequency 1 kHz. To use efficiently the camera readout the frequency was slowed down to 500 Hz by a mechanical chopper phase locked to the laser. The laser beam was split by a 60/40 beam splitter into two parts. The more intense beam, the pump, was delayed by the optical delay line with respect to the probe. Pump was chopped once more down to 250 Hz, to allow heterodyning the photo-induced signal. The less intense beam was focused on a sapphire crystal for generating white light supercontinuum. Due to instability of this light, it was further split in two parts: the probe and the reference. Pump and probe beams were finally spatially overlaid on the crystal surface with the aid of a microscope objective (InFocus, model KC, Infinity, NA = 0,05), the same as used in the experiments on (EDO-TTF)$_2SbF_6$ compounds. Both pulses were polarized parallel to the long crystal axis ***a*** for better penetration of the laser (Fig. 6.11 – next page).

During the analysis we used double reference method and avoided outliers in averaging. Care was taken to ensure the correct sign of the optical density change. The benefits of with this method were briefly described in chapter 3. To check the zero time between pump and probe, we generated cross-phase modulation (XPM) in the thick neutral filter. The XPM effect provides a reliable signal across the whole spectrum.

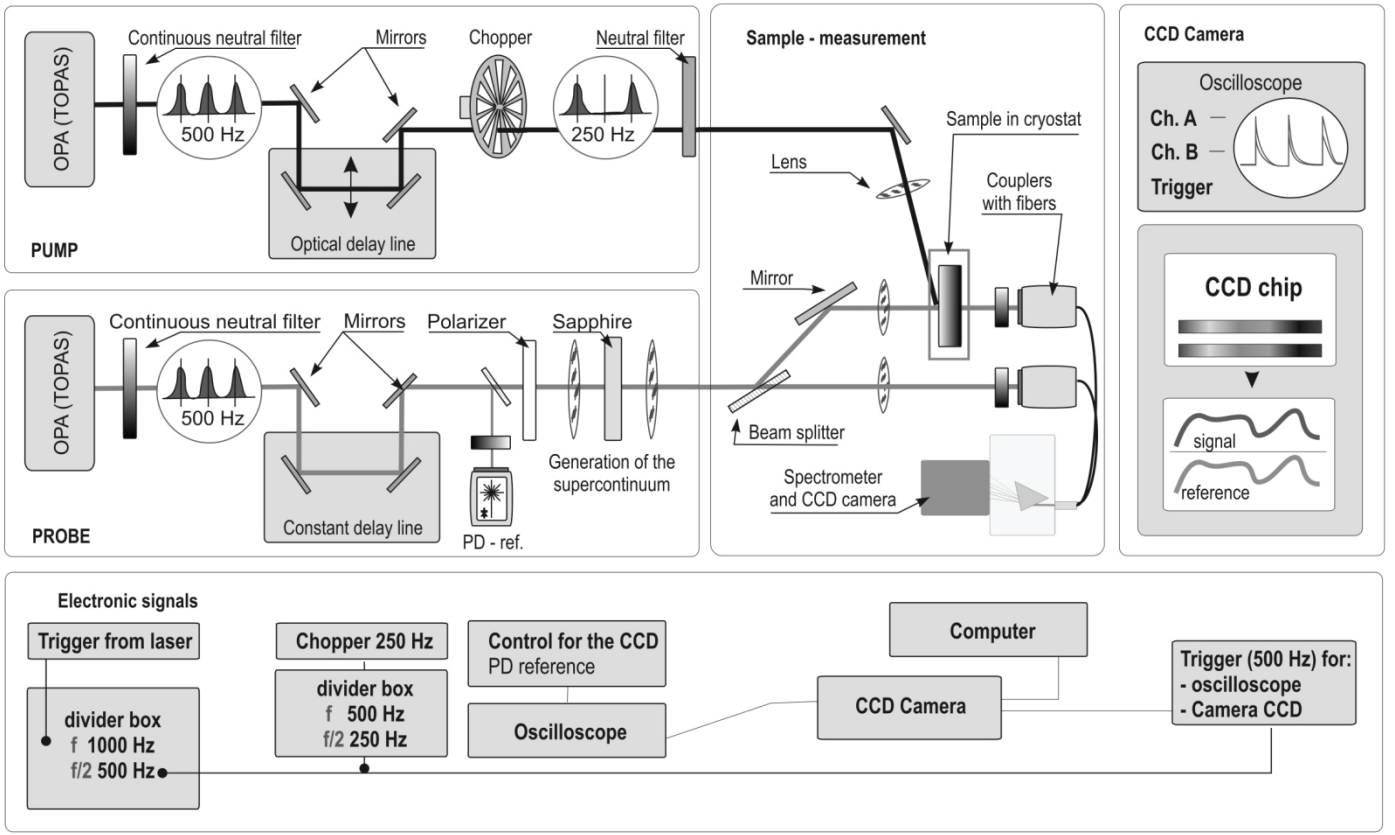


**Fig 6.11:** Experimental setup used with [(TPA)FeIII(TCC)]$SbF_6$ experiments with "white-light" probe. On the left side was presented scheme of the laser beams and most important elements in the experimental setup. On the right side was shown electronic connections and idea of detection with CCD camera.

*Generation of the supercontinuum*. Supercontinuum is a nonlinear effect induced in a dense optical medium, for example in sapphire, calcium fluoride ($CaF_2$) or fused silica. During our experiments we focused (lens, f=150 mm) the beam at 800 nm on the surface of the crystal. The peak intensity at the focal point was enough to generate supercontinuum, which by its nature is a threshold effect. After generation, white light was recollimated by the achromatic lens (f=150 mm) to reduce chromatic aberrations at the focal plane.

The exact description of this phenomena is difficult, because many effects contribute to white light generation, such as: stimulated Raman scattering, self phase-modulation effect, optical Kerr effect, self focusing effect. White light generation starts inside the crystal at the focal point, so before leaving the medium, therefore GVD (group velocity dispersion) affects supercontinuum. In our studies, the GVD resulted in a strong chirp, 10 fs/THz, which we later used to our advantage in single shot measurements (described in next section).

#### 6.2.2.3 Single shot measurements

For single shot measurements we used exactly the same experimental setup as described above, with only one modification: a shutter was placed before the sample on the pump beam pathway. In these studies we fully exploited the fast readout time of our customized CCD chip, able to record single spectra at 500 Hz. The scheme presented in Fig. 6.12 (next page) shows the experimental setup.

With a capable detector, the critical part of the experiment was to analyze the obtained spectra, which had to be indexed with the respect the occurrence of the pump pulse. Detailed description about pulses taken to the analysis was provided in chapter 5.

## 6.3 Cryogenics setup

We used an open cryojet stream of gas nitrogen, which is standard in X-ray diffraction studies. Alternatively, for measurements below nitrogen temperature, we used a closed cryostat filled with gas helium. The latter cryostat was also used in the measurements with microscope of the spin-crossover compounds.

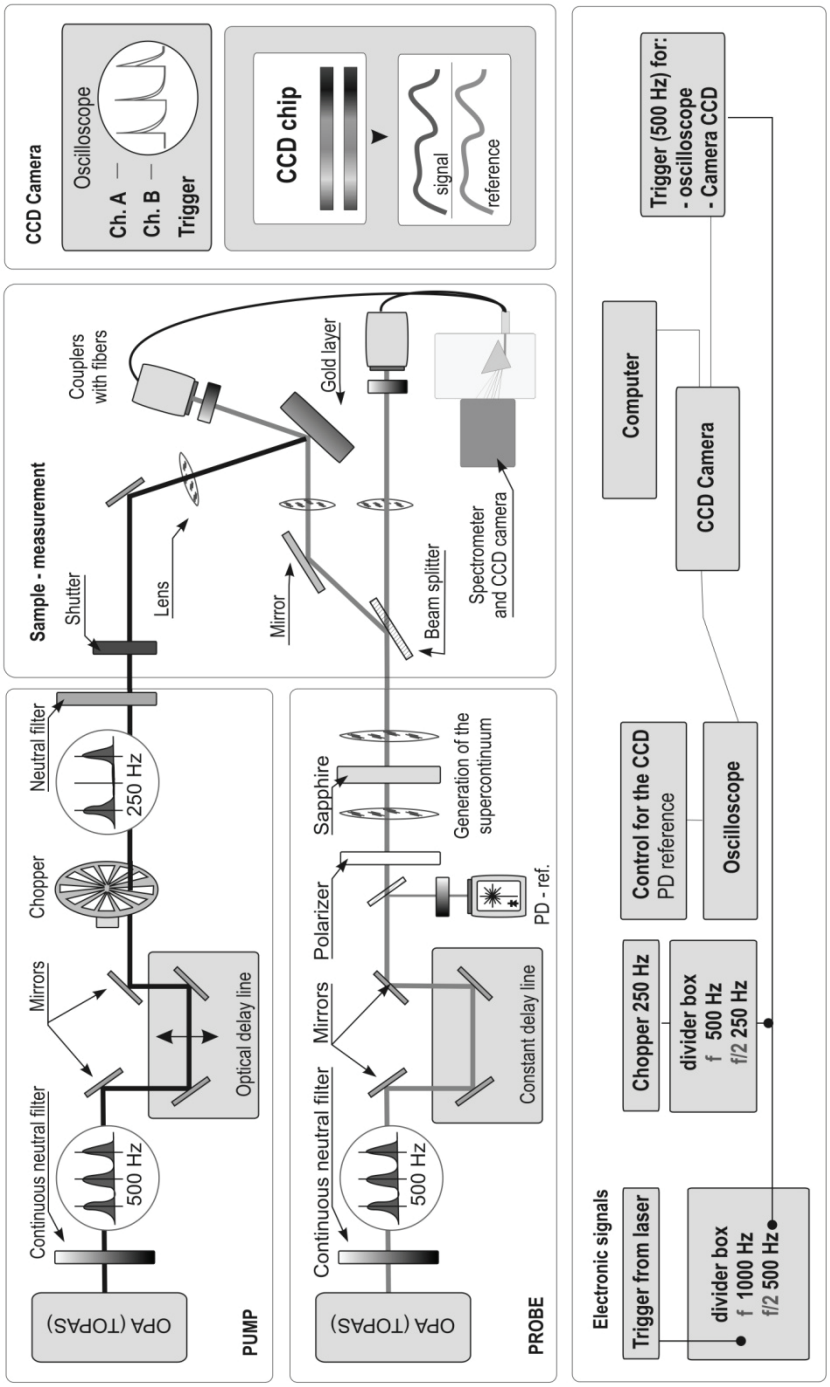


**Fig 6.12:** Experimental setup used in single shot measurements was similar to those presented on Fig. 6.11. Changes relied on the different detection path and on additional shutter, placed before the sample. Electronic connections was the same.

**References:**

[1] S. Mukamel, *Principles of Nonlinear Optical Spectroscopy*, Oxford University Press, NY (1995)
[2] D.E. Spence et al., *Opt. Lett*. **16,** 42 (1991)
[3] A. Rundquist et al., *Appl. Phys. B* **65,** 161 (1997)
[4] R. Naskręcki, *Femtosecond transient absorption spectroscopy. Photophysical study of the excited states of molecules and short - living individua*, Wydawnictwo Naukowe UAM, Poznan 2000
[5] J-C. Diels et al., *Ultrashort Laser Pulse Phenomena,* Academic Press (1995)
[6] Users Manual: *Mira*, Coherent (2005)
[7] C. Rulliere, *Femtosecond Laser Pulses*, Springer-Verlag, Berlin (1998)
[8] Users manual: *Legend USP*, Coherent (2005)
[9] Users manual: *Legend Elite II*, Coherent (2010)
[10] W. Kaszub et al., *Acta Phys. Pol. A* **121**, 325 (2012)
[11] M. Lorenc et al., *Phys. Rev. Lett*. **103**, 028301 (2009)
[12] Users manual: *SR830*, Stanford Research Systems (2006)
[13] V. Klimov et al., *Opt. Lett*. **28**, 277 (1998)
[14] J.H. Scofield et al., *Am. J. Phys.* **62,** 129 (1994)
[15] A. Temple, *Am. J. Phys* **43**, 801 (1975)
[16] M. Servol et al., in preparation
[17] N. Moisan et al., *C. R. Chimie* **11**, 1235 (2008)
[18] M. Lorenc et al., *Phys. Rev. B* **85**, 054302 (2012)
[19] E. Collet et al., *Acta Crystallogr. B* **65**, 474 (2009)
[20] C. D'Amico et al., *J. Phys. Chem. C*, **116**, 3719 (2012)
[21] Users manual: *Acton CCD*, Princeton Instruments (2009)

Chapter 7:

# General conclusions

# 7. General conclusions

This work presents results of experiments performed on two types of compounds, more precisely spin-crossover and charge transfer organic crystals, in order to understand the physical mechanisms of photo-induced transformations in a material driven by an ultra-short laser pulse. The experimental work realized during the thesis was largely dedicated to the new developments of the pump-probe optical setups.

## 7.1 Spin-crossover crystals

In the first family of compounds (spin-crossover) we monitored changes of absorbance of the crystal, triggered by the femtosecond laser pulse. For performing the measurements we applied two new experimental setups: by synchronizing the lasers to cover a very broad range of time delays between pump an probe pulses to monitor the evolution of the photo-excited material on specific wavelengths, and by probing with supercontinuum to observe broad spectral changes of the new state. We have concluded that that the transformation driven by a light pulse follows a complex pathway through a sequence of steps, from molecular to material scale.

Following laser pulse excitation we can distinguish three main steps, successively corresponding to femtosecond, nanosecond and microsecond time window. In the first step, purely photo-induced, we observed a molecular process leading to a small increase of $X_{HS}$ fraction, which is manifested by a plateau of the optical density change with time. Next step, completed in less than 1 ns was attributed to an elastic process, related to the expansion of crystalline volume triggering a large increase of transformed molecules from LS to HS state. During this step associated to the pressure relaxation of the sample we have to consider elastic interactions caused by both: the swelling of photo-excited molecules and the lattice heating – both being the valid physical origins of an increase of pressure inside the crystal. Over the microsecond timescale thermal processes take place and lead to the thermal activation between LS to HS states and as well as temperature homogenization of the crystal, which remains adiabatically isolated from its cryogenic environment.

### 7.2 Organic crystal $(EDO\text{-}TTF)_2SbF_6$

We made several interesting observations on another compound, namely one of the $(EDO\text{-}TTF)_2XF_6$ family exhibiting insulator-to-metal phase transition, the $(EDO\text{-}TTF)_2SbF_6$. The results obtained from pump-probe optical measurements present some differences with the reported giant photo-response in the prototype $(EDO\text{-}TTF)_2PF_6$. Photo-induced ultra-fast dynamics implying several coherent optical phonon modes has been clearly observed. We also conclude that the photo-induced phenomena triggered by the femtosecond laser pulse are more localized than in the prototype compound. Indeed, comparison between results from Raman spectroscopy and time resolved studies at low temperatures, showed a weak but significant softening with temperature of the three main phonon modes in frequency domain, but not with the excitation density. In addition, results collected inside the hysteresis and the absence of nonlinearity of the optical response, seem to favour a physical picture of a localised photo-induced state rather than of a phase transition with long range order at thermal equilibrium.

### 7.3 Single shot

Using new experimental set-up based on fast spectral readout we proved feasibility of single shot measurements by recording a temporal sequence of an irreversible photo-induced process. During test experiments we observed that a single laser pulse of high fluency strips a dielectric surface of gold layer. The single shot setup installed during this thesis work, is a promising tool for new insights into the physics of phase transitions, in particular inside a bistable regime.

## List of publications, conferences and scientific activity

**Scientific publications with the results of the thesis:**

M. Lorenc, Ch. Balde, **W. Kaszub**, A. Tissot, N. Moisan, M. Servol, M. Buron, H. Cailleau, P. Chasle, P. Czarnecki, M. L. Boillot, E. Collet
***"Cascading photoinduced, elastic, and thermal switching of spin states triggered by a femtosecond laser pulse in an Fe(III) molecular crystal"***
Phys. Rev. **B 85**, 054302 (2012)

**W. Kaszub**, E. Collet, H. Cailleau, M. Servol, M-L. Boillot, A. Tissot, M. Lorenc
***"White light snapshot of non-equilibrium high spin state in a molecular crystal"***
Acta Phys. Pol. **A 121**, 324 (2012)

**and other publications:**

P. Kurzynski, **W. Kaszub**, M. Czechlewski,
*"**Mutually unbiased bases and complementary spin 1 observables**"*
J. Phys. A: Math. Theor. 43 (2010) 265303

**In preparation (with results from thesis):**

M. Servol, **W. Kaszub**, N. Moisan, M. Lorenc, D. Boschetto, A. Moréac, H. Cailleau, S. Koshihara, M. Maesato, X. Shao, Y. Nakano, H. Yamochi, G. Saito, E. Collet
***„Optical probing of an out of equilibrium photoinduced transition: observation of coherent dynamics in the photo-induced state of $(EDO)_2SbF_6$"***

**W. Kaszub**, E. Collet, R. Naskręcki, H. Cailleau, B. Arnaud, M. Lorenc
***„Broadband detection of electron temperature in vicinity of Fermi level in gold"***

**Conferences, schools, seminars:**
*with posters, oral presentations*

**W. Kaszub**, E. Collet, B. Arnaud, H. Cailleau, R. Naskrecki, J. Kubiicki, M. Lorenc
poster entitled:.„***Single shot spectroscopy of gold under ultrashort intense irradiation***"
4th Photoinduced Phase Trasitions And Cooperative Phenomena „PIPT4", Wrocław, Poland, 2011

---

M. Servol, **W. Kaszub**, N. Moisan, M. Lorenc, D. Boschetto, A. Moréac, H. Cailleau, S. Koshihara, M. Maesato, X. Shao, Y. Nakano, H. Yamochi, G. Saito, E. Collet,
co-author of the oral presentation entitled.***„Out of equilibrium coherent precursor dynamics of a photo-induced phase transition in molecular material of (EDO-TTF)SbF"***
4th Photoinduced Phase Trasitions And Cooperative Phenomena „PIPT4", Wrocław, Poland, 2011

---

**W. Kaszub**, E. Collet, M. Buron, H. Cailleau, R. Naskrecki, C. Balde, M-L. Boillot, M. Lorenc,
poster entitled.***„Structural and optical fingerprints of spin-crossover in a single crystal of [(TPA)Fe(III)(TCC)]PF$_6$"* **(awarded as 2nd Prize of Poster session)**
4th International School and Symposium on Multifunctional Molecule-based Materials, „ISSMMM", Argonne, USA, 2011

---

M. Servol, **W. Kaszub**, N. Moisan, M. Lorenc, D. Boschetto, A. Moréac, H. Cailleau, S. Koshihara, M. Maesato, X. Shao, Y. Nakano, H. Yamochi, G. Saito, E. Collet,
co-author of the oral presentation entitled. ***"Multi-phonon dynamics of the ultra-fast photoinduced insulating-to-metal transition in (EDO-TTF)SbF"***
23rd General Conference of the Condensed Matter Division of the European Physical Society, „CMD 23", Warszawa, Poland, 2010

---

**W. Kaszub,** M. Servol, N. Moisan, M. Lorenc, D. Boschetto, A. Moréac, H. Cailleau, S. Koshihara, M. Maesato, X. Shao, Y. Nakano, H. Yamochi, G. Saito, E. Collet,
poster entitled. ***"Out of equilibrium coherent precursor dynamics of a photo-induced phase transition in molecular material of (EDO-TTF)SbF"***
23rd General Conference of the Condensed Matter Division of the European Physical Society, „CMD 23", Warszawa, Poland, 2010

---

**W. Kaszub,** M. Servol, N. Moisan, M. Lorenc, D. Boschetto, A. Moréac, H. Cailleau, S. Koshihara, M. Maesato, X. Shao, Y. Nakano, H. Yamochi, G. Saito, E. Collet,
poster entitled. ***"Out of equilibrium coherent precursor dynamics of a photo-induced phase transition in molecular material of (EDO-TTF)SbF"***
4eme Reunion Annuelle du GDR „Magnetisme et Comutations Moleculaires", Montpelier, France, 2010

---

**W. Kaszub,** M. Servol, N. Moisan, M. Lorenc, D. Boschetto, A. Moréac, H. Cailleau, S. Koshihara, M. Maesato, X. Shao, Y. Nakano, H. Yamochi, G. Saito, E. Collet,
poster entitled. ***"Out of equilibrium coherent precursor dynamics of a photo-induced phase transition in molecular material of (EDO-TTF)SbF"***
4th International Conference on Molecular Materials „MOLMAT 2010", Montpelier, France, 2010

---

**W. Kaszub**, E. Collet, M. Buron, H. Cailleau, R. Naskrecki, C. Balde, M-L. Boillot, M. Lorenc,
poster entitled. ***„Structural and optical fingerprints of spin-crossover in a single crystal of [(TPA)Fe(III)(TCC)]$PF_6$"***
1st International Conference on Ultrafast Structural Dynamics, Lausanne, Switzerland, 2010

---

3rd International Advanced School: Molecular Switching and Functional Materials, Rennes, France, 2009

---

**W. Kaszub,** M. Servol, N. Moisan, M. Lorenc, D. Boschetto, H. Cailleau, S. Koshihara, M. Maesato, X. Shao, Y. Nakano, H. Yamochi, G. Saito, E. Collet,
poster entitled. ***"Observation of coherent dynamics in the photo-induced state of (EDO-TTF)SbF"***
5th International Symposium on Molecular Materials: Electronics, Photonics and Spintronics, Rennes, France, 2009

---

P. Kurzyński, W. Kaszub, M. Czechlewski,
poster entitled. ***„Mutually Unbiased Bases and Complementary Spin 1 Observables"***
Conference Quantum Optics VII, Zakopane, Poland, 2009

---

**W. Kaszub**
oral presentation: *„Spektroskopia korelacji fluorescencji jako narzędzie do obserwacji pojedynczych molekuł" (Fluorescent Correlation Spectroscopy as a tool to observation of a single molecules)*
V$^{th}$ Student Seminar of Biomolecular and Medical Physics, Kraków, Poland, 2009

Colloque de l'Association française de cristallographie, Rennes, 2008

BIO Biznes Finances Innvations 2008, Gdynia, Poland, 2008

**W. Kaszub**
oral presentation: *„Współczynnik załamania światła – czy zawsze stały?" (Refractive index – always constant?)*
IV$^{th}$ Student Seminar of Biomolecular and Medical Physics, Poznań, Poland, 2008

**W. Kaszub**, W. Giera
oral presentation: *„Optical birefringence induced by an intense laser beam in tRNA"*
Students Conference of Nature Physics, Poznań, Poland, 2007

**W. Kaszub**, W. Giera
oral presentation: *„Indukowanie dwójłomnosci optycznej w tRNA za pomoca wiazki laserowej" (Optical birefringence induced by an intense laser beam in tRNA)*
III$^{rd}$ Student Seminar of Biomolecular and Medical Physics, Kraków, Poland, 2007

II$_{nd}$ Student Seminar of Biomolecular and Medical Physics, Kraków, Poland, 2006

**W. Kaszub**, W. Giera
oral presentation: *„Lasery impulsowe – droga do skrócenia czasu" (Pulse lasers – race against time)*
IV$^{th}$ Polish session of Students Association of Physics, Kraków, Poland, 2005

12$^{th}$ International Seminar „Neutron Scattering Investigation in Condensed Matter", Ciążeń, (Poland), 2005

11$^{th}$ International Seminar „Neutron Scattering Investigation in Condensed Matter", Poznań, (Poland), 2004

10th International Seminar „Neutron Scattering Investigation in Condensed Matter", Poznań, (Poland), 2003

"*Soft Mat Control*", Erasmus intensive program (Universite de Rennes1, Adam Mickiewicz University, Saarbrücken University), Poznan, Poland (2 weeks), 2012

4th International School on Multifunctional Molecule-based Materials, Argonne, USA (1 week), 2011

3rd International Advanced School: Molecular Switching and Functional Materials, Rennes, France (1 week), 2009

*„Workshop of heavy ions accelerations"* – Heavy Ion Laboratory, Warsaw (Poland), 2005

*„Biophysics summer school"* – Joint Institute of Nuclear Research, Dubna (Russia), 2005

*„Summer school of neutron scattering"* – Forschungszentrum Julich, Julich (Germany), 2005

*„Low temperatures summer school"* – Pavol Jozef Safarik University, Kosice (Slovakia), 2004

*„Neutron scattering school"* – Joint Institute of Nuclear Research, Dubna (Russia), 2004

*„Nanoscience school"* – Institute of Physics PAS Warsaw (Poland), 2002

# Posters

# Optical probing of an out of equilibrium photoinduced transition: Observation of coherent dynamics in the photo-induced state of $(EDO\text{-}TTF)_2SbF_6$


**Wawrzyniec Kaszub[1,2], Nicolas Moisan[1], Marina Servol[1], Maciej Lorenc[1], Hervé Cailleau[1,3], Ryszard Naskrecki[2], Shin-ya Koshihara[3,4], Mitsuhiko Maesato[5], Hideki Yamochi[4,6] & Eric Collet[1,3]**

[1]*Institut de Physique de Rennes, UMR CNRS-University Rennes 1 campus Beaulieu, Rennes, 35042, France*
[2]*Quantum Electronics Laboratory, Faculty of Physics, Poznan, Poland,*
[3]*Non-equilibrium Dynamics Project, ERATO-JST, Tsukuba, Ibaraki, Japan,*
[4]*Department of Materials Science, Tokyo Inst. of Technology, 2-12-1, Oh-okayama, Meguro, Tokyo, 152-8551, Japan,*
[5]*Division of Chemistry, Graduate School of Science, Kyoto University, Sakyo-ku, Kyoto, 606-8501, Japan*
[6]*Research Center for Low Temperature and Materials Sciences, Kyoto University, Sakyo-ku, Kyoto, 606-8502, Japan*


## Introduction

Schematic views of the lattice and electronic structural changes accompanying the M-I phase transition in (EDO-TTF)$_2$PF$_6$[1].

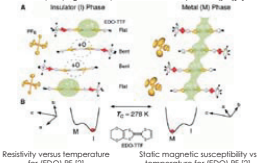


In the $(EDO\text{-}TTF)_2SbF_6$ systems investigated electronic excitations initiated by an ultrashort laser pulse perturb the entire atomic network. It generates coherent collective molecular motions, optical phonons, which can rapidly lead to new state (less than 1ps). $(EDO\text{-}TTF)_2XF_6$ family of comounds undergoe metal-insulator transition upon temeprature. This molecular nm crystal also features a gigantic photoresponse to the femtosecond pulse, comparable to the thermally [3] induced transition, indicating that highly cooperative phenomena are at work upon photoexcitation. However, the metastable photoinduced phases, induced via coherent processes, seems to be different from the thermally equilibrated one [3] .

The phonon frequencies correspond to Raman modes (ambient pressure)

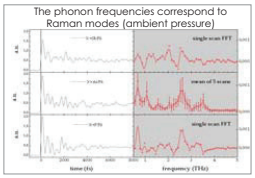


Thermal and photoinduced Metal - Insulator transition [4]

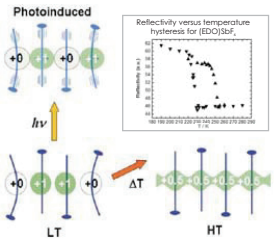


## Different wavelenghts and temperatures

The phonon frequencies resolved at different wavelenghts (closed criostat)

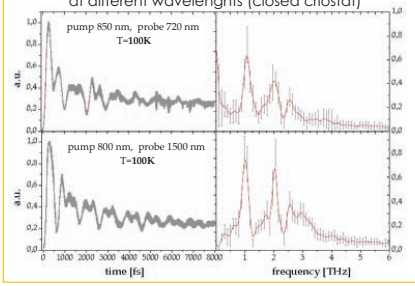


Using different pump and probe wavelenghts, we can observe different behaviour of the oscillation diagram. Main frequencies of the FFT spectrum are the same, but IR wavelength showed deeper oscillations. This contrasts with the trend observed in the case of $(EDO\text{-}TTF)_2PF_6$ [4].

The phonon frequencies resolved at different temperatures (closed criostat)

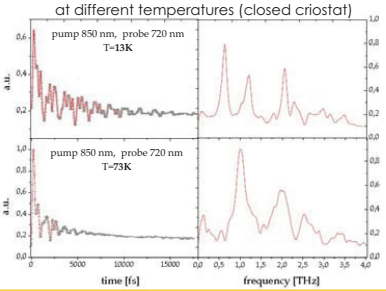


Time-reolved measurements showed that the oscillations last longer at very low temperatures. There are fewer thermal phonons on which the coherent phonon will scatter.
FFT plots showed also changes in phonon frequencies at different temperatures.

Time dependance of oscillations at 100K and 200K [7]

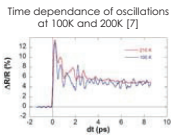


## 3D analysis technique

Time dependance of phonon frequencies

There are mainly 2 phonons observed at high temperatures (>180K), whereas at lower tempertaures (<180K) at least as 4 appear in the time-gated FFT pattern. The origin and relevance of the troughs (dark blue) on the 2D maps need clarification. By changing the width of the timegate for the FFT we adjust the time-frequency resoltion [5].

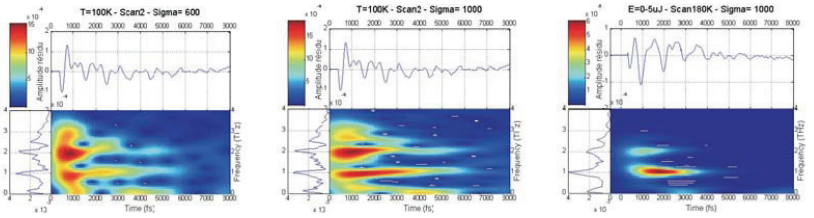


## Threshold measurements

Our experiments on $(EDO\text{-}TTF)_2SbF_6$ showed no clear indication of a threshold behaviour. The photoinduced reflectivity change after 5 ps increases linearly with the excitation density. Either this phenomena has got a remrkably low threshold or the true photoinduced phase stabilises later than thermalisation time of the coherent phonon. Lack of nonlinear reponse was also reported recently, on a different material undergoing photoinduced Metal-Insulator phase [6].

Signal from PD versus excitation density (closed criostat, T=100K)

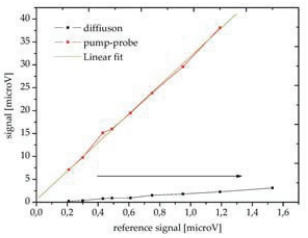


## Conclusions and outlook

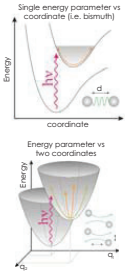


Conclusions:

1. We can observe a certain number of coherent phonons.
2. Decreasing temperature from 100K to 10K, we can observed that phonons are better resolved.
3. Coherent phonons seem to have different thermalisation times.
4. The photo-induced spectrum it is possible, is different from the metallic spectrum, indicating that the photo- induced phase is a new phase.

Outlook:

- Temperature dependent Raman.
- Selective switching of only one of the phonon modes.
- Measurements of the lifetime of the photoinduced state
- Observation of the switch from photoinduced to the temperature induced metallic phase.

## References


[1] M. Chollet *et al.* Science **307**, 86 (2005)
[2] A. Ota *et al.* J. Mat. Chem. **12** (2002) 2600
[3] M. Lorenc *et al.* J. Phys: Conf. Series **148** (2009) 012001
[4] K. Onda *et al.* Phys. Rev. Lett. **101**, 067403 (2008)
[5] A. Tomeljak *et al.* Phys. Rev. Lett. **102**, 066404 (2009)
[6] Y. Okimoto *et al.* Phys. rev. Lett. **103**, 027402 (2009)
[7] N. Moisan, Ph.D. Thesis, Universite de Rennes 1, 2008


## Support


Région Bretagne, ANR, ERATO Japan, METROPOLE Rennes, ZIK

# Single shot spectroscopy of gold under ultrashort intense irradiation

**Wawrzyniec Kaszub[1,2], Eric Collet[1], Brice Arnaud[1], Hervé Cailleau[1], Ryszard Naskrecki[2], Jacek Kubicki[2], Maciej Lorenc[1]**

[1] *Institut de Physique de Rennes, UMR CNRS-University Rennes 1 campus Beaulieu, Rennes, 35042, France*
[2] *Faculty of Physics, Adam Mickiewicz University, ul. Umultowska 85, 61-614 Poznan, Poland*

## Introduction and idea of experiment

CCD camera
for single shot experiment

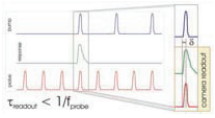

Dynamics of CCD (customised) chip
readout rate 500 Hz

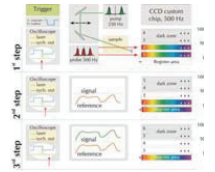

Idea of single shot experiment
using chirped white light as a probe pulse

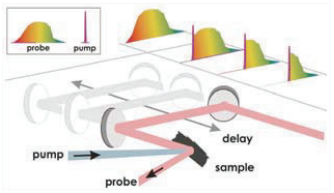


Geometry of experiment (a)
and sample surface after experiment (b)

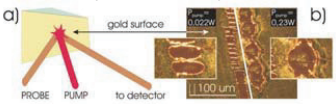


Band structure of gold

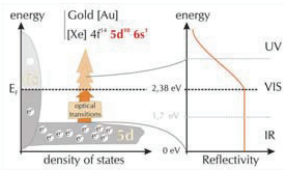


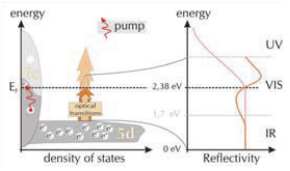


Stationary reflectance of gold...

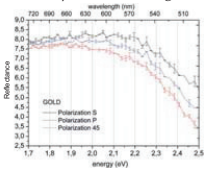


...and its substrate

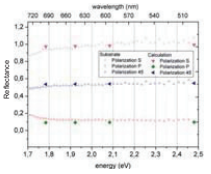


## Single shot, analysis method and results

Experiments with different pump power

Reversible

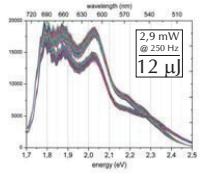


Irreversible

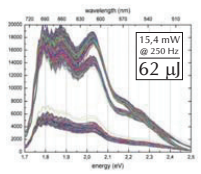


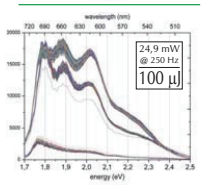


Analysis method

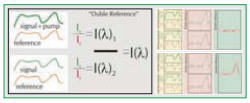


Experiment pulses description

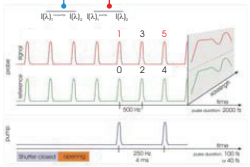


Description of experiment data

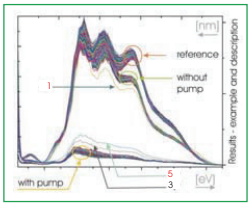


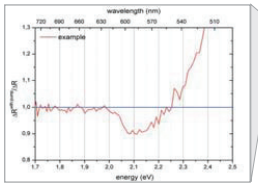


Single shot example
Curves after double reference analysis
blue corresponds to situation before shot,
red - corresponds to situation during shot

Measurements inside chirped probe
Red circles corresponds to chirp curve
obtained in another experiment.

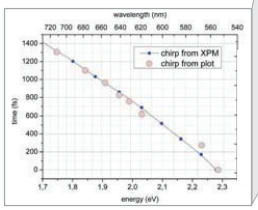


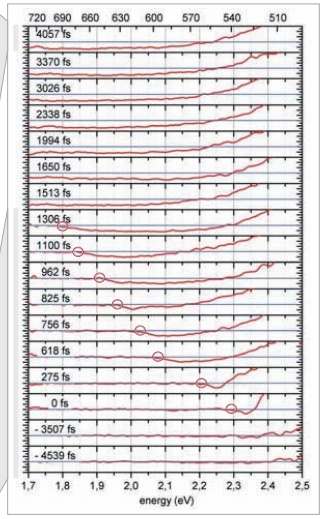


## Discussion

Analysis of three pulses: before pump, "pump" and after pump (substrate only)

Empty crcles corresponds to theoretical calculations

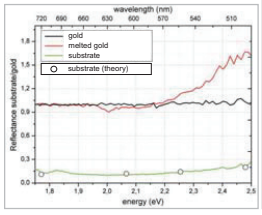


ANALYSIS

Scheme of pulses taken from experiment to reflectivity calculations pulse after pump

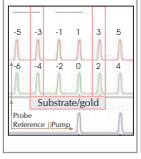


Comparison between stationary and time resolved experiment

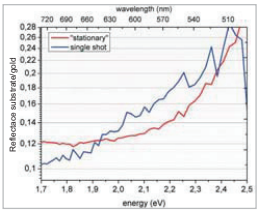


## Conclusions

1. Spectral and temporal response of hot plasma above melting point has been observed
2. Single shot 1.5 ps chirped white light reveals apectral and temporal information at once
3. Melting of band structure with a single shot of intense femtosecond pulse
4. Outline: application to irreversible phase transitions in molecular crystals, transition dynamics inside thermal hysteresis


## Bibliography

[1]. J. Hohfeld et al., *Chem. Phys.* ***251***, 237 (2000)
{2]. R.W. Schoenlein et al., *PRL* ***58***, 1680 (1987)
[3]. P. Poulin, K. Nelson, *Science* ***313*** 1756 (2006)
[4]. K. Sokolowski-Tinten et al., *PRL* ***81*** 224 (1998)

*"Dobry wieczór we Wrocławiu"* (Good evening in Wroclaw), history on: http://www.molecki.transport.pwr.wroc.pl/neony/dwww/

## Support

ANR
MET ROPOLE Rennes
Région Bretagne

# Out of equilibrium coherent precursor dynamics of a photo-induced phase transition in molecular material of $(EDO\text{-}TTF)_2SbF_6$


**Wawrzyniec Kaszub[1,2], Nicolas Moisan[1], Marina Servol[1], Alain Moreac[1], Maciej Lorenc[1], Hervé Cailleau[1,3], Ryszard Naskrecki[2], Shin-ya Koshihara[3,4], Mitsuhiko Maesato[5], Hideki Yamochi[4,6] & Eric Collet[1,3]**

[1]*Institut de Physique de Rennes, UMR CNRS-University Rennes 1 campus Beaulieu, Rennes, 35042, France*
[2]*Quantum Electronics Laboratory, Faculty of Physics, Poznan, Poland,*
[3]*Non-equilibrium Dynamics Project, ERATO-JST, Tsukuba, Ibaraki, Japan,*
[4]*Department of Materials Science, Tokyo Inst. of Technology, 2-12-1, Oh-okayama, Meguro, Tokyo, 152-8551, Japan,*
[5]*Division of Chemistry, Graduate School of Science, Kyoto University, Sakyo-ku, Kyoto, 606-8501, Japan*
[6]*Research Center for Low Temperature and Materials Sciences, Kyoto University, Sakyo-ku, Kyoto, 606-8502, Japan*


## $(EDO\text{-}TTF)PF_6$

Schematic views of the lattice and electronic structural changes accompanying the M-I phase transition in $(EDO\text{-}TTF)_2PF_6$ [1].

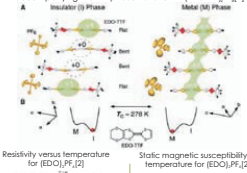


Resistivity versus temperature for $(EDO)_2PF_6$ [2]

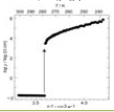

Static magnetic susceptibility vs temperature for $(EDO)_2PF_6$ [2]

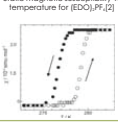

## EDO family

Thermal and photoinduced Metal - Insulator transition [4]

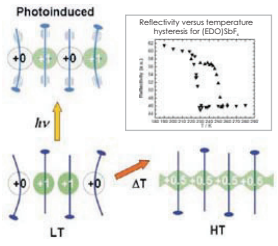


## Experimental and analysis

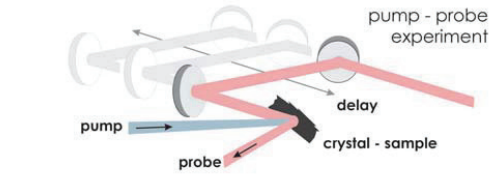


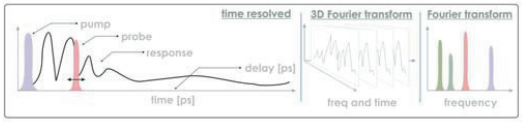


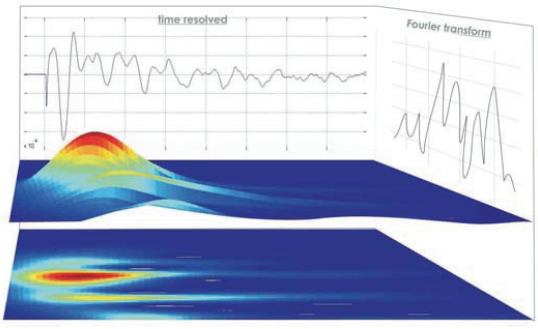


## Idea

The phonon frequencies correspond to Raman modes [3]

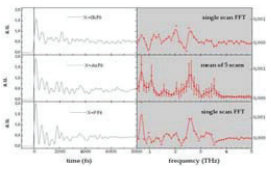


Single energy parameter vs coordinate (i.e.

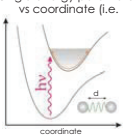


Energy parameter vs two coordinates

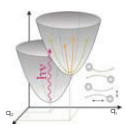


## $(EDO\text{-}TTF)PF_6$

Time dependance of oscillations at 100K and 200K [7]

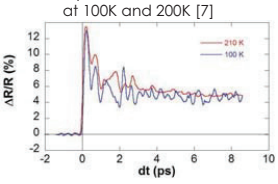


## Results

The phonon frequencies resolved at different temperatures

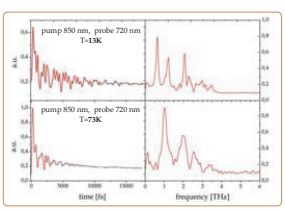


The phonon frequencies resolved at different wavelengths

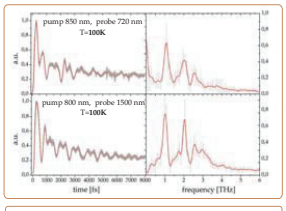


Raman Spectra at different temperatures

Raman spectra were obtained using duble monochromator and Ti:Saphire laser - wave-length: 747,475 nm.

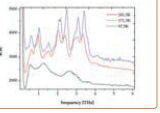

## 3D analysis technique

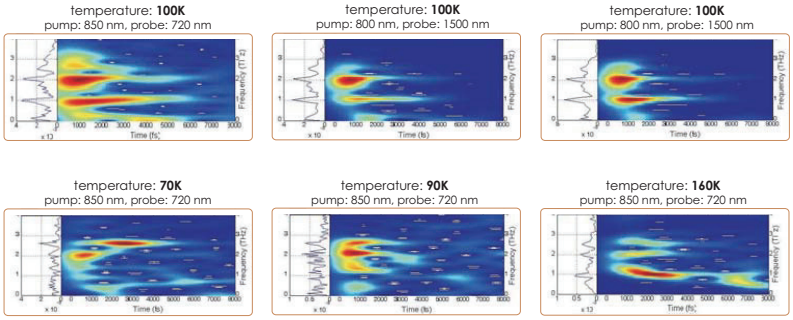


## Conclusions

1. We can observe a certain number of coherent phonons.
2. Phonons are better resolved when temperature is decreased from 100K to 10K
3. Coherent phonons seem to have different thermalisation times (multiple coordinates).
4. The photo-induced phase spectrum is different from the metallic phase spectrum, indicating that the photo- induced phase is a new one.

## Support


Région Bretagne · Metropole Rennes · ANR · ERATO Japan


## References


[1] M. Chollet *et al.* Science **307**, 86 (2005)
[2] A. Ota *et al.* J. Mat. Chem. **12** (2002) 2600
[3] M. Lorenc *et al.* J. Phys: Conf. Series **148** (2009) 012001
[4] K. Onda *et al.* Phys. Rev. Lett. **101**, 067403 (2008)
[5] A. Tomeljak *et al.* Phys. Rev. Lett. **102**, 066404 (2009)
[6] Y. Okimoto *et al.* Phys. rev. Lett. **103**, 027402 (2009)
[7] N. Moisan, Ph.D. Thesis, Universite de Rennes 1, 2008

# Structural and optical fingerprints of spin-crossover multiscale dynamics in a single crystal of [(TPA)Fe(III)(TCC)]$PF_6$


**Wawrzyniec Kaszub[1,2], Hervé Cailleau[1], Ryszard Naskrecki[2], Eric Collet[2], Marylise Buron[2], Marina Servol[2], Cherif Balde[1], Marie - Laure Boillot[3], Maciej Lorenc[1]**

[1]*Institut de Physique de Rennes, UMR CNRS-University Rennes 1 campus Beaulieu, Rennes, 35042, France*
[2]*Quantum Electronics Laboratory, Faculty of Physics, Poznan, Poland,*
[3]*Institut de Chimie Moleculaire et Materiaux d'Orsay, UMR CNRS 8182, Universite Paris-Sud, 91405 Orsay, France*


## Introduction

A challenging field of research for chemists and physicists community concerns the study of bistable molecular materials.

Controlling with an ultrashort laser pulse molecular states in a solid material represents a next step in ultrafast science, ensuing the now established field of femtochemistry. Molecular materials, and among them spin-crossover systems, offer the possibility to be directed between different macroscopic states by using appropriate electronic excitations as, contrary to dilute solutions, all the constituent molecules in solids can be photoactive. This opens new avenues for light-control of various photoswitchable functions (magnetic, optical, conduction...), with some direct consequences for future developments of information technologies.

Relaxation Process

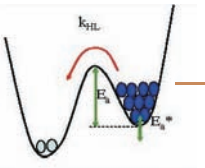


Ultra - fast photoswitching dynamics

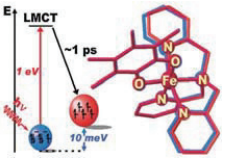


## Spin crossover phenomenon

Switching between S=1/2 and S=5/2

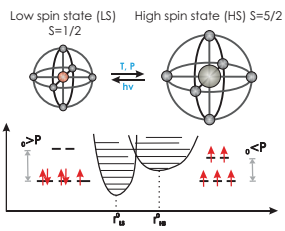


In an octahedral environment, the iron(III) metal ion is in a high spin state (S=5/2) at high temperature and in a low spin state (S=1/2) at low temperature. Change between HS and LS states can be induced by tuning temperature (T), pressure (P) or by applying irradiation (hν).

In this study, we examine the photoswitching dynamics of [(TPA)Fe(TCC)]PF6 compound.

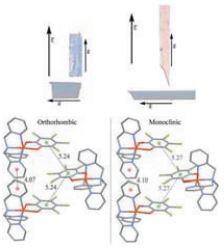


Magnetic, structural and optical properties correlation in [(TPA)Fe(TCC)]PF

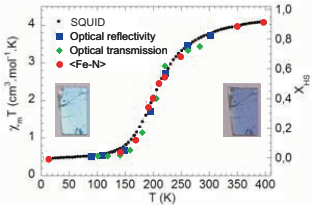


## Pump probe experiments

### Femtosecond optical pump-probe experiments

Pump probe experimental setup

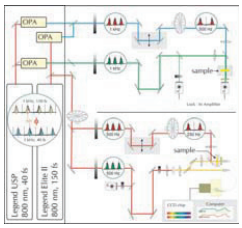


Heterodyne detection with synchronised laser amplifiers

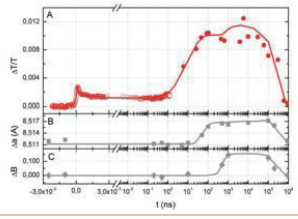


Sub - 100fs broadband absorption spectroscopy

Benchmarking of the spectrometer ND Filter bleaching

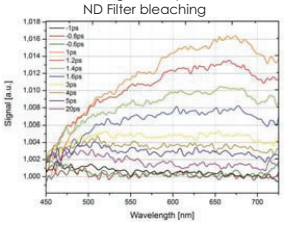


Temperature - dependent spectrum

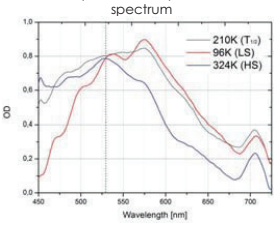


## X-Ray and optical studies

### X-Ray Diffraction and Optical Time-Resolved studies

Time depend structural changes at 180K

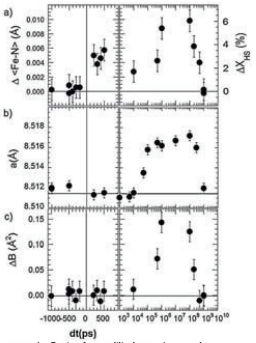


e) Out-of-equilibrium dynamics

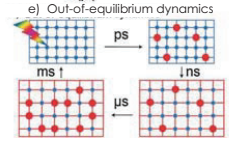


Optical Time depend transmission at 180K

d) Optical Time Resolved measurements

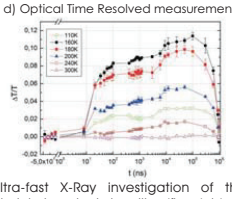


Ultra-fast X-Ray investigation of the photoinduced spin transition (fig. a), b), c)) and Optical Time-Resolved (fig. d)) confirm the existence of three consecutive steps from sub-picosecond up to the millisecond. Fig. e) is the schematic picture of the multiscale dynamics.

1. The sub-picosecond non-thermal molecular switching from LS to HS state,
2. The unit cell volume expansion on 2 ns time scale,
3. Significant thermal effects which lead to additional LS to HS conversion.
4. Relaxation to the Low spin state on ms time scale

## Conclusion

The out-of-equilibrium dynamics towards the macroscopic switching, when triggered by ultrashort laser pulse, involves consecutive steps over different time scales. The above results shed new light on the complex switching pathway from the molecular to materiallength and time scales. This is important for the design of materials with enhanced functionality. The spin-crossover compounds are known to be highly photo-switchable. The next step will be to study in real time these irreversible conversions in materials posessing high degree of cooperativity.

## References


1) E. Collet *et al.*, Z. Kristallog. **223** (2008) 272
2) E. Collet *et al.*, Acta Cryst. B **65** (2009) 474
3) M. Lorenc *et al.*, PRL **103** (2009) 028301
4) H. Cailleau *et al.*, Acta Cryst. A **66** (2010) 189


## Support

# Out of equilibrium coherent precursor dynamics of a photo-induced phase transition in molecular material of $(EDO\text{-}TTF)_2SbF_6$


**Wawrzyniec Kaszub[1,2], Nicolas Moisan[1], Marina Servol[1], Alain Moreac[1], Maciej Lorenc[1], Hervé Cailleau[1,3], Ryszard Naskrecki[2], Shin-ya Koshihara[3,4], Mitsuhiko Maesato[5], Hideki Yamochi[4,6] & Eric Collet[1,3]**

[1]*Institut de Physique de Rennes, UMR CNRS-University Rennes 1 campus Beaulieu, Rennes, 35042, France*
[2]*Quantum Electronics Laboratory, Faculty of Physics, Poznan, Poland,*
[3]*Non-equilibrium Dynamics Project, ERATO-JST, Tsukuba, Ibaraki, Japan,*
[4]*Department of Materials Science, Tokyo Inst. of Technology, 2-12-1, Oh-okayama, Meguro, Tokyo, 152-8551, Japan,*
[5]*Division of Chemistry, Graduate School of Science, Kyoto University, Sakyo-ku, Kyoto, 606-8501, Japan*
[6]*Research Center for Low Temperature and Materials Sciences, Kyoto University, Sakyo-ku, Kyoto, 606-8502, Japan*


## $(EDO\text{-}TTF)PF_6$

Schematic views of the lattice and electronic structural changes accompanying the M-I phase transition in $(EDO\text{-}TTF)_2PF_6$ [1].

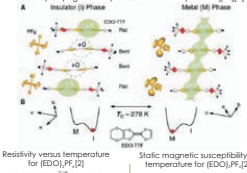


Resistivity versus temperature for $(EDO)_2PF_6$ [2]

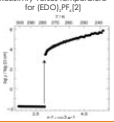

Static magnetic susceptibility vs temperature for $(EDO)_2PF_6$ [2]

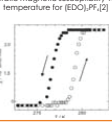

Thermal and photoinduced Metal - Insulator transition [4]

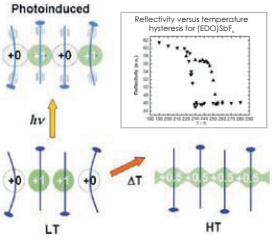


## EDO family and experiment

The phonon frequencies correspond to Raman modes [3]

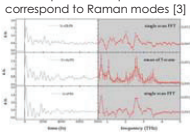

Time dependance of oscillations at 100K and 200K [7]

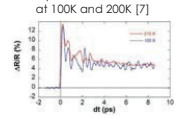


Experimental Setup

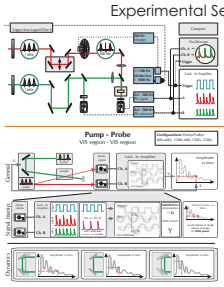


Idea

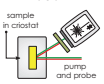


Overlap

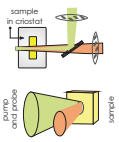


## Experimental and analysis

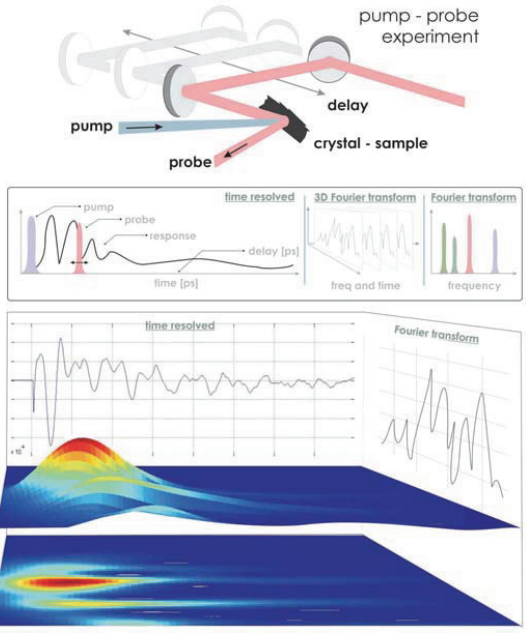


## Results

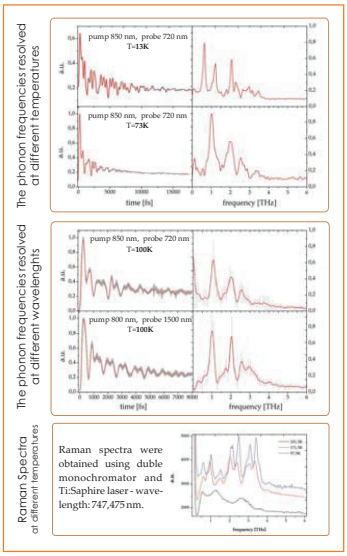


## 3D analysis technique

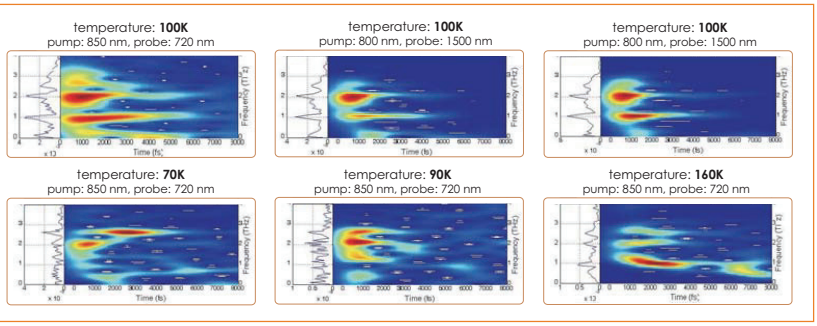


## Conclusions

1. We can observe a certain number of coherent phonons.
2. Phonons are better resolved when temperature is decreased from 100K to 10K
3. Coherent phonons seem to have different thermalisation times (multiple coordinates).
4. The photo-induced phase spectrum is different from the metallic phase spectrum, indicating that the photo- induced phase is a new one.

Single energy parameter vs coordinate (i.e. bismuth)

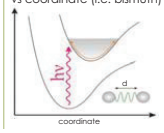


Energy parameter vs two coordinates

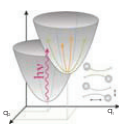


## Support


Région Bretagne · Métropole Rennes · ANR · ERATO Japan


## References


[1] M. Chollet *et al.* Science **307**, 86 (2005)
[2] A. Ota *et al.* J. Mat. Chem. **12** (2002) 2600
[3] M. Lorenc *et al.* J. Phys: Conf. Series **148** (2009) 012001
[4] K. Onda *et al.* Phys. Rev. Lett. **101**, 067403 (2008)
[5] A. Tomeljak *et al.* Phys. Rev. Lett. **102**, 066404 (2009)
[6] Y. Okimoto *et al.* Phys. rev. Lett. **103**, 027402 (2009)
[7] N. Moisan, Ph.D. Thesis, Universite de Rennes 1, 2008

**Sujet :** TRANSITIONS DE PHASE PHOTOINDUITES DANS LES MATERIAUX MOLECULAIRES

L'objectif principal de ce travail de thèse de doctorat est l'étude de transformations photo-induites par un pulse laser dans des matériaux moléculaires. Les résultats ont été obtenus grâce à l'utilisation de techniques optiques pompe-sonde. Ceci a nécessité des développements expérimentaux innovants, incluant des premières tentatives de techniques « single shot ».

Dans un matériau à transition de spin, où la lumière peut induire la commutation d'un état non magnétique à un état magnétique, nous avons pu suivre pour la première fois la dynamique de la transformation sur plusieurs ordres de grandeurs en temps, de 100 femtosesecondes à la milliseconde. Ceci a permis de montrer que le processus se produit en plusieurs étapes successives, de l'échelle de la molécule à celle du matériau.

Un composé organique à transfert de charge, qui présente une transition métal-isolant, a aussi été étudié. Une dynamique mettant en jeu plusieurs modes de phonons optiques cohérents a clairement été observée. Le comportement en fonction de l'intensité du pulse laser et de la température permet de conclure que l'état photo-induit à partir de la phase isolant diffère de la phase métallique observée à l'équilibre thermique.

La mise en place du nouveau montage optique « single shot » va permettre d'observer des changements d'état irréversible, comme dans un régime d'hystérèse. Ce montage a été testé en observant le comportement non thermique d'une couche mince d'or.

---

**Subject:** PHOTOINDUCED PHASE TRANSITIONS IN MOLECULAR MATERIALS

The main purpose of this Ph. D. thesis is to study the photo-induced transformations by a laser pulse in molecular materials. The results have been obtained thanks the use of pump-probe optical techniques. This required innovative experimental developments, including first attempts with a single shot technique.

In the spincrosover family of molecular materials, in which light may induce the switching from a non magnetic to a magnetic state, for the first time we followed the transformation dynamics over ten decades in time scale, from 100 femtoseconds to a millisecond. It reveals that the process follows a complex pathway from molecular to material scale through a sequence of steps.

A charge transfer organic compound, which exhibits an insulatior-to-metal phase transition, has also been investigated. A dynamics implying several coherent optical phonon modes has been clearly observed. The behaviour as a function of laser pulse intensity and temperature shows that the state photo-induced from the insulating phase differs from the metallic phase at thermal equilibrium.

The newly developed single shot set-up proved able of recording changes upon an irreversible transformation, for instance inside a hysteresis regime. This set has been tested by observing photo-induced damages of a thin gold layer.